

TIME DOMAIN ANALYSIS OF SPIROGRAMS

by

MARTIN RAYMOND MILLER, B Sc, MB BS, MRCP

A Thesis presented for the Degree of Doctor of Medicine
in the University of London

1983



The Medical College
St. Bartholomew's Hospital
London EC1

ABSTRACT

Spirograms are widely used simple tests of ventilatory lung function. This thesis evaluates their analysis in the time domain as a means of improving their yield of diagnostic information.

The most precise method for recording spirograms was determined. Errors due to non-instantaneous cooling of gas within spirometers were found to be greater than the known non-linearity of pneumotachographs when recording simulated spirograms.

The analysis of spirograms in the time domain involves considering the spirogram as a cumulative distribution of transit times and deriving the statistical moments of this distribution. A valid procedure for comparing the moments of truncated spirograms has been proposed and these truncated moments have been shown to be highly reproducible within individuals and retain discriminatory ability.

A multi-exponential model of the spirogram has been considered in detail as a means of overcoming errors inherent in the moments of some spirograms. The most satisfactory technique for applying this model to describe spirograms has been determined and the model was found to reflect correctly abnormalities in spirograms for commonly found ventilatory disorders.

A cross-sectional population survey of a male workforce was carried out to determine whether time domain analysis of spirograms detects abnormalities hitherto unappreciated. Normal values for conventional and time domain spirometric indices were determined.

Smokers were found to have two types of spirogram abnormality previously not recognised. The more commonly found abnormality was evident early within the spirogram, and the other was only evident in the tail of the spirogram. These findings do not agree with current hypotheses that smoking damage should be first manifest in the terminal part of a maximal forced expiratory manoeuvre. Alternative hypotheses are proposed.

Time domain analysis of spiograms has been found to demonstrate hitherto unrecognised changes in spiograms due to smoking.

TIME DOMAIN ANALYSIS OF SPIROGRAMS

CONTENTS

Abstract	2
Acknowledgements	7
Abbreviations	9
List of Figures	11
List of Tables	15

CHAPTER 1

BACKGROUND

Introduction	17
Historical Review	18
Current Perspective	22

CHAPTER 2

SPIROGRAMS IN THE TIME DOMAIN

Introduction	25
Statistical Considerations	26
Computation of the Moments of Spirograms	30
Truncation of Spirograms	36
Discussion	41

CHAPTER 3

METHODS

Introduction	44
The Computer	45
The Pump	46
The Spirometers	50
Pneumotachographs	51

CHAPTER 3 (contd.)

Performance and calibration of the pneumotachograph	54
(i) Linearity	54
(ii) Calibration	57
Effect of gas temperature on PT calibration	61
Choice of recording device	66
(i) Effect of air temperature	67
(ii) Effect of time constant of signal	72
(iii) Effect of connecting tubing	73
Discussion	73
Procedure for recording a spirogram	75

CHAPTER 4

MOMENT ANALYSIS OF SPIROGRAMS

Introduction	77
Repeatability Study	78
(i) Subjects	78
(ii) Methods	78
(iii) Results	79
Discussion	83

CHAPTER 5

A MULTI EXPONENTIAL MODEL OF THE FORCED EXPIRATORY SPIROGRAM

Introduction	89
The Model	91
Fitting the model to spiograms	95
(i) The Algorithm	95
(ii) Testing the Algorithm	99

CHAPTER 5 (Contd.)

Sequential mu and sigma for real spiograms	101
Selection of mu and sigma to describe a spiogram	110
The model and recognised ventilatory abnormalities	116
Discussion	119

CHAPTER 6

POPULATION SURVEY

Introduction	124
The Sample Population	126
Procedure	127
Analysis of recorded MFEM	128
Normal Values for men	129
Abnormalities in male smokers	140
(i) Identification of abnormal smokers	140
(ii) Patterns of abnormality	143
Discussion	151

CHAPTER 7

CONCLUSIONS

Recording Spiograms	167
Time Domain Analysis	169
Appendix A	171
Appendix B	172
Appendix C	176
References	179

ACKNOWLEDGEMENTS

The idea to pursue a more rigorous analysis of the maximal forced expiratory manœuvre was suggested to me by Dr. A. C. Pincock, Senior Lecturer in the Department of Medicine, University of Birmingham. Dr. Pincock has given invaluable support, advice and technical help throughout the work of this thesis. In particular, he masterminded the development of the microcomputer laboratory arrangement and he designed and developed the pump and thermo-regulatory devices used in the pump and for the pneumotachograph. The construction of the pump would not have been possible without the engineering skill of Colin Williams and Rick Whiting of the Department of Medicine Workshop and the many electronic aspects of the project required the patient skill of Roger James of the Dept. Medicine Workshop.

I am indebted to Dr. D. M. Grove, Lecturer in the Department of Statistics, University of Birmingham who triumphed over the many mathematical and statistical problems raised by this study. In particular he supplied the mathematical code necessary for using the multi-exponential model and he helped with the testing of the integration and optimisation procedures required by the model.

I thank the University of Birmingham Computer Centre for the facility of their Dec 20-60 computer and thank Mr. Paul Ramsay of the University of Birmingham Microprocessor Systems Laboratory for supplying the computer interface with the Dec 20-60. I thank Professor R Hoffenberg and Professor J M Bishop for the facility to carry out this work in the University of Birmingham Department of Medicine and I am grateful to Dr. Malcolm Green, Senior Lecturer

at the University of London for his advice on the preparation of this thesis.

For their financial support during this work I acknowledge the Birmingham Regional Health Authority who were supporting me as a Sheldon Clinical Research Fellow at the start of this work and I acknowledge the UK Medical Research Council for a project grant to complete this work. I acknowledge the University of Birmingham Faculty of Medicine Rowbotham Bequest and Scott-Moncrieff Bequest for the funds to purchase the microcomputer essential for this study.

I am indebted to my wife, Jan Miller, for patiently typing the manuscript.

ABBREVIATIONS

The following familiar abbreviations have been used within the text of this thesis without further definition.

FVC	Forced vital capacity
FEV _n	Forced expiratory volume at n seconds
FEV _n %	FEV _n expressed as % of FVC
PFR	Peak expiratory flow
FEF _n %	Forced expiratory flow when n% of FVC has been expired
FEF _{75-85%}	Mean flow between 75% and 85% of FVC expired.
FMF	Mean flow between 25% and 75% of FVC
FET	Forced expiratory time
ATPS	Ambient temperature and pressure, saturated
BTPS	Body temperature and pressure, saturated
L	Litres
mls	Millilitres
s	Seconds
ms	Milliseconds
L/s	Litres per second
DC	Direct current

ABBREVIATIONS (contd.)

The following abbreviations have been used but with initial definition within the text

PT	Pneumotachograph
RSS	Rolling seal spirometer
WSS	Water seal spirometer
MFEM	Maximal forced expiratory manoeuvre
FES	Forced expiratory spirogram
α_1	First moment of the spirogram
α_2	Second moment of the spirogram
MR	Moment ratio = $\sqrt{\alpha_2 / \alpha_1}$
A/D	Analog to digital
D/A	Digital to analog
CAL	Chronic airflow limitation
TTV	Theoretical terminal volume achievable if a spirogram could continue to infinite time.
MBC	Maximal breathing capacity
ID	Internal diameter

LIST OF FIGURES

2.1	Spirograms and frequency distribution of transit times for a normal subject and a subject with chronic airflow limitation.	28
2.2	The first moment of a spirogram expressed as an area	31
2.3	Two approaches to frequency of sampling for spirograms	32
	a) equal volume increment method	
	b) equal time increment method	
2.4	Percentage error in computing α_1 of single exponentials using	34
	a) equal volume increment sampling	
	b) equal time increment sampling	
2.5	Sequential α_1 , α_2 and moment ratio for a normal spirogram	37
3.1	Laboratory equipment configuration	47
3.2	The pump	49
3.3	Pneumotachograph differential pressure record for various constant flows	55
3.4	Pneumotachograph linearity	56
3.5	Flow profile from brass calibrating spirometer	60
3.6	Percentage error of pneumotachograph flow reading	65

3.7	Percentage recording error for pneumotachograph, water sealed spirometer and rolling seal spirometer.	70
	a) pump and ambient temperature at 19°C	
	b) pump at 37°C ambient at 19°C	
4.1	Mean within person co-efficient of variation of the sequentially derived spirometric indices	80
4.2	Mean discriminatory ability of the sequentially derived spirometric indices	82
4.3	The sequential moments and moment ratio for a young normal subject	84
4.4	The sequential moments and moment ratio for a middle-aged normal subject	85
4.5	The sequential moments and moment ratio for a stable asthmatic subject	86
4.6	The sequential moments and moment ratio for a subject with chronic obstructive lung disease	87
5.1	Theoretical spirograms and flow-volume curves with constant mu	92
5.2	Theoretical spirograms and flow-volume curves with constant sigma	93

5.3	Relationship between residual and changes in mu and sigma	96
	a) contour plot	
	b) 3 dimensional plot	
5.4	Testing the algorithm; sequential mu and sigma for a single exponential	100
5.5	Sequential mu and sigma and theoretical spiograms for a young normal subject	103
5.6	Sequential mu and sigma and theoretical spiograms for a middle-aged normal subject	105
5.7	Sequential mu and sigma and theoretical spiograms for a second young normal subject	107
5.8	Sequential mu and sigma and theoretical spiograms for a young stable asthmatic	108
5.9	Sequential mu and sigma for a young normal subject	109
5.10	Sequential mu and sigma for a man with an extrathoracic airway obstruction	111
	a) before operation	
	b) after operation	
5.11	Two theoretical spiograms and the original. A better fit from an earlier mu and sigma value	113

5.12	Two theoretical spiograms and the original. Equally good fit yet different mu and sigma values.	- 14 - 114
6.1	Age and height distribution for the 'normal' men	131
6.2	Relationship between $FEF_{75\%}$ and age for the 'normal' men	132
6.3	Plot of mu and sigma versus age for the 'normal' men	134
6.4	Plot of $\alpha_1 100\%$ versus age and the standardised residual versus predicted $\alpha_1 100\%$ for the 'normal' men	136
6.5	Plot of $\log_e (\alpha_1 100\%)$ versus age and the standardised residual versus predicted $\log_e (\alpha_1 100\%)$ for the 'normal' men.	137
6.6	Age and height distribution of the male smokers	141
6.7	Patterns of spirometric abnormalities in the asthmatics	144
6.8	Patterns of spirometric abnormalities in the 'normal' men	146
6.9	Pattern I of spirometric abnormality in the male smokers	147
6.10	Pattern II of spirometric abnormality in the male smokers	149
6.11	Pattern III of spirometric abnormality in the male smokers	150

LIST OF TABLES

2.1	Moment ratio values for 4 single exponentials with different truncation.	39
2.2	Moment ratio values for 2 spiograms with identical dispersion of time constants.	40
3.1	Viscosity of dry and saturated inspired and expired air at different temperatures	53
3.2	Calibration factors for the pneumotachograph calibrated with air at 25°C and 37°C.	62
3.3	List of variables recorded for the series of temperature experiments	69
3.4	Percent and absolute errors for the pneumotachograph and water sealed spirometer recordings with changes in ambient temperature.	71
3.5	Percent and absolute errors for the pneumotachograph and water sealed spirometer recordings with changes in time constant of volume profile.	72
4.1	Group results for reproducibility study	79
4.2	Correlation matrix for selected spirometric indices	81
5.1	Comparison of recorded spirometric indices and those predicted by the model using 3 methods for selecting μ and σ .	117

5.2	Mu and sigma values for subjects with recognised ventilatory abnormalities.	118
6.1	Regression equations for men for conventional spirometric indices.	133
6.2	Regression equations for men for the natural log of α_1 and $\sqrt{\alpha_2}$.	138
6.3	Regression equations for men for moment ratio, mu and sigma	139
6.4	The number of male smokers and 'normals' found to be abnormal for each spirometric index	142
6.5	The number of smokers with Pattern I and Pattern II with specific groups of symptoms.	151

BACKGROUND

INTRODUCTION

The main purpose of the lungs is to effect gas exchange between the blood and air so that cellular metabolism can take place. It may therefore seem that the only pertinent test of lung function is to study this gas exchange by measuring arterial blood gas tensions and analysing expired gas. However, the lungs have tremendous reserve which enables adequate oxygenation of blood both at rest and on extreme exercise when the oxygen demand may have increased by 20 fold or more. Hence a disease process may have a pronounced effect on certain aspects of the way the lungs work with little change occurring in overall gas exchange at rest.

Because of this no single test of lung function adequately describes the performance of the lungs. This performance can be broadly divided into two related aspects, firstly, the transport of gas in and out of the lungs (i. e. ventilation) and its control, and secondly, the exchange of gas between air and blood. The last 50 years have seen a phenomenal improvement in the ability to investigate, and thus understand, the intricate details of gas exchange, ventilation and its control. Consequently there is now a profusion of tests available for studying lung function. However, if in normal clinical practice an assessment of the ventilatory and gas exchanging performance of the lungs is required, only a small number of relatively simple tests are usually used.

The purpose of this thesis is to determine whether improved recording and a more rigorous analysis of one of the simplest and most widely used of the tests of ventilatory lung function, namely the forced expiratory spirogram, can improve its yield of clinically useful information.

HISTORICAL REVIEW

The rigorous investigation of ventilatory function in man was founded by Hutchinson in 1846 ⁽¹⁾, although 15 years earlier Thackrah ⁽²⁾ had described his equally extensive but less thorough study. In Hutchinson's exemplary treatise he first reviewed the work already done by others concerning lung function and then having drawn a distinction between the chemical and mechanical aspects of respiration he devoted his attention to the second of these. He carefully described a device, which he called a spirometer, for recording the total volume of gas that a subject could slowly exhale after a maximal full inspiration and he called this volume the vital capacity. His observations on the way some subjects may inadequately perform the vital capacity manoeuvre are as pertinent today as they were then. He recorded the vital capacity in over 2000 subjects and drew conclusions on the influence of age, height, weight and disease on the vital capacity.

Bain in 1870 ⁽³⁾ praised the work of Hutchinson but was dismayed at its lack of impact on the medical practice of the day. He described the first waterless portable spirometer, a design which is still widely used.

Following this early work the vital capacity (VC) was measured and documented in certain diseases. Peabody in 1917^(4, 5) noted that subjects with cardiac disease with a low VC were more dyspnoeic when they were stressed with a raised inspired carbon dioxide tension than were cardiac patients with a normal VC. Dreyer and Burrell^(6, 7) and Cameron⁽⁸⁾ separately documented VC in cases of pulmonary tuberculosis and they found that a low VC was associated with more severe disease and that if the clinical condition improved then the VC would increase.

It was soon realised that measurement of VC, which is essentially a static volume, gave little information about the common clinical problem of breathlessness associated with asthma and chronic bronchitis. The first established dynamic test of ventilatory function was the maximal breathing capacity (MBC)⁽⁹⁾. The MBC was defined as the maximal voluntary ventilation per minute, usually being measured over a period of 15 seconds. This test was fairly widely used and although it had the merit of being the first test to reflect the flow resistive properties of the lungs it suffered by being also largely dependent on the subject's motivation and strength, and its measurement was influenced by the procedure adopted and by the type of equipment used.

In an attempt to overcome the deficiencies of MBC as a dynamic test of ventilatory function the measurement of the forced expired volume in a much shorter length of time during a single exhaled breath was first proposed by Tiffeneau⁽¹⁰⁾, and subsequently by Gaensler⁽¹¹⁾ in 1951. Gaensler described a spirometer for

- 20 -

measuring timed volumes and found that the forced expiratory volume in 1 second (FEV_1) had a higher correlation with MBC than did FEV_2 or FEV_3 . FEV_1 and FVC were found to distinguish between subjects with airflow limitation, normal subjects and subjects with either loss of lung volume from lung resection or a restrictive ventilatory defect. He found that FEV_1 expressed as a percent of FVC ($FEV_1\%$) was highly reproducible and dramatically reflected improvements in an asthmatic subject after use of a bronchodilator aerosol.

Although the measurement of static lung volumes and its subdivisions was well established before 1951, the static tests had not proved helpful in assessing the common clinical problem of airflow limitation.

Following Gaensler's work the recording of a single breath maximal forced expiratory manoeuvre (MFEM) has become an accepted means for testing ventilatory lung function and the plot of expired volume against time (called the spirogram) offers a useful visual representation of the test, with FEV_1 , FVC and $FEV_1\%$ being numerical indices derived from it.

At about the same time as Gaensler's work was presented a more detailed consideration was being made of the mechanical properties of the lungs which limited expired flow. Dayman in 1951⁽¹²⁾ noted the relationship between lung elastic recoil and the maximal flow achieved in patients with emphysema. Later Fry and associates⁽¹³⁾ demonstrated that as the expiratory driving pressure during an MFEM increased, so expiratory flow increased to a maximum beyond which further rises in pressure failed to produce an increase in flow. The maximum flow so

achieved was determined by the lung volume at which the measurements were made. The relationships between driving pressure, flow and volume led to the suggestion by Fry and Hyatt ^(14, 15) that if an MFEM were represented just by a plot of flow against volume much information would be available and there was then no need to record the driving pressure. They observed that after approximately 15 to 25% of the FVC had been expired the maximal expiratory flow during an MFEM was largely independent of effort.

Leuallen and Fowler in 1955 ⁽¹⁶⁾ proposed a flow measurement derived from the spirogram as a sensitive index of ventilatory function. Although expiratory flow had been measured by many workers before 1955 it had not by then been fully standardised as an index of ventilatory function. Leuallen and Fowler defined the maximal mid-expiratory flow (MMF) as the slope of the chord joining 25% and 75% of expired FVC on a spirogram and this equals the mean flow over the mid-half in volume of the spirogram. They found that MMF was more sensitive than FEV_1 , FEV_3 and MBC in detecting abnormal ventilatory function in subjects with chronic bronchopulmonary disease. MMF is largely independent of effort and is still widely used today. The use of a different flow measurement was reported by Higgins in 1957 ⁽¹⁷⁾. He used a Wright peak flow meter, which was later fully described in 1959 by Wright and McKerrow ⁽¹⁸⁾, to record the peak expiratory flow (PEF) achieved during an MFEM. Higgins found that PEF correlated fairly well with MBC but was easier to perform and record and was as sensitive as MBC to smoking habit. PEF was subsequently found to have a wide range of normal values ⁽¹⁹⁾ and this, together with it being effort dependent, has limited its application in diagnosis.

The work of Fry and Hyatt ^(14, 15) led to an increased understanding of how expired flow is limited during an MFEM and this was expressed by the two theories proposed by Mead ⁽²⁰⁾ and Pride and Permutt ⁽²¹⁾. These theories helped to clarify the determinants of maximal expiratory flow during an MFEM and it was thus thought that maximal expiratory flow-volume (MEFV) curves were more informative than spiograms and were likely to supercede them as a test of ventilatory function.

Fry and Hyatt recognised that intrapulmonary airflow limitation produced a change in the shape of the MEFV curve different from that due to a fixed extrathoracic airway obstruction ⁽¹⁴⁾. Green and others ⁽²²⁾ noted a change in the shape of MEFV curves with age and felt that the variability of MEFV curves amongst normal subjects represented true differences but that this variability would limit the use of the MEFV curve in diagnosis and management of individual subjects with ventilatory disorders. Various methods have been tried to describe the shape of MEFV curves ⁽²²⁻²⁵⁾ but none have found wide acceptance and one approach has been shown to be limited by its high variability within individuals ⁽²⁶⁾.

CURRENT PERSPECTIVE

The forced expiratory spiogram, which is both simple to perform and easy to record, remains one of the most widely used tests of ventilatory lung function. Because of the problems associated with the use of MEFV curves in clinical practice they have not been widely adopted, although they are extremely useful for the diagnosis

of extrapulmonary airway obstruction⁽²⁷⁾. However, with a view to improving the yield of information from the MFEM an alternative approach to the description of the spirogram, and MEFV curve, has been proposed. Spirograms represent the same information as MEFV curves but in a different form, and when a spirogram and its corresponding MEFV curve are standardised for volume, they both contain information only about the timing of the MFEM. This led to the consideration of the MFEM in the time domain rather than flow or volume domain.

This approach was first proposed in an abstract by Fish, Permutt Menkes and colleagues in 1974⁽²⁸⁾ and more fully by Tockman, Permutt, Menkes and others in 1976⁽²⁹⁾. They considered the volume standardised spirogram as a cumulative distribution of transit times and analysed this distribution to determine the mean transit time and an index of dispersion of transit times. Fish et al⁽²⁸⁾ found that when asthmatics were challenged with methacholine their mean transit time increased with no change in dispersion. Tockman et al⁽²⁹⁾ found that in smokers the mean transit time and the root mean square of the transit times increased with age twice as much as they did in non-smokers.

Following this lead several groups of workers have applied this technique in different ways^(24, 30-33). Analysis of the spirogram in the time domain has been found to be more sensitive than conventional, and often more complicated lung function tests, in detecting abnormalities in young smokers⁽²⁴⁾ and in young asthmatics.⁽³⁰⁾

Because of the apparent potential that this form of analysis might improve the clinical application of the spirogram, the study presented in this thesis was undertaken to test and validate time domain analysis of the spirogram.

CHAPTER 2

SPIROGRAMS IN THE TIME DOMAIN

INTRODUCTION

The major emphasis of spirogram analysis in the past has been in the volume domain with timed volume measurements such as the forced expiratory volume in one second (FEV_1). FEV_1 remains the single most validated and clinically useful test of ventilatory function for the assessment and management of air flow limitation. The effect of cigarette smoking on airflow has been extensively researched and the careful longitudinal survey of Fletcher⁽³⁴⁾ demonstrated the value, as well as the limitation, of FEV_1 . The problem with FEV_1 has been in interpreting whether a subject with a slightly low FEV_1 has always had a low FEV_1 or whether the subject is beginning to develop chronic airflow limitation. This dilemma has limited the usefulness of FEV_1 as a test to apply to individuals as a means of identifying the early stages of chronic airflow limitation.

Airflow limitation means that a longer time is required to deliver a certain volume. Therefore the forced expiratory time (FET) was studied⁽³⁵⁾ as a means of identifying airflow limitation, but its poor within person repeatability has limited its application. The analysis of the spirogram in the time domain, rather than the volume domain, has been further pursued, firstly by Fish et al⁽²⁸⁾, then by other colleagues at Johns Hopkins University, Baltimore⁽²⁹⁾ and also by other groups of workers^(24, 30-33). They proposed that the spirogram should be considered as a distribution of transit

times and analysed to obtain a mean transit time of the spirogram.

The immediate advantages of this form of analysis are that the mean transit time, which is the mean time taken for a quantity of gas to be expired, is sensitive to the whole spirogram and is volume standardised.

Thus subjects with different forced vital capacities can be directly compared in terms of mean transit time. Before considering this further it is first necessary to examine the statistical methods for analysing such distributions.

STATISTICAL CONSIDERATIONS

Any distribution can be analysed by the statistical technique of moments⁽³⁶⁾. The "R"th moment of any distributed variable is defined as the average "R"th power of the distributed variable throughout its distribution. Hence the first moment of a distributed variable is its mean. If the spirogram is considered as a distribution of transit times then the first moment of spirogram is the mean transit time for a unit volume of gas to be expired. In calculating the moments the variable can be measured with respect to any point within the distribution. Thus when working with a normal distribution the square root of the second moment measured with respect to the mean is the standard deviation i. e. root mean square deviation from the mean. It is evident that the first moment with respect to the mean will be zero.

When the Johns Hopkins group^(28, 29) considered transit time analysis of spiograms they realised that the second and higher moments would be especially sensitive to a distorted distribution of transit times such as that which might occur when airflow limitation

causes an increase in the population of long transit times. They chose to derive the higher moments of the spirogram measured with respect to the origin of the spirogram. The study in this thesis and the work of others⁽²⁴⁾ have followed this lead. Other groups of workers^(30, 31) have exclusively measured the higher moments with respect to the mean transit time. Although analysis about the mean is not incorrect, it is less likely to be helpful in identifying a population of prolonged transit times for the following reasons.

The frequency distribution of transit times of a normal spirogram approximates to a single decaying exponential, figure 2.1, and even in the presence of marked chronic airflow limitation the overall shape of the distribution is similar. If interest lies in identifying a population of prolonged transit times then the method of analysis should be chosen appropriately. Analysing about the mean of the distribution to derive the second and higher moments would be unhelpful for two reasons. Firstly, it diminishes the importance of those transit times in the region of the mean and there is no reason why these have less relevance to the problem of identifying a population of prolonged transit times. Secondly, when the mean transit time is prolonged deriving the second moment about the mean not only emphasises the presence of the very long transit times but to an increasing extent also that of the very short transit times. This is because derivation of the second moment about the mean involves summing the second power of the difference between the mean transit time and all the individual transit times. Hence all those transit times terminating within one second either side of the mean have their contribution reduced. If the mean is greater than 1 second

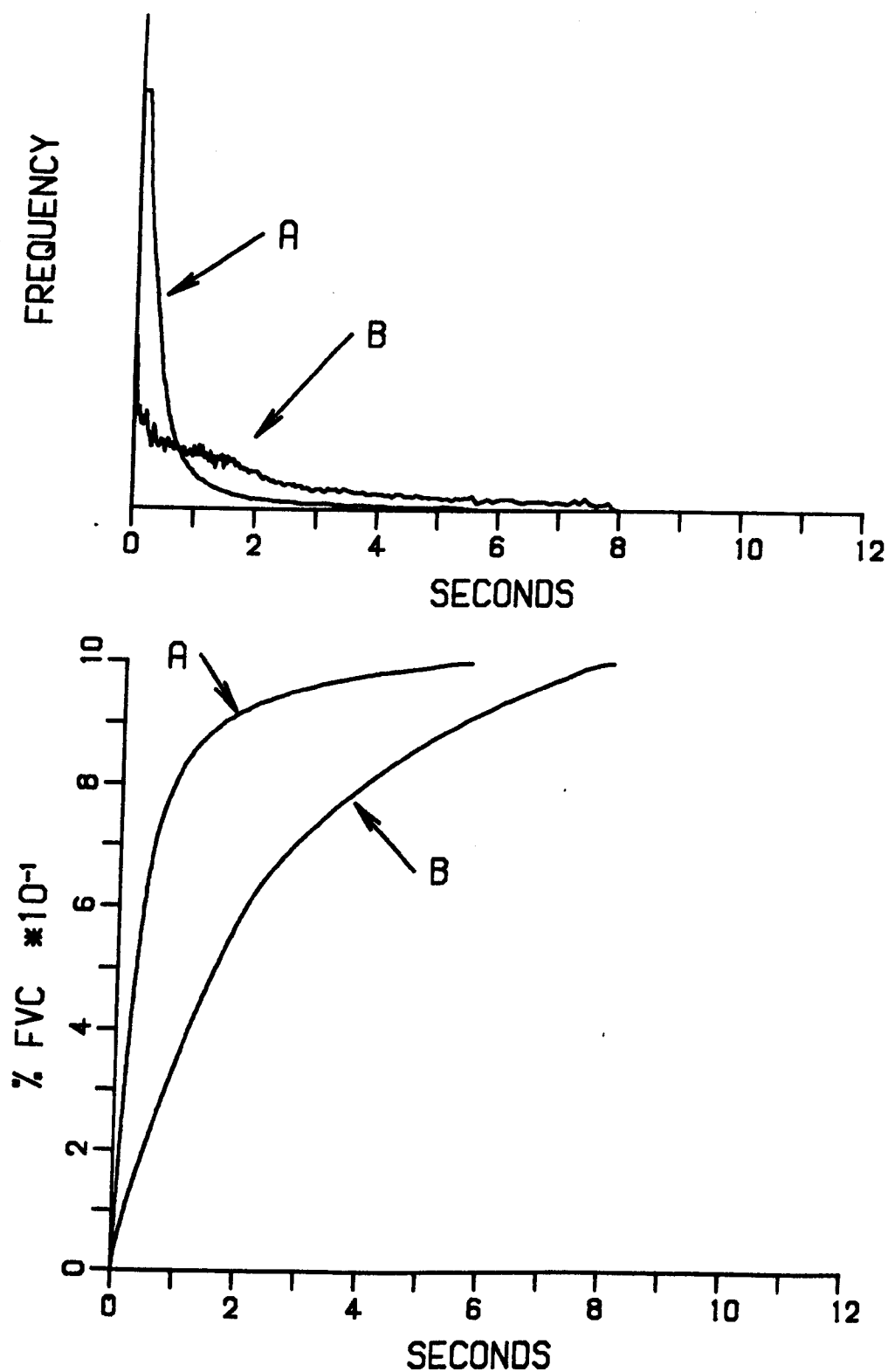


Figure 2.1 Spirograms and frequency distribution of transit times for a normal subject (A) and a subject with chronic airflow limitation (B).

then the very shortest transit times begin to make an important contribution to the higher moments. This conflict of influence may confound the interpretation of the result. Analysis about the origin of the spirogram avoids these problems and in the higher moments diminishes the contribution of only those transit times of less than 1 second, which would be desirable since interest lies in identifying a population of long transit times.

The choice of whether to analyse about the mean or any other point in a distribution depends entirely on the shape of the distribution being considered and on the point of interest within the distribution. For these reasons it is usual practice with a normally distributed variable, such as the height of men in the general population, to derive the variance about the mean and not the variance about the origin of the distribution. The variance with respect to zero height would be valid statistically but not very helpful.

The following convention has been followed for nomenclature. α_1 has been used to denote the first moment about the origin of the spirogram, i. e. the mean transit time. α_2 denotes the second moment with respect to the origin and $\sqrt{\alpha_2}/\alpha_1$ has been called the moment ratio (MR). The moment ratio is a dimensionless index of dispersion of transit times and can be considered as an index of dispersion of the time constants for emptying of the lungs.

COMPUTATION OF THE MOMENTS OF SPIROGRAMS

The Johns Hopkins group⁽²⁹⁾ calculated the moments by dividing the FVC into 50 equal volume increments and the elapsed time corresponding to the midpoint of each volume increment was recorded and averaged to give the mean transit time i. e. α_1 . Neuburger and colleagues⁽³¹⁾ divided the FVC into 0.11 s time intervals and the corresponding volume increments were recorded. The moments can then be derived by numerical integration from:

$$\alpha_r = \frac{\sum_{n=1}^N \left[dv_n (tt_n)^r \right]}{FVC}$$

where dv_n is the 'n'th volume increment, tt_n is the mean time taken from the start of the spirogram for this volume increment to be expired and N is the total number of increments considered. This procedure was validated by comparison with planimetry⁽³¹⁾ because the first moment about the origin of a volume standardised spirogram equals the area between the spirogram and the volume axis, figure 2.2.

Theoretical considerations can indicate the optimal method for storing spirograms digitally so that the moments can be computed by numerical integration with the least quantitising errors. By considering single exponentials whose moments can be found precisely from definite integrals (see Appendix A) it is possible to determine precisely the quantitising errors for the moments using numerical integration with different sampling frequencies.

Spirogram co-ordinates can be stored in a computer either at specified volume increments, figure 2.3a, or at specified time

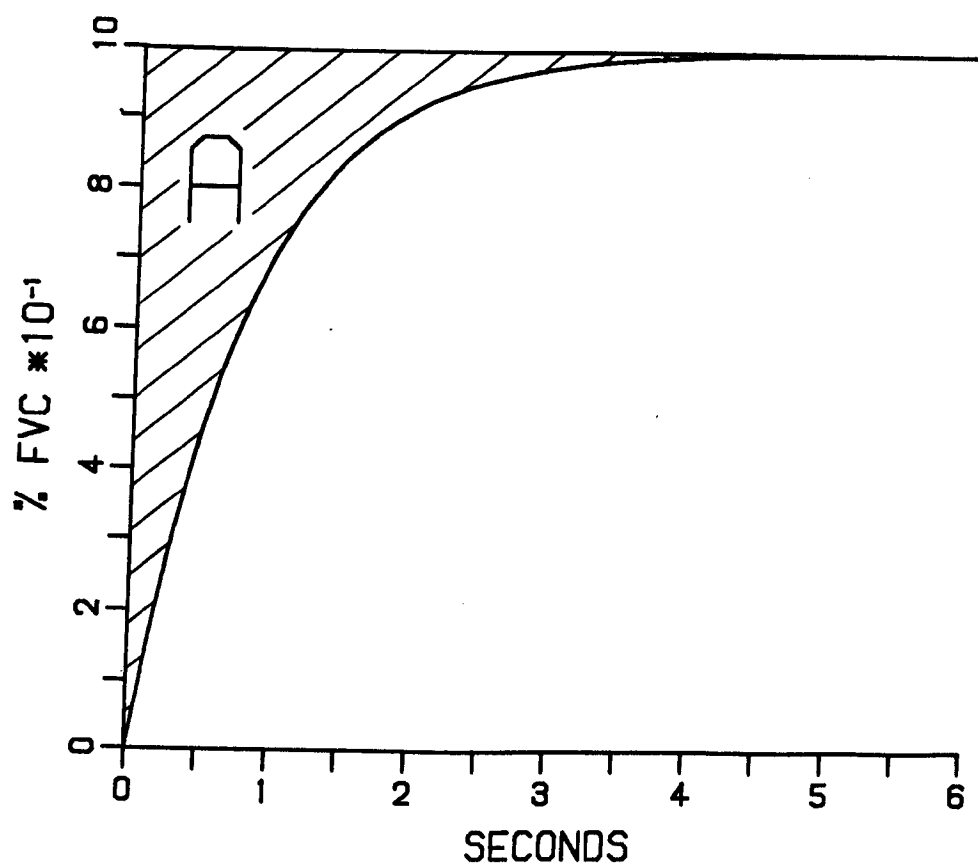


Figure 2.2 The first moment of a spirogram expressed as an area (A).

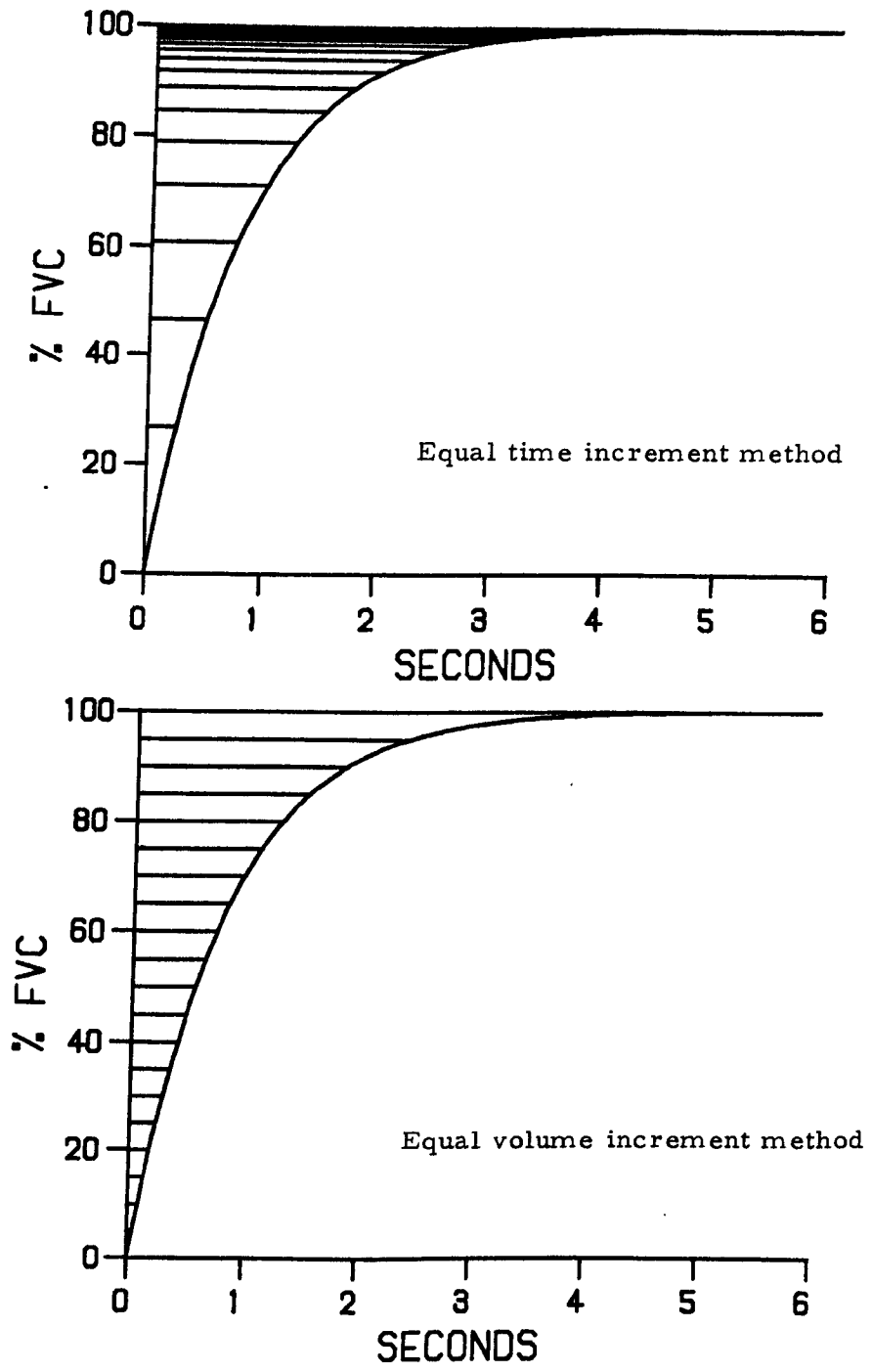


Figure 2.3 Two approaches to frequency of sampling for spiograms.

increments, figure 2.3b. Figure 2.4 shows the percent error in computed first moment of 3 single exponentials of time constant 0.4 s, 0.8 s and 2.4 s for different numbers of volume increments of storage and different duration time increments. Single exponentials are similar to volume standardised spiograms and these three time constants span the physiological range.

With the time increment sampling (dt) method the errors vary considerably with the time constant of the exponential and the errors are greatest for the shortest time constant exponential. However, there is only a 0.5% overestimate of α_1 for the 0.4 s time constant exponential if dt is 0.1 s. With the equal volume increment sampling (dv) method the errors for different time constant exponentials are roughly the same. The errors for the 0.4 s time constant are almost identical to the 0.8 s time constant and are not shown. The errors with the dv method are larger than those for the dt method and only approach 0.5% if the number of volume increments is 250. This is equivalent to 8 ml increments for an FVC of 2.0 L.

The reason for the errors for each method is that the volume increment method (dv) does not sample the tail of the spiogram frequently enough and the time increment method (dt) does not sample the early part of the spiogram frequently enough. Because the early part approximates to a straight line so the dt method is more precise. Jordanoglou and colleagues⁽³²⁾ have derived the mean transit time by dividing the volume axis into between 12 and 35 increments. This will lead to substantial and variable errors. The 50 volume increment

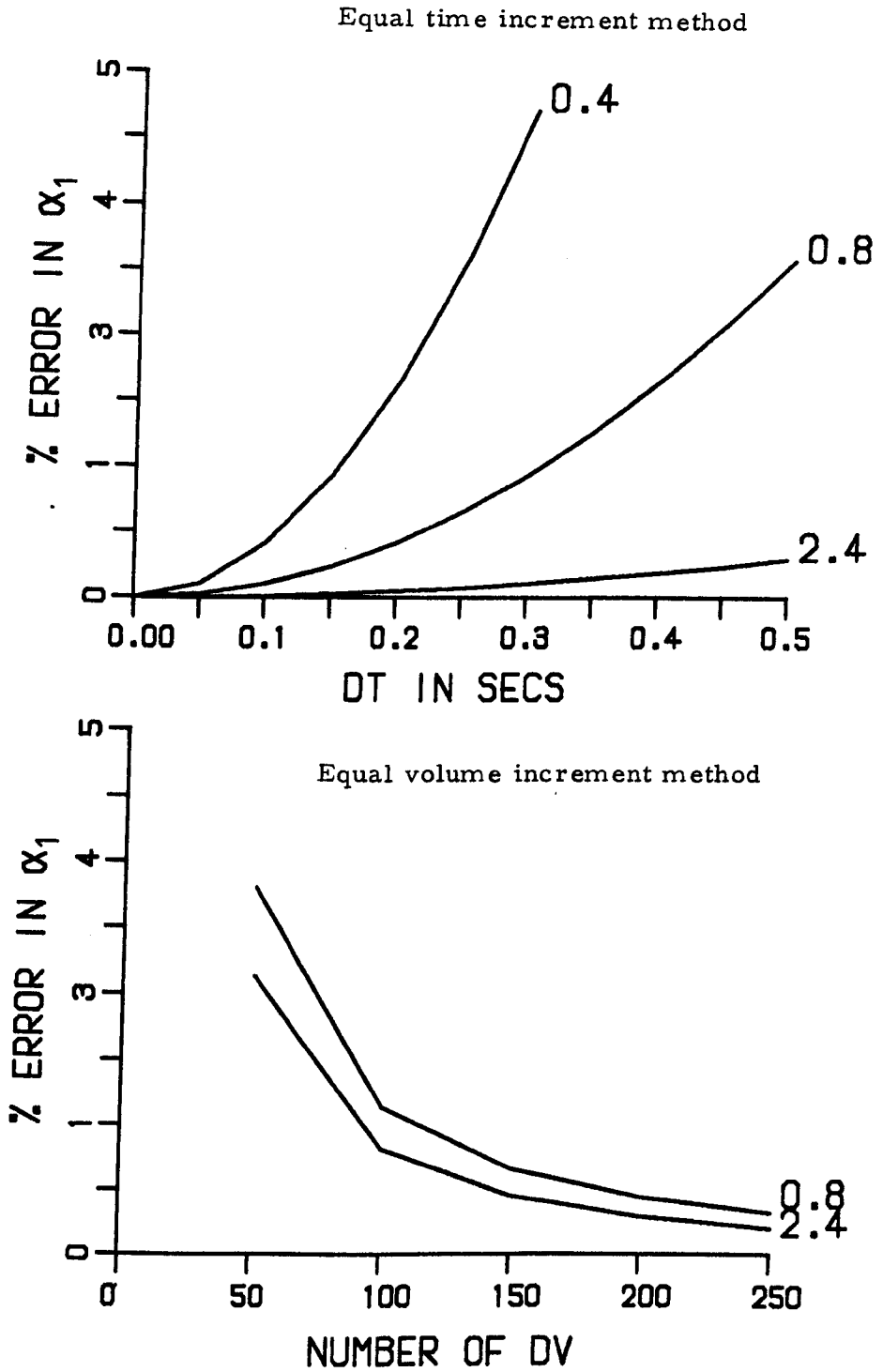


Figure 2.4 Percentage error in computing α_1 of single exponentials of time constants 0.4, 0.8 and 2.4 s using two methods of sampling.

method used by the Johns Hopkins group ⁽²⁹⁾ leads to a 3% over-estimate of α_1 .

For precise description of the spirogram, allowing exact calculation of the moments, a compromise between the volume and time increment method was used in this study for storing spiograms digitally. In order to increase the sampling frequency early on, spiograms were recorded digitally whenever the volume increment exceeded 20 mls or time increment exceeded 0.1 s whichever occurred the sooner. The first moment integrated from single exponentials stored in this way was precise with an error in α_1 of less than 0.05% when FVC was 1.0 L, irrespective of the time constant. For an FVC larger than this, the error would be smaller still. All the above calculations assume perfect sampling of the signal and so estimates of the moments based on hand drawn lines ⁽²⁹⁾ from analog output of spiograms will contain additional errors.

A further important consideration with regard to the computation of the moments of the spirogram relates to defining the origin of the spirogram. All spiograms are slightly sigmoid shaped at the start because it takes a finite time before peak flow is reached. This time varies between individuals and varies within individuals from blow to blow. It has therefore been proposed that for all timed events during a spirogram the origin of the spirogram should be defined by back extrapolation from peak flow on the spirogram at constant peak flow to intersect the time axis at the new time zero ⁽³⁷⁾. This procedure is obligatory for calculation of the moments of the spirogram. If it is not performed then the mean transit time includes a contribution related

to the time taken to achieve peak flow and this contribution is adding 'noise' and not 'signal'. Performing the back extrapolation by hand can lead to considerable errors in defining the new time zero. In this study the back extrapolation was performed by an algorithm which found peak flow from the spirogram co-ordinates held in the computer and then calculated the new origin of the spirogram precisely.

From spirogram co-ordinates stored digitally, as described above, the moments can be derived with precision by simple numerical integration. This integration procedure can be performed in a sequential manner with the instantaneous sequential moments being standardised by the instantaneous total expired volume. Figure 2.5 shows a normal spirogram plotted together with the sequential α_1 , α_2 and moment ratio (MR). It can be seen that α_1 rises more steeply early on and increases more slowly later in the spirogram. α_2 increases more slowly initially and rises more steeply later because of the influence of the longer transit times. MR rises steeply from close to unity in the first 0.25 s of the spirogram and increases steadily thereafter.

TRUNCATION OF SPIROGRAMS

All recorded spiograms are in a sense truncated in that the expiration was not able to continue to infinite time to see what expired volume could then be achieved. An MFEM is terminated by a number of factors which include chest wall mechanics, breath hold time, airway closure and effort. Different factors operate in different subjects⁽³⁸⁾, with chest wall mechanics being dominant in some young subjects whose MFEM comes to an abrupt halt after a short

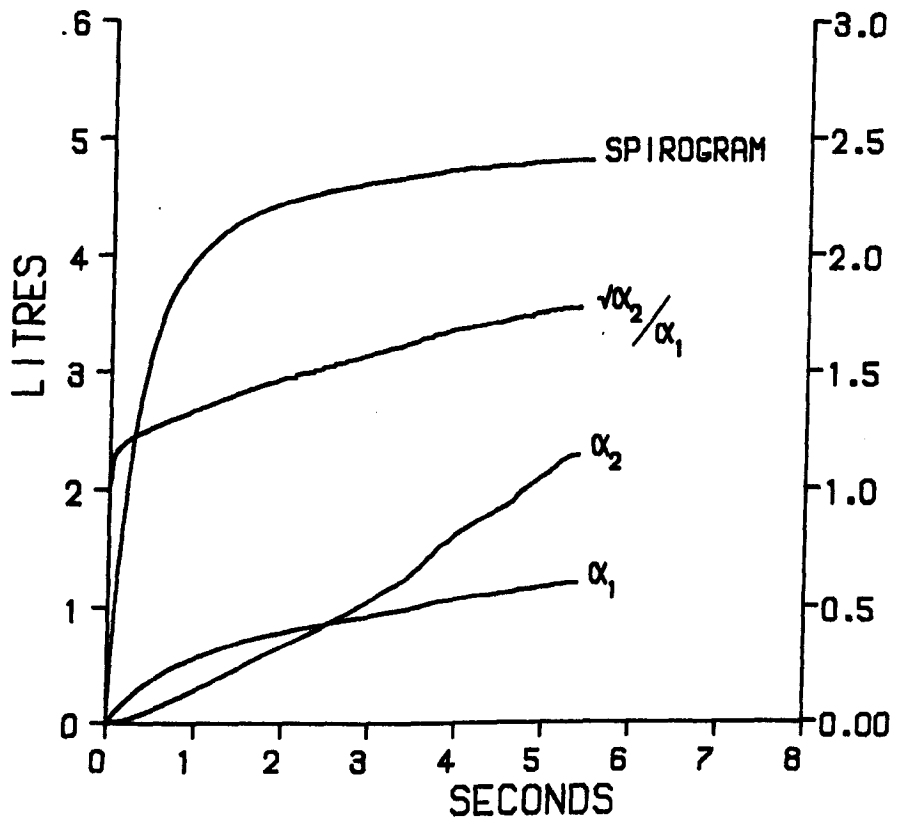


Figure 2.5 Sequential α_1 , α_2 and moment ratio for a normal spirogram

forced expiratory time (often 1 to 1.5s) with a sharp fall off in flow.

Other older subjects and especially those with airflow limitation have their MFEM curtailed due to breath hold time being exceeded or airway closure.

The impact of this truncation on moment analysis of spiograms was not at first fully appreciated; an arbitrary method for standardising the moments of a subject's spiogram was adopted by some workers (24, 29-31). This involved only analysing the first 6 seconds of the spiogram and the hope was that this could allow valid comparisons of one subject with another to be made. This convention was accepted without question.

The effect of inevitable truncation can be seen in figure 2.5 which shows a normal spiogram plotted together with the sequential α_1 , α_2 and MR. It can be seen that if the spiogram had stopped 100 mls sooner than it did, the moments and MR would have been considerably underestimated. If a recorded spiogram is asymptotic to a line parallel to the time axis then there is effectively no truncation and a precise estimate of α_1 is obtained. If it is not asymptotic then it is not possible to know what the α_1 would have been if the spiogram had been able to continue to an asymptote. Permutt and Menkes⁽³⁹⁾ demonstrated the effect truncation of spiograms had on moment analysis of spiograms and proposed a mathematical model of forced expiration in order to overcome this problem. Their model will be discussed later in this thesis.

The work presented here ⁽⁴⁰⁾ was the first challenge to the convention of 6 second truncation for standardisation of the moments. A satisfactory convention for truncating spiograms must apply not only to spiograms but also to all similarly shaped curves. If the convention does not apply to simpler but similar curves then there is no reason to expect it to be true for complex curves such as spiograms.

First consider single exponentials of the form

$$v = 1 - e^{-t/D} \quad (i)$$

where v is the volume expired by time t and D is the time constant. From definite integrals the moments and MR can be determined at any specified time or volume of truncation of such exponentials (see Appendix A). Because MR is an index of dispersion of both the transit times and time constants for such curves and all single exponentials will have the same dispersion irrespective of time constant it follows that a valid convention for truncation will yield constant MR irrespective of time constant.

The table below shows the MR values at different volumes and times of truncation for single exponentials of the type in equation (i).

Table 2.1

Time Constant	Truncation at % terminal vol.			Truncation at time in secs.		
	20%	60%	100%	2	6	10
0.75	1.1656	1.2014	1.4142	1.2921	1.4085	1.4141
1.00	1.1656	1.2014	1.4142	1.2589	1.3922	1.4129
1.50	1.1656	1.2014	1.4142	1.2236	1.3464	1.3988
2.00	1.1656	1.2014	1.4142	1.2058	1.3073	1.3742

It can be seen that truncation with respect to time is incorrect and erroneously suggests these single exponentials have differing dispersion of time constants. Truncation with respect to the theoretical terminal volume achieved at time infinity (TTV) is a valid procedure with the MR being constant at given truncation irrespective of the time constant.

The same observations pertain if any mixture of single exponentials is used. To see if this is true for real spiromograms it is necessary to test two different spiromograms which are known to have the same dispersion of time constants. The only way to obtain two such spiromograms is to take any subject's recorded spirogram and generate another spirogram from it by multiplying all the time co-ordinates of the spirogram by a constant factor. Although for a real spirogram the FVC is not necessarily the TTV that could be achieved if the expiration continued to infinite time the FVC for the real spirogram and the generated spirogram will bear the same relationship to TTV so that truncation with respect to volume will not be disturbed by this procedure. The table below shows MR values for these two spiromograms with truncation with respect to time and volume.

Table 2.2

Truncation at	50% FVC	75% FVC	3 s	4 s
original spirogram	1.1719	1.2087	1.4432	1.5091
generated spirogram	1.1719	1.2087	1.3543	1.4141

Again truncation with respect to time leads to the erroneous conclusion that the two spiromograms have differing dispersion of time constants. Only truncation with respect to volume is valid.

DISCUSSION

These observations on truncation present a serious limitation to the use of moment analysis of spiograms. Truncation with respect to time is clearly incorrect and analysing spiograms in this way precludes valid comparisons of one spiogram with another. These observations question the validity of the findings of some groups of workers (24, 29, 30).

Truncation with respect to theoretical terminal volume (TTV) presents its own problems since TTV is not known for a real spiogram. Hence there is an inevitable error due to the fact that all recorded spiograms are truncated when obtained. This inevitable truncation is most pronounced in subjects with airflow limitation and in a few young subjects where chest wall mechanics seem to terminate the MFEM. In the majority of normal subjects the spiogram is approximately asymptotic and so inevitable truncation errors are minimal. Hence this form of analysis is best applied to normal spiograms and is unsuitable for use on subjects with severely truncated spiograms. Not realising these limitations moment analysis has been applied to the spiograms of subjects with airflow limitation who are therefore liable to have these truncation errors. Liang et al⁽³⁰⁾ found that bronchodilators did reduce mean transit time significantly in asthmatics but the changes in $FEF_{50\%}$, $FEF_{75\%}$ and $FEV_1\%$ were more impressive and consistent. They analysed about the mean to derive a co-efficient of variation and index of skewness of transit times, which were not significantly changed and in some subjects 'worsened'. Their results are confounded by truncation errors and inappropriate analysis about the mean, but despite this they found that in their asthmatic subjects

of all the indices derived the mean transit time was abnormal in the largest number of subjects and had the most extreme abnormalities.

That this form of analysis should be confined to essentially asymptotic spiograms is not too serious a limitation. There are satisfactory indices already available for detecting established airflow limitation but, as yet, there is no index to detect changes in spiograms which presage the onset of serious airflow limitation. Such an index would necessarily be derived from essentially asymptotic spiograms where the use of moment analysis would not be fraught with inevitable truncation errors.

However, the errors in the moments due to inevitable truncation can, paradoxically, be reduced by earlier truncation of the recorded spiogram. In figure 2.5 it can be seen that if this spiogram had been able to continue for a further 100 mls the moments and MR would be much higher because in this region they are generally rising more steeply than the spiogram. Suppose then, that in this example, the difference between the recorded FVC and the theoretical terminal volume is 100 mls. If one chose to truncate the spiogram and the moments at 90% of FVC then the absolute error in defining the correct truncation point would be 90 mls, since it has been shown one must truncate with respect to TTV for valid comparisons to be made. However, the difference this 90 mls makes in α_1 , α_2 or MR at 90% FVC is much smaller than the difference the 100 mls makes at 100% FVC because at 90% FVC the spiogram is rising more steeply than α_1 , α_2 or MR. Therefore the moments truncated at 90% FVC will be closer to the true moments at 90% TTV and so comparisons of these truncated

moments between subjects will be more valid than comparing the moments derived up to 100% FVC.

This paradoxical reduction in error by earlier truncation has the drawback that with earlier truncation the very prolonged transit times are not being considered. However, those areas within the lungs which are emptying slowly do so from the start of the MFEM. Therefore the distribution of even the early transit times may be abnormal and the long transit times may not need to be considered (see figure 2.1). This aspect of truncation will be considered in more detail in Chapter 4.

CHAPTER 3

METHODS

The study in this thesis requires the accurate recording of forced expiratory spiograms (FES). As water seal spirometers (WSS) and dry rolling seal spirometers (RSS) are known to record volume with an acceptable degree of precision⁽⁴¹⁾ it would seem at first reasonable to use such a device for this study. However, these spirometers allow cooling of expired gas to occur as the expired volume is recorded. To date it has been assumed that this cooling is nearly instantaneous i. e. the time constant of cooling for the device is very short in relation to the time constant of the FES, thus allowing the use of a correction factor to adjust the volume results from ambient temperature and pressure, saturated (ATPS) to body temperature and pressure, saturated (BTPS). Doubt has been cast on the validity of the temperature correction⁽⁴²⁻⁴⁵⁾.

It is evident that if this cooling is not instantaneous and occurs progressively then the shape of the FES will be distorted and this distortion would not be rectified by the application of the ATPS to BTPS correction factor. Only precise knowledge of the thermal time constant of the device would allow suitable correction of the distortion. Flow meters have better dynamic characteristics than spirometers but their response is known to be slightly non-linear⁽⁴⁶⁾ and so they have not been widely used for recording spiograms. However, a heated pneumotachograph should not suffer from problems of cooling of expired gas because the flow is measured at a stable temperature.

Therefore in order to determine which device records an MFEM most faithfully it was necessary to assess the degree of distortion of spiograms due to cooling in spirometers and see if the errors incurred were greater than those resulting from the known non-linearity of pneumotachographs.

The equipment used in this study formed part of a computerised laboratory arrangement which was developed during the course of the study. This arrangement allowed many different procedures to be run consecutively without changing the configuration of the equipment. Furthermore, digital recording at high frequency by computer allows a more detailed and rapid interpretation of data.

THE COMPUTER

A general purpose microcomputer (Cromemco System Three with 64K bytes of random access memory) was used rather than a system dedicated to pulmonary function testing as this allowed greater flexibility in the laboratory. Rather than use the computer's own internal clocks to determine the sampling frequency a separate programmable quartz interrupt clock (10 kilocycle crystal) was interfaced with the computer (figure 3.1) allowing software control of sampling frequency (interrupt interval range 0.1 ms to 25.4 ms in 0.1 ms increments). A 16 channel bit analog to digital (A/D) converter (Analog Devices DAS 1128) was interfaced with the computer so that 16 separate devices were permanently linked to the computer via the pre-amplifiers. The pre-amplifiers were either 0 to 1 or 0 to 10 gain amplifiers, depending on the device, and had 2 pole

Butterworth filters. The 16 input channels could be sampled in any order at the frequency determined by the clock with 0.3 ms taken per input channel sampled.

Output options (see figure 3.1) included 8" computer floppy disks, DEC-writer printer terminal for hardcopy results, Tektronix T4010 graphics terminal, incremental XY plotter for hardcopy graphics, Perex perifile 6041 digital cassette tape recorder (DC300A cassettes) which was double buffered to allow on-line data storage in real time, and 16 digital outputs for control of solenoids and other pieces of equipment. A 2 channel 12 bit D/A converter (Data Translation Inc. module DT212) was interfaced with the computer in order to drive a servo controlled pump and to give a real time analog display of signals on a Tektronix type 611 storage oscilloscope. The microcomputer was interfaced with the University of Birmingham computer Centre's DEC 20-60 computer to facilitate data handling and permit the use of sophisticated algorithms required later in this study.

THE PUMP

In order to test a volume recording device dynamically it is essential to be able to generate a reproducible volume-time profile which approximates to a spirogram. Spirometers have been tested using normal subjects repeatedly^(43, 44, 47, 48) but since an individual has an inherent variability in performing an MFEM this method of testing a device is not ideal. Using a waveform generator to test spirometers is more satisfactory and various types have been used^(41, 49).

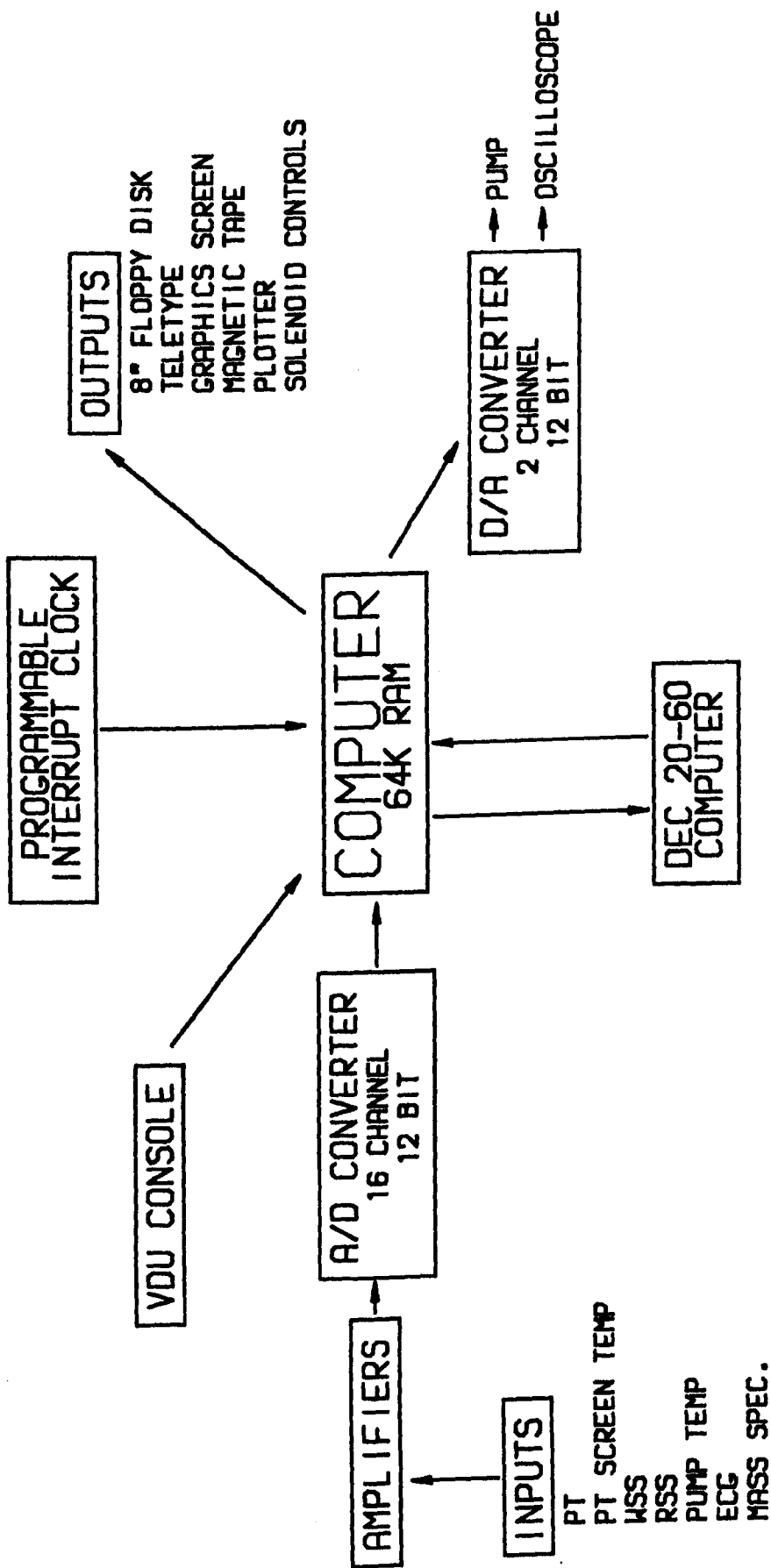


Figure 3.1 Laboratory equipment configuration.

This study has used a pump (figure 3.2) developed by the engineering workshop of the University of Birmingham Department of Medicine which was specifically for testing volume and flow measuring devices. The pump consists of a 30 cm long clear plastic cylinder of 20.0 ± 0.0025 cm internal diameter terminated by a 70 cm long smooth walled fibreglass cone. The piston was sealed by a double knife-edged polytetrafluoro ethylene seal and was driven from a central rod by a rack and pinion. A permanent magnet printed armature DC servo motor was connected directly to the pinion and a 15 turn positional potentiometer. The servo motor was driven by a DC amplifier from the output of the D/A converter which was updated by the computer. The displacement of the piston was measured using a vernier optical microscope. The pump's internal temperature was controlled by a heating coil placed at the outflow of a small axial flow fan placed centrally in the cylinder at the junction of the cylinder and cone. The temperature was regulated by a proportional output thermostat using a platinum resistance thermometer. The interior of the pump was humidified by a water saturated gauze in a dish attached to the piston.

The response of the D/A converter and pump was tested by sending increasing digital values to the D/A converter and pump. After each increment in digital output the displacement of the piston was measured using the optical vernier microscope. The volume of gas discharged for a given digital output to the pump was calculated from the known cross-sectional area of the pump and the measured displacement of the piston. The pump's response to digital output was linear



Figure 3.2 The Pump

over its 6 L range with a residual standard deviation from the regression line of 3 ml. The pump's slewing rate was 30 L/s which was sufficiently fast to allow adequate testing of flow meters up to 15 L/s.

THE SPIROMETERS

Two types of spirometer were evaluated, a water seal spirometer (WSS) and a dry rolling seal spirometer (RSS). The WSS was of conventional bell and counter balance design with water columns of unequal annular radii to reduce oscillations⁽⁵⁰⁾. The lightweight plastic bell (145 gm) of 178 mm diameter activated a single turn plastic film potentiometer which was attached directly to the counter balance. The linearity of this device was tested statically through its 7 L range by successively discharging 250 mls volume increments from the pump and recording the output of the spirometer through the A/D converter. The regression line of discharged volume against bit value from the A/D converter had a residual standard deviation (RSD) of 8 mls. This device therefore fulfilled accepted performance criteria^(51, 52).

The RSS used was a type 840 Ohio 10 L spirometer which was used unmodified. When the RSS linearity was tested statically through its 10 L range the RSD from the regression line was 26 mls and thus the RSS fulfilled accepted performance criteria^(51, 52). This larger RSD was probably due to a slight change in resistance offered by the seal of this device as it passed through the 4 to 6 L region of its volume range. There was no overt deformity of the cylinder to account for it.

PNEUMOTACHOGRAPHS

A heated Fleisch No. 4 pneumotachograph (PT)⁽⁵³⁾ was used for this study. A PT works on the principle of offering a viscous resistance to the flow of gas across a resistive element which in the case of a Fleisch PT is a series of individual fine parallel capillaries filling the 60 mm diameter casing. The pressure difference (P) between two arbitrary points in a flow stream can be given approximately from the Navier Stokes equation,

$$P = P_a + P_c + P_f$$

where P_a is the pressure increment due to linear acceleration or deceleration of the flow stream occurring between the two points, P_c is the increment due to convective acceleration between the two points and P_f is the increment due to frictional losses in the flow.

P_a can be minimised by placing the lateralappings close together and P_c is minimised by ensuring that the inlet and outlet apertures of the PT are identical.^(54, 55) In this way the pressure drop across the PT can be simplified to $P = P_f$, which from the Hagen-Poiseuille formula for fully developed lamina flow becomes:

$$P = P_f = \frac{8\mu LQ}{\pi R^4}$$

where μ is the gas viscosity, R is half the diameter of the tube, L is the length of the tube and Q is the rate of flow. Hence pressure drop across the resistive element is proportional to flow and depends on gas viscosity and not gas density. However, if flow is not lamina Γ ,

$$P_f \propto \frac{\mu Q^2}{\text{density}}$$

Hence the pressure drop is no longer linearly related to flow and now depends on gas density as well as viscosity. The design of the Fleisch No. 4 PT is such that flow remains laminar over most of the range 0 - 15 L/s.

The pressure drop across the resistive element was measured with a variable capacitance transducer (Furness Controls Ltd., Bexhill, type FC 040) which was connected to the PT via short (8 cm) rubber tubes of equal length to minimise resonance and phase lag in response. (54) The transducer was manufactured with a linearity better than 0.5%, frequency response of 50 HZ and temperature effect of 0.1% full deflection per °C above 20°C.

The viscous resistance of the PT element can be altered by condensation of water from expired air and so it is customary to heat the element to prevent this. The temperature of expired air is approximately 33°C (56, 57) and so the element's temperature must be higher than this. In this study the PT element has been heated to 40°C and the temperature controlled at this level by means of a proportional thermostat whose thermocouple was placed in one of the capillaries of the resistive element of the PT. Under steady state conditions the screen temperature remains at $40.0 \pm 0.1^\circ\text{C}$. It is necessary to control the temperature of the PT head very precisely as the temperature alters the performance of the PT considerably. This change due to temperature is by two mechanisms. Firstly, the viscosity of air rises with increase in temperature and secondly, the heating effect of the PT head expands the gas as it passes through the PT.

If one assumes that the viscosity of a composite gas such as air is made up in proportion from the viscosities of its constituent gases then the viscosity of air, dry or saturated with water vapour can be determined using Sutherlands formula

$$\eta_t = \eta_{273} \left[\frac{273 + C}{t + C} \right] \left[\frac{t}{273} \right]^{1.5}$$

where t is the absolute temperature, η_t is the viscosity at temperature $t^{\circ}\text{K}$, η_{273} is the viscosity at 273°K and C is one of Sutherland's constants (58). Table 3.1 shows the viscosity of inspired and expired air at different temperatures both dry and saturated assuming barometric pressure of 760 mm Hg.

Table 3.1

Viscosity of Air in Micropoises

Temp $^{\circ}\text{C}$	Inspired		Expired	
	Dry	Saturated	Dry	Saturated
20	182.5	180.4	180.0	178.0
25	184.9	182.2	182.4	179.7
30	187.3	183.6	184.8	181.2
35	189.7	184.8	187.2	182.4
37	190.7	185.1	188.1	182.7
40	192.1	185.6	189.5	183.2

Inspired Air = $0.2095 \text{ O}_2 + 0.7809 \text{ N}_2 + 0.0003 \text{ CO}_2 + 0.0093 \text{ Ar}$

Expired Air = $0.16 \text{ O}_2 + 0.7907 \text{ N}_2 + 0.04 \text{ CO}_2 + 0.0093 \text{ Ar}$

It is apparent that water vapour pressure has a considerable influence on the overall viscosity of air, such that saturated air at 35°C has the same viscosity as dry air at 25°C .

The second way that heating the PT alters its performance is because gas flowing through the PT is heated and expanded, thus increasing the true flow in proportion to the difference between the gas temperature and that of the flow head according to ^{CHARLES'S} ~~Boyle's~~ law. This assumes 100% efficiency of heating the gas by the PT. The efficiency will diminish with increasing flow rates and with increasing difference between the temperature of the gas and that of the PT head. With the PT at 40°C and assuming 100% heating efficiency then gas at 25°C will expand by 5% on passage through the PT whereas gas at 37°C will expand by 1%.

It is evident that the temperature and composition of the gas flowing through the PT, together with the temperature and heat capacity of the PT are important factors in determining the pressure drop registered across the PT.

PERFORMANCE AND CALIBRATION OF THE PNEUMOTACHOGRAPH

(i) Linearity

The linearity of response of the PT was assessed by discharging the pump through the PT at a constant flow i. e. driving the pump with a ramp function. Figure 3.3 shows the actual signal recorded from the PT with increasing flows. Resonance was evident which was quite stable except at the highest flow 15 L/s. In order to estimate the bit value corresponding to the given flow the signal was numerically averaged over its second half. Figure 3.4 shows a plot of the bits thus recorded from the A/D converter against flow with a regression line derived from the first 4 points up to a flow of 4 L/s. This regression

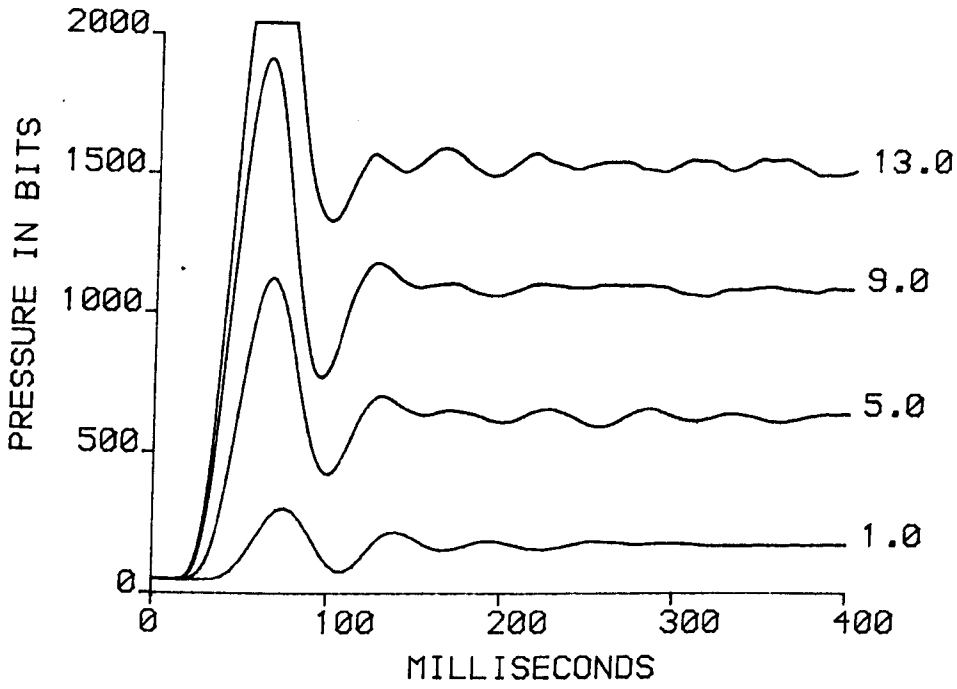


Figure 3.3 Pneumotachograph differential pressure record for constant flows of 1.0, 5.0, 9.0 and 13.0 L/s.

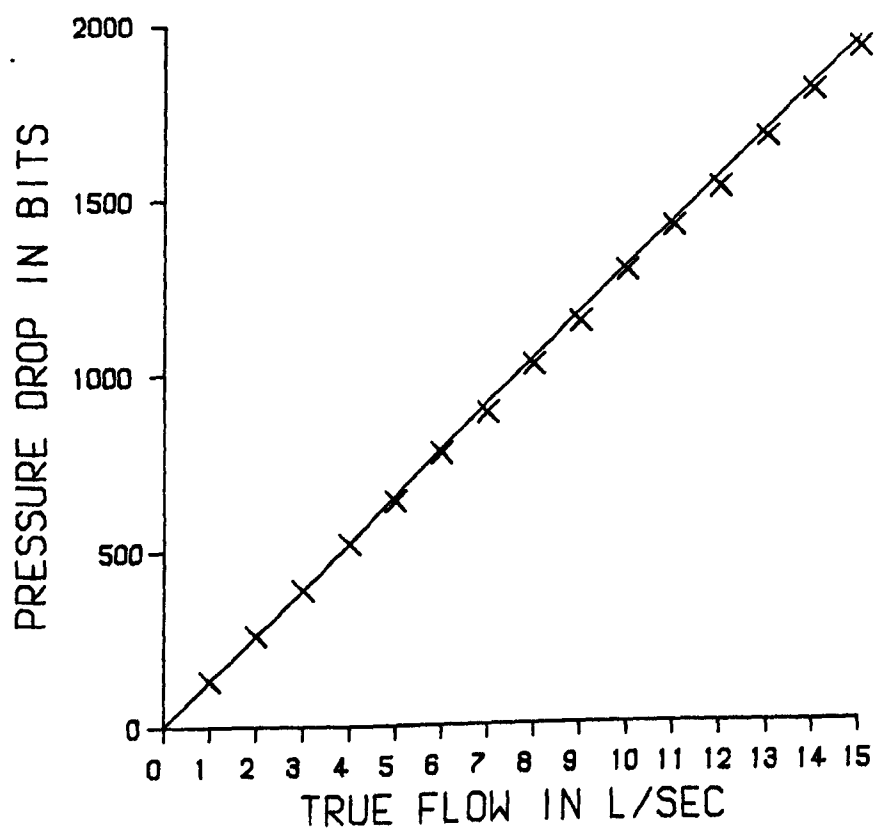


Figure 3.4 Pneumotachograph Linearity.

line is used to illustrate that with flows greater than 4 L/s, the points all fall slightly below this line. One possible explanation for this break point in the response at 4 L/s is that since the internal diameter of the proximal end of the PT casing is 28 mm the Reynolds number at this point exceeds 2000 when the flow is greater than 4 L/s and the change from laminar to turbulent entry flow may have subtly altered the characteristics of the device. This explanation is going to be tested in studies outside the context of this thesis. However, a regression line drawn using all the data has a RSD of 7 bits (i. e. RSD of 0.05 L/s, with 15 L/s full scale for 2000 bits).

The non-linearity of pneumotachographs is usually seen at high flows with a pressure drop across the PT screen in excess of that anticipated, because turbulence leads to a square law relationship between pressure and flow (vide supra)⁽⁵⁵⁾. This non-linearity is known to be dependent on the upstream geometry and Finucane et al⁽⁴⁶⁾ found a similar result to ours when using a similar upstream geometry. Their findings confirm that the upstream flow conditions have a pronounced effect on the performance of a PT.

(ii) Calibration

The usual practice for calibrating pneumotachographs is to discharge a known volume of gas through the PT, integrate the flow to give volume and equate the integrated volume with the true volume in order to obtain a calibration factor. In this way the complete recording system, PT, transducer and A/D converter are calibrated as one unit. This procedure is usually carried out by using a hand driven syringe of 1 L (or up to 4 L) capacity and the gas used is room air at ambient

temperature. Several errors may arise from this procedure. Although the viscosity of dry room air at 25°C is the same as saturated expired air at 37°C (table 3.1) the degree of heating and expansion of gas on passage through the heated PT head will be different for gas at 25°C and gas at 37°C . This means that a correction factor should be applied for the temperature difference. However, the efficiency of heating the air from 25°C to PT head temperature of 40°C will not be perfect and will differ from that of heating expired air to 40°C . Furthermore, an adequate control of the flow rate from the syringe is necessary to ensure a reproducible and pertinent range of flows.

For these reasons, in this study two different means of calibration were investigated. One used the pump and the other a brass spirometer. The spirometer had a heavy brass bell which was counterbalanced by two pulleys and weights. The bell fell under gravity when released by a solenoid trigger and it was held central during its fall by a rod with a linear bearing. An air damper was attached to this rod which engaged a dash-pot after 70% of the drop was completed in order to slow the fall of the bell. The length of the drop was determined by the position of the trigger and the air damper on the rod. From the length of the drop and the known dimensions of the brass bell the volume discharged was calculated. The water in the spirometer was heated by a heating jacket around the outer case of the reservoir and the temperature was maintained at 37°C by a proportional thermostat. The whole device was enclosed by a polyethylene bag to reduce heat losses. The speed of the fall of the bell was set by adjusting the number of counterbalance weights used so that the peak flow of the gas discharged was approximately 7L/s .

Figure 3.5 shows the flow profile recorded from this device.

The slight oscillation of the water following the drop caused the flow to go negative transiently so the calibration procedure recorded the flows through the PT every 4 ms for a total of 6 s. This was 4 s longer than the drop took thus allowing the flow oscillation to settle. The summed bit values from the A/D converter from this procedure were equated with the known volume discharged (4.157 L) and a volume calibration factor for the device (CAL_V) was obtained.

$$CAL_V = \frac{\sum_{n=1}^j (B_n - B_0)}{4.157}$$

where B_n is the bit value recorded after the 'n'th interval of 4 ms and B_0 is the bit value recorded when the flow was zero. Dividing this volume calibration factor by 4 (because of the 4 ms sampling interval) converts it to an instantaneous flow calibration factor.

Preamplifier gain was set at 1.9 to give a 15 L/s full range at + 2000 bits from the A/D converter. Repeated calibrations with this device showed an excellent degree of reproducibility with a co-efficient of variation of 0.1% for 5 calibrations. This variation represents a maximum volume error of 17 mls in 4.157 L.

The second method for calibrating the PT was using the pump with a double-exponential volume profile. This profile was derived in the computer as a reverse single exponential (0.8 s time constant) immediately followed by the same single exponential to give a sigmoid volume profile. This meant that peak flow was achieved

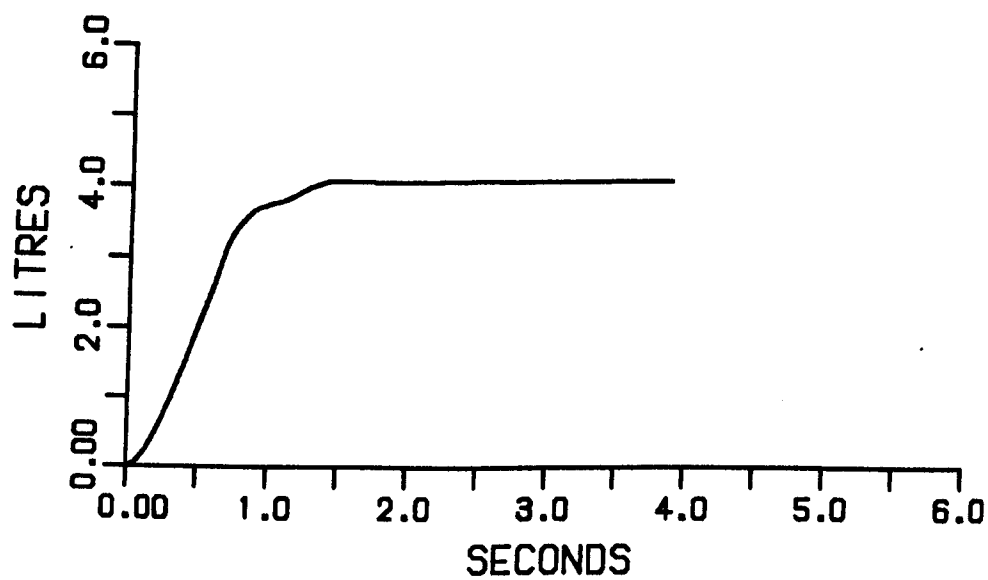
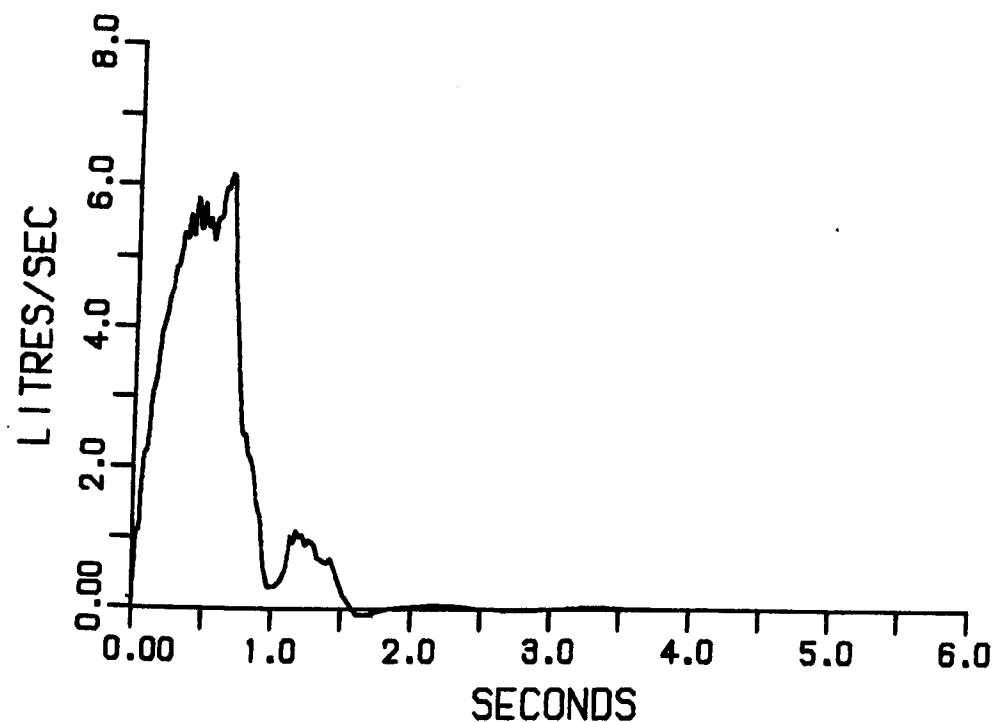


Figure 3.5 Flow and volume profiles from brass calibrating spirometer.

half-way through the profile and minimised any resonance that might be set up in the pump by generating peak flow instantly at the start of the profile. Using this profile with the air in the pump heated to any specified temperature and saturated with water vapour, a known volume (5.6 L) could be discharged through the PT (PFR = 6.5 L/s) and a calibration factor calculated as above. This method of calibration was just as reproducible as that using the brass spirometer.

The brass spirometer was used to calibrate the PT whenever the PT was used to record subjects because this calibration was quicker to perform. Calibration with the pump was used for those experiments designed to assess the effect of temperature on recording spirograms because the calibration then was using the device subsequently used for the experiment. The calibrations with the pump were slightly more tedious to perform because of the longer time taken for the pump to reach the correct temperature and because of the necessity to measure the piston's displacement optically. This latter problem has been solved subsequent to the completion of the experiments and studies in this thesis by using an optical shaft encoder within the pump.

EFFECT OF GAS TEMPERATURE ON PT CALIBRATION

To determine the effect of gas temperature on calibration the PT (heated to $40.0 \pm 0.1^{\circ}\text{C}$) was calibrated a) eight times with gas in the pump at ambient 25°C saturated and b) eight times with gas in the pump at 37°C saturated; the resulting calibration factors are shown below .

Table 3.2

<u>a) gas at 25°C</u>	<u>b) gas at 37°C</u>
1. 0.02866	0.03022
2. 0.02871	0.03027
3. 0.02866	0.03026
4. 0.02862	0.03031
5. 0.02862	0.03026
6. 0.02870	0.03026
7. 0.02868	0.03021
8. 0.02867	0.03019
mean 0.02868	mean 0.03023
SD 0.00003	SD 0.00005
COV 0.11%	COV 0.18%

At both temperatures the calibrations were highly reproducible.

The difference in calibration factors is for two reasons:

(i) the gas at 25°C is expanded to a greater extent as it is heated to 40°C than is the gas at 37°C so the 25°C calibration factor is smaller. This discrepancy between the two experiments is due to the 12°C difference in start temperature so that the factor, C_E , to correct for this discrepancy is given by

$$C_E = \frac{273 + 37}{273 + 25} = 1.04027$$

(ii) Both gases are recorded at a temperature of 40.0°C (assuming 100% heat efficiency) when dry air has a viscosity of 192.1. However, the gas which was at 25°C has a lower partial water vapour pressure than the gas at 37°C, 24 and 47 mm HG respectively. The corrected viscosities are therefore 187.9 for the gas which was at 25°C and 185.2 for that which was at 37°C. This effect also makes the 25°C

calibration factor smaller than that for 37°C. The factor, C_V , to correct for the viscosity difference is given by

$$C_V = \frac{187.9}{185.2} = 1.01458$$

Therefore the total correction factor, C_T , is given by

$$C_T = C_E \times C_V = 1.04027 \times 1.01458 = 1.05544$$

The observed relationship between the calibration factors at 25°C

$$\text{and } 37^\circ\text{C} = \frac{0.03023}{0.02868} = 1.05404$$

Hence the known changes occurring due to gas expansion and

different gas viscosity explain to within the tolerance of measurement

the observed difference between the calibration factors. Mouth air temperature is thought to be about 33°C (56, 57),

and it can be computed that the relationship between the calibration

factors obtained with gas at 25°C and with gas at 33°C should be

1.03590. Hence calibrating with room air at 25°C would lead to

a 3.6% underestimate of expired flow and volume; if, erroneously,

a standard correction factor from ATPS (25°C) to BTPS is used (1.075)

this will lead to a 3.8% overestimate.

It is evident from the above experiments and reasoning that errors can easily be incurred during the calibration of pneumotachographs.

A further small error arises since alveolar air has a composition and viscosity different from room air, 183 and 186 micropoises respectively at 40°C saturated, but this error is generally ignored.

When using the brass spirometer for a series of calibrations with the water at 25°C and then at 37°C the mean calibration factors from 8 calibrations were 0.02847 (± 0.00006) and

- 64 -

0.02945 (\pm 0.00003) respectively. The calibration factor for 25°C gas is comparable to that achieved with the pump. The calibration factor with the water at 37°C is lower than that found using the pump. The recorded calibration factor is appropriate for a gas temperature of 32 - 33°C, which is closer to mouth temperature. This lower gas temperature arises because of the inefficient heating of the gas within the spirometer which, unlike the pump, does not have an internal fan.

Therefore for clinical use in recording spiograms the brass spirometer was found to be a satisfactory method for calibrating the PT with gas approximately at mouth temperature. Using a calibration factor derived in this way to convert the bit values achieved from the linearity experiment into real flows gives an estimate of the overall error using the PT. These errors are expressed graphically in figure 3.6. The maximal percentage error was 3.4% at 1.0 L/s (absolute error = 0.03 L/s) and the maximal absolute error was 0.08 L/s at 7 L/s (percent error = 1.2%). The results are better than the standards set for flow meters (51).

When using this method for calibration and recording an MFEM the flows and volumes recorded are being standardised to mouth temperature and not to 37°C. This represents a break from convention. When measuring static lung volumes it seems reasonable to adjust the recorded volumes to 37°C which is the assumed temperature of the gas resident within the lungs during tidal breathing. During an MFEM, which follows shortly after a maximal inspiratory manoeuvre, this assumption is less likely to be valid and measurement of flows and

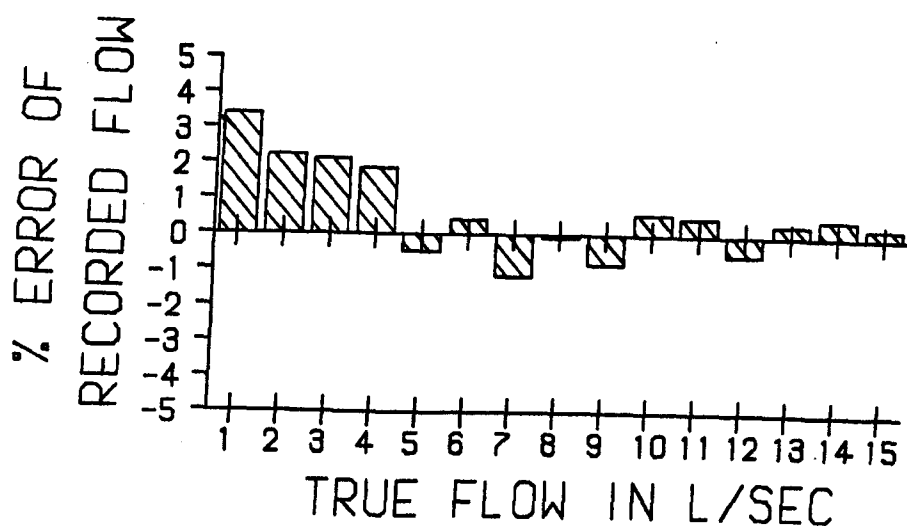


Figure 3.6 Percentage error of pneumotachograph flow reading.

volumes in relation to mouth temperature seems more sensible.

Further investigation of this point would be desirable but is outside the scope of this thesis.

The points outlined above about the effect of temperature and viscosity on pneumotachographs are not new ⁽⁵⁹⁾ but they have not always been fully appreciated when these devices are used. The confused thinking on these effects was demonstrated by Von der Hardt and Zywiets ⁽⁶⁰⁾ who erroneously concluded in their equation 11 that the effect of temperature on viscosity and on gas expansion partially compensated for each other; whereas for a given flow into a heated PT the pressure drop across the screen is increased by the rise in viscosity with rise in temperature and is further increased by the acceleration of the gas within the PT as it is heated. Also it has been suggested ⁽⁶¹⁾ that a simple BTPS correction factor can be used if a PT is calibrated with dry room air and this is evidently not a valid procedure.

^C CHOICE OF RECORDING DEVICE

If the object of this thesis is to evaluate methods of spirogram analysis it might seem reasonable that the spiograms, which are a representation of expired volume against time, should be recorded with an appropriate volume measuring device such as a spirometer. It has long been accepted that spirometric data such as FVC and FEV₁ need to be corrected from the ambient temperature and pressure saturated (ATPS) of the spirometer to the body temperature and pressure saturated (BTPS) prevailing in the lungs prior to expiration.

However, this assumes that the spirometer or recording device has a very short thermal time constant in relation to the time constant of the maximal forced expiratory manoeuvre (MFEM). If this assumption is incorrect then errors will arise if BTPS correction is used leading to an overestimate of the expiratory volume. These errors should not occur if expired volume is derived by integrating the output of a heated pneumotachograph as the flow will be recorded at constant temperature.

As non-instantaneous cooling of gas within spirometers will distort the shape of spirograms the effect of this cooling will be most marked on indices sensitive to this shape i. e. the first moment of the spirogram α_1 and the moment ratio ($MR = \sqrt{\alpha_2 / \alpha_1}$)

It was therefore necessary to measure the magnitude of the errors due to this cooling in spirometers and compare them with the errors due to the known non-linearity of pneumotachographs.

(i) Effect of air temperature

In order to test the RSS, WSS and PT under the same conditions we used the pump to deliver identical volume profiles to each device at the same ambient temperature, first with the air in the pump at ambient and then with the air in the pump at 37°C saturated. The volume profile used was a single exponential function of the form

$$v = 1 - e^{-t/D}$$

where v is the volume delivered by time t and D is the time constant.

In the first experiments the time constant used was 0.8 s which is in the middle of the range encountered in normal spiograms. This exponential function was preceded by a brief geometrically increasing volume-time run-in so that peak flow was achieved 120 ms after the start of the profile. The resulting profile was an improvement for three reasons (i) the profile was more akin to the actual spiogram, (ii) the inertia of the pulley system by the WSS was no longer exceeded at peak flow and (iii) an artefact due to resonance in the pump was reduced.

When each device was tested with this volume profile with air at ambient and then at 37°C the resulting recorded spiogram was stored in computer memory as was the original computer derived exponential function which drove the pump. For both the recorded and original 'spiogram' back extrapolation was performed to find new time zero ⁽³⁷⁾ and the ten spirometric indices in the table 3.3 below were computed. The results for the WSS and RSS were corrected to BTPS and the original and recorded results were then compared and the percentage error in the recorded result calculated.

Table 3.3

Table of the ten variables derived from each recording and their true values for the two time constants used

	Time constant 0.8 s	Time constant 2.4 s
FVC	5.60 L	4.92 L
FEV ₁	3.99 L	1.74 L
FEV _{0.5}	2.59 L	0.96 L
PFR	6.30 L/s	2.25 L/s
FEF _{50%}	3.50 L/s	1.13 L/s
FEF _{75%}	1.75 L/s	0.58 L/s
FMF	3.19 L/s	1.02 L/s
FEF _{75-85%}	1.37 L/s	0.48 L/s
α_1	0.80 s	2.10 s
MR	1.41	1.32

Figure 3.7a shows the percentage error for each device for each index when tested with the air in the pump and ambient temperature at 19°C and figure 3.7b shows the percentage error when the air in the pump was at 37°C saturated and ambient at 19°C.

When tested with ambient air the three devices record the specified volumes with satisfactory precision. Instantaneous flows from spirometers are known to be noisy and the peak flow is consistently slightly overestimated due to the resonance in the pump. The RSS was not as precise as the WSS for the flow measures and this perhaps relates to the slightly variable resistance offered by the rolling seal over its 10 L range. For all these experiments the RSS was always tested over the same part of its range so that these errors were constant.

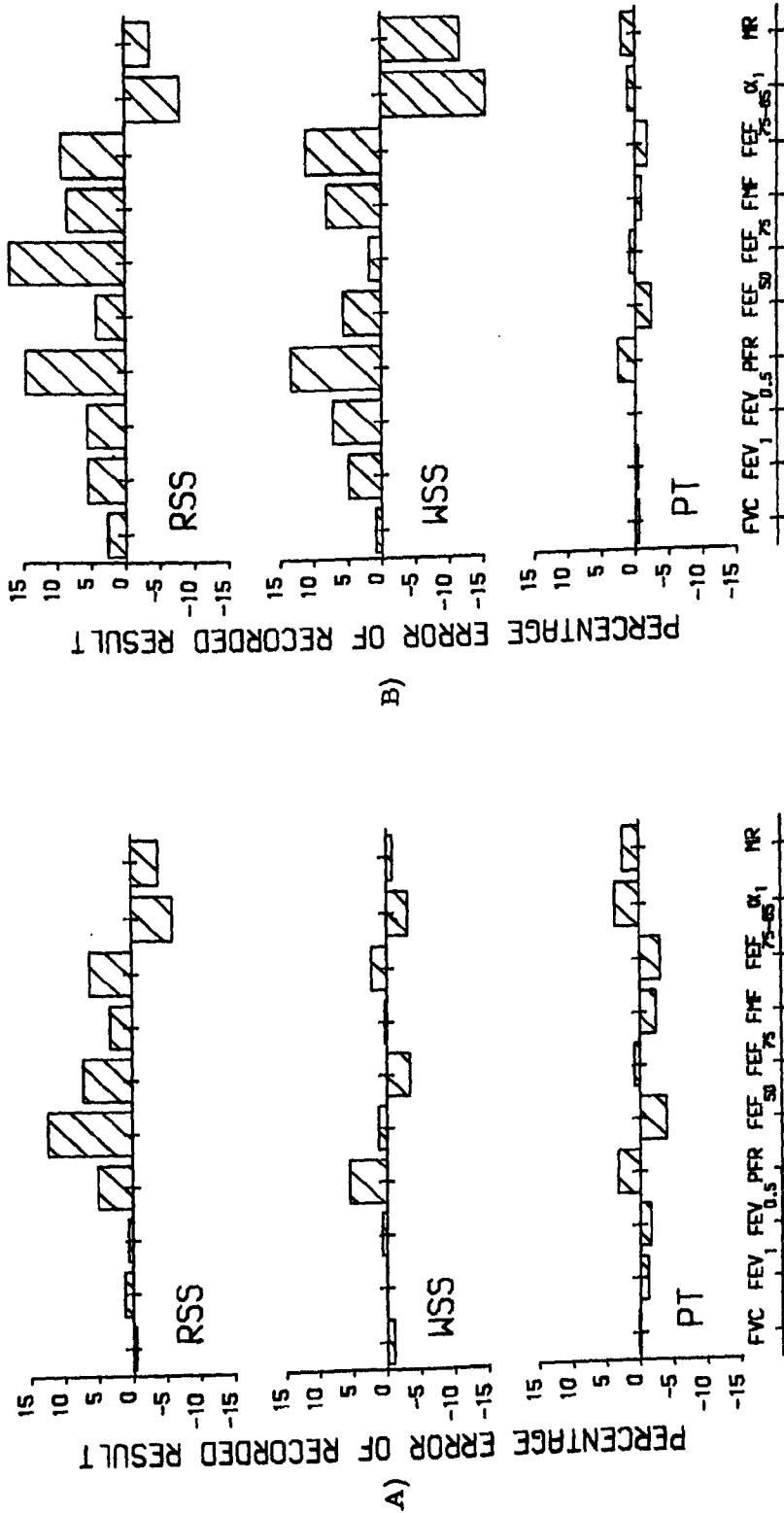


Figure 3.7

Percent recording error for pneumotachograph (PT), water sealed spirometer (WSS) and rolling seal spirometer (RSS)
 A) pump and ambient temperature at 19°C
 B) pump at 37°C, ambient at 19°C, RSS and WSS results corrected to BTPS

From figure 3.7b it is evident that substantial errors result when using the WSS and RSS due to non-instantaneous cooling and that the PT response is unchanged. The PT has to be calibrated with gas at the testing temperature so the response should be consistent. The maximal error observed was for α_1 and MR with the WSS at -16% and -14% respectively.

The experiments were repeated with the WSS and the PT at higher ambient temperature of 21°C and then 23°C to assess how the errors depended on ambient temperature. The percent and absolute error for 3 spirometric indices for the WSS and PT with changes in ambient temperature are shown below. (Time constant of signal = 0.8 s, test gas = air at 37°C saturated, FEV₁ for WSS corrected to BTPS).

	19°C	<u>Table 3.4</u>		<u>PT</u>	
		<u>WSS</u> 21°C	23°C	19°C	23°C
FEV ₁ %	+5	+4	+4	0	1
ml	188	169	156	-14	30
α_1 %	-16	-15	-13	1	-1
s	-0.13	0.12	0.10	0.01	-0.01
MR%	-14	-13	-10	2	1
	-0.21	-0.18	-0.14	0.03	0.01

As expected the errors reduce with higher ambient temperature. If one considers the absolute errors for α_1 with a true value of 0.802 and recorded values of 0.671, 0.682 and 0.698 for 19°C, 21°C and 23°C ambient respectively, they are in rough proportion to give zero error at 38°C ambient. Given the precision of the measurements of temperature this is a satisfactory confirmatory result.

(ii) Effect of time constant of signal

If the errors demonstrated in the previous section were only related to ambient temperature for a given spirometer then they could be corrected fairly readily. However, the errors should also depend on the relationship between the time constant of cooling for the spirometer and the time constant of the spirogram. Hence the errors incurred by BTPS correction would be maximal if the cooling time constant were long in relation to the time constant of the spirogram and minimal if this relation were reversed.

To test the influence of this relationship the previous experiments were repeated using the WSS and PT with ambient temperature at 23°C and with a 2.4 s time constant signal. The percentage and absolute error of 3 spirometric indices for the WSS and the PT with changes in time constant of signal are shown below. (Ambient temperature = 23°C, test gas = air at 37°C saturated, FEV₁ for WSS corrected to BTPS)

<u>Table 3.5</u>				
	<u>WSS</u>		<u>PT</u>	
	0.8 s	2.4 s	0.8 s	2.4 s
FEV ₁ %	4	5	1	3
ml	160	91	30	49
α ₁ %	-13	-4	-1	-2
s	-0.10	-0.09	-0.01	-0.04
MR%	-10	1	1	0
	-0.14	0.01	0.01	0.0

The errors using the WSS are substantially reduced with the longer time constant, as expected. The errors using the PT are increased with the 2.4 s time constant signal but for FEV₁ and FVC they are still within accepted guidelines⁽⁵¹⁾. The reason for this

increase in error is that with the 2.4 s time constant signal all the flows fall within that range which our PT and calibration procedure, slightly overestimate (figure 3.6). - 73 -

(iii) Effect of connecting tubing

The length of tubing leading to a spirometer has been found to influence the spirometer's cooling characteristics⁽⁴¹⁾. For practical reasons in the previous experiments the RSS was connected to the pump by 50 cm plastic tubing (internal diameter 28 mm) and the WSS was connected by 15 cm of this tubing. In order to assess whether the length of tubing influenced the magnitude of the errors the WSS was tested with a 0.8 s time constant single exponential volume profile using air at 37°C saturated and constant ambient temperature of 21°C first with 15 cm and then 50 cm of this tubing.

Using 15 cm of tubing the errors for FEV_1 , α_1 and MR were +4%, -15% and -13% respectively, which reduced to +3%, -14% and -10% respectively when 50 cm of connecting tube was used.

DISCUSSION

Hitherto the MFEM has usually been recorded using either a WSS or RSS. Previous testing of these devices with ambient air and single exponential volume profiles has demonstrated their linearity and precision.⁽⁴¹⁾ The experiments presented here demonstrate that despite their linearity the distortion of spirograms due to non-instantaneous cooling produces substantial errors which are far greater than those incurred by the non-linearity of a heated PT.

Previous workers have appreciated the problem of non-instantaneous cooling in spirometers^(42 - 45). Some workers have demonstrated errors using human subjects to generate spirograms^(44, 45). The errors found by Perks et al⁽⁴⁴⁾ included errors due to within person variability and possible errors due to the effect of the extreme ambient temperatures used on the recording device. Tashkin et al⁽⁴⁵⁾ recorded subjects through a PT and then into a WSS in series with the PT and found errors with the WSS of 6% in FEV₁ and 10% in FEF₇₅₋₈₅ at an unspecified ambient temperature.⁽⁴¹⁾ These errors are similar to those presented here. Gardner et al⁽⁴¹⁾ using a waveform generator found that temperature effects might cause a maximal overestimate of 3% in FEV₁ using a BTPS correction with a WSS or RSS. However, they were not explicit about the ambient temperature or how the experiment was conducted. Interestingly, their estimates of the time constant of cooling for a Stead-Wells spirometer was 1.4 s with single tubing and 0.9 s with double connecting tubing. These are of the order to produce pronounced effects on the recording of spiograms.

Of the two spirometers tested in this study the RSS was not as good as the WSS when tested with ambient air but it was not so affected by cooling errors. The experiments with the WSS and different lengths of tubing showed that this factor could not explain the difference found between the WSS and RSS.

The conclusions drawn from these experiments are that, contrary to current practice, an MFEM should be recorded with a heated PT in order to obtain maximum recording fidelity. The technical demands for using a PT may be deemed excessive for routine clinical purposes and the errors found in conventional indices when using spirometers are not likely to produce errors in clinical decisions. However, for research procedures and especially for any work involving the moments of the spirogram or description of the shape of spiograms and flow-volume curves the use of a PT is necessary.

PROCEDURE FOR RECORDING A SPIROGRAM

The following computer controlled routine is carried out when an MFEM of a subject is recorded using the heated PT.

Prior to the start of the MFEM the signal from the pressure transducer of the PT is sampled every 4 ms via the A/D converter for 100 ms and the average reading for the zero offset is stored in the computer and this zero offset is subsequently always subtracted from the signal reading to give the true reading. The signal is then sampled every 4 ms and recording does not commence until the flow signal exceeds a specified threshold value (150 mls/s). Once this threshold is reached the flow signal is sampled every 4 ms and the flow numerically integrated with respect to time using the trapezoid rule (61) to give expired volume. Instantaneous flow, expired volume and elapsed time are stored in computer memory arrays whenever the volume increment since the last triplet of data was stored exceeds

20 mls or the time increment exceeds 0.1 s whichever occurred the sooner.

In this way the MFEM is stored with frequent sampling when flow is fast and yet with an adequate sampling frequency when flow is low. For an MFEM the recording ceases as soon as flow becomes zero or negative and for a flow volume loop, when the inspiratory flows are required, the recording procedure is terminated manually. The number of data triplets stored in the computer for an MFEM varies from 100 to 350 depending on the subject. From the stored arrays of data back extrapolation is performed from peak flow at constant peak flow to establish a new time zero⁽³⁷⁾ which defines the onset of the blow; all timed events are subsequently referenced to this time zero. The spirogram and flow-volume curve are displayed on a graphics screen and algorithms compute conventional spirometric data from the stored arrays using linear interpolation where necessary.

The integration of flow was checked using a cubic interpolation routine⁽⁶²⁾ in order to estimate the magnitude of error due to using the trapezoid rule rather than a more sophisticated algorithm. The maximum difference throughout the integration was only 8 mls for a blow of 4.5 L and so the trapezoid rule was deemed satisfactory.

MOMENT ANALYSIS OF SPIROGRAMS

INTRODUCTION

It has been proposed that α_1 , the first moment of the spirogram or mean transit time, is a sensitive test of lung function^(28 - 32). Its merits are that it is standardised for lung volume and it is sensitive to the whole spirogram.

Any satisfactory test of lung function should be repeatable within individuals and able to detect true differences between individuals. The moments of the spirogram are dependent on the forced expiratory time (FET) and although it is known that FET is increased by airflow limitation FET has a large within and between subject variation⁽⁶⁴⁾ which limits its usefulness. Therefore, the moments may similarly have limited application.

From Chapter 2 it is evident that the moments can be derived up to any point within the spirogram by halting the integration at the specified point. These truncated moments are standardised by the volume at truncation. Following the theoretical findings presented in Chapter 2 it was necessary to determine if the truncated moments of the spirogram were more repeatable within subjects than those of the full spirogram and to see if the discriminatory ability of the truncated moments was better than those of the full spirogram. Therefore the within subject and between subject variability of the truncated moments over 5 days was assessed in 21 normal subjects.

(i) Subjects

Twenty-one untrained subjects from the hospital and university staff agreed to participate. They comprised 10 men and 11 women of age range 21 to 59 years (mean 35.0, median 29 years) of whom 11 were lifelong non-smokers, 7 were ex-smokers (mean duration 5 years) and 3 current smokers (mean duration 27 years). None had any respiratory symptoms or ~~were~~^{was} on any medication known to influence pulmonary function and none was convalescent from or suffering from a respiratory infection.

(ii) Methods

On the first test day each subject had two test blows to familiarise them with the equipment, then each subject had 5 MFEM recorded on each of five consecutive days. A blow was rejected if time to peak flow exceeded 300 ms or there was a cough during the manoeuvre. Smokers abstained from tobacco for 2 hours prior to testing. The PT was calibrated each day prior to testing and each subject was recorded at approximately the same time on each day.

For each recorded spirogram conventional spirometric indices were derived (PFR, FEV₁, FEV₃, FVC, FMF, FEF_{50%}, FEF_{75%}), the sequential moments were computed and the first two moments (α_1 and α_2) and the moment ratio ($MR = \sqrt{\alpha_2 / \alpha_1}$) were determined after 75%, 80%, 85%, 90%, 95% and 100% of the FVC had been expired.

(iii) Results

Table 4.1

	Group mean	Group min	Group max	Group SD	Mean within-person COV%	B/W
FVC litres	4.52	2.41	7.86	1.22	3.3	58.7
FEV ₁ %	94.4	76.7	100.0	5.0	1.7	8.1
FEV ₁ %	77.5	54.7	93.6	7.7	2.4	14.5
PEFR l/s	9.24	5.41	14.75	2.14	4.1	25.5
FMF l/s	3.64	1.57	6.25	1.01	6.5	17.3
FEF ₂₅₋₇₅ % l/s	3.63	1.21	7.07	1.10	8.6	11.2
FEF ₂₅₋₇₅ % l/s	1.36	0.26	3.40	0.65	12.7	13.4
α_1 75% s	0.319	0.198	0.681	0.088	5.6	15.0
α_1 80% s	0.367	0.219	0.836	0.107	6.1	14.6
α_1 85% s	0.427	0.245	1.031	0.134	6.8	13.2
α_1 90% s	0.507	0.275	1.284	0.172	7.8	11.8
α_1 95% s	0.623	0.310	1.616	0.299	9.3	10.5
α_1 100% s	0.813	0.366	2.093	0.319	10.9	9.4
α_1 75% s ²	0.182	0.056	0.989	0.133	12.8	14.7
α_1 80% s ²	0.256	0.070	1.560	0.209	14.4	13.3
α_1 85% s ²	0.377	0.090	2.488	0.341	16.6	12.0
α_1 90% s ²	0.597	0.114	4.095	0.586	20.4	10.7
α_1 95% s ²	1.060	0.155	7.086	1.086	25.4	9.7
α_1 100% s ²	2.287	0.253	13.279	2.298	29.2	8.3
$\sqrt{\alpha_1/\alpha_1}$ 75%	1.267	1.134	1.461	0.056	1.3	9.2
$\sqrt{\alpha_1/\alpha_1}$ 80%	1.295	1.155	1.509	0.067	1.4	10.2
$\sqrt{\alpha_1/\alpha_1}$ 85%	1.335	1.184	1.552	0.083	1.7	10.6
$\sqrt{\alpha_1/\alpha_1}$ 90%	1.391	1.217	1.663	0.109	2.1	10.3
$\sqrt{\alpha_1/\alpha_1}$ 95%	1.478	1.259	1.923	0.146	2.8	9.6
$\sqrt{\alpha_1/\alpha_1}$ 100%	1.641	1.305	2.184	0.189	4.1	6.5
FET 75% s	1.021	0.505	2.811	0.376	8.8	10.9
FET 80% s	1.278	0.579	3.696	0.519	9.8	10.7
FET 85% s	1.643	0.684	4.978	0.734	11.3	10.1
FET 90% s	2.274	0.841	6.698	1.110	13.6	9.5
FET 95% s	3.392	1.129	9.344	1.763	15.9	8.5
FET 100% s	6.149	1.900	15.172	2.954	17.9	6.1

SD = Standard Deviation
 COV% = Co-efficient of Variation
 B/W = Between subject variance divided by within subject variance

Table 4.1 shows the results for each variable for the group of subjects as a whole. The mean within person co-efficient of variation over the 5 days (i. e. all 25 blows per subject) for each of the computed indices is shown graphically in figure 4.1. All the sequentially derived indices became progressively less repeatable with later truncation. α_1 has tolerably good repeatability especially with early truncation whereas α_2 is less repeatable than FET. MR is highly repeatable and with early truncation is more repeatable than any of the other tests.

To assess whether discriminatory ability was reduced by earlier truncation an analysis of variance was performed on the natural logs of the results. This log transformation was performed in order to standardise the variances as the results showed that for

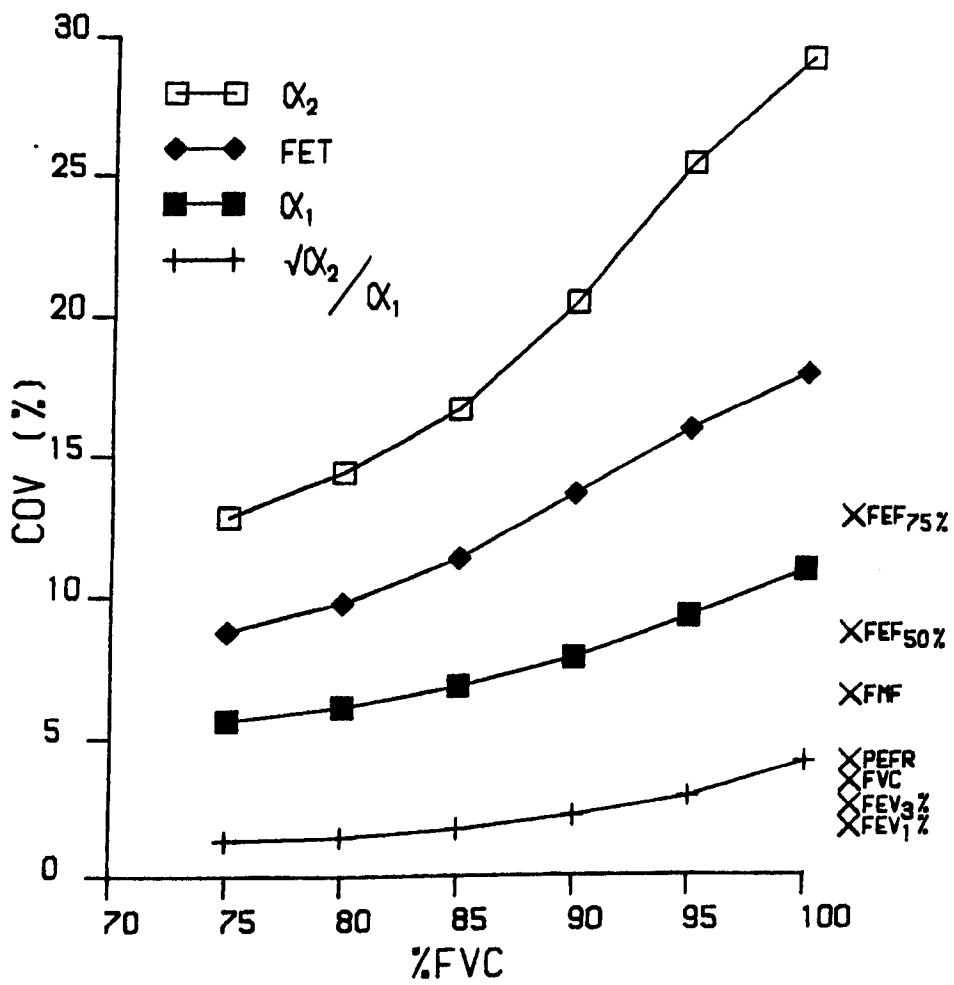


Figure 4.1 Mean within person co-efficient of variation of the sequentially derived spirometric indices.

the majority of the variables the standard deviation was proportional to the mean. For each log variable the mean within subject variance (W) and the between subject variance for the whole group (B) was computed. The ratio B/W is an index of the discriminatory ability of a variable for our group of subjects. The B/W ratio is the same as a signal to noise ratio.

Figure 4.2 shows the B/W ratio for the sequentially derived variables together with that of some of the conventional spirometric indices. The B/W ratio falls with later truncation for all the sequentially derived variables, except that of MR. MR has a maximal B/W ratio at 85% of FVC which falls sharply after 95% FVC.

To determine whether α_1 or MR contained novel information about the spirogram a correlation matrix was derived as shown below.

	FEF 75%	FEV 3%	FEV 1%	MR 100%	α_1 100%	MR 90%	α_1 90%	MR 75%
α_1 75%	-0.25	-0.66	-0.90	0.00	0.78	0.28	0.93	0.57
MR 75%	-0.79	-0.85	-0.80	0.51	0.84	0.85	0.79	
α_1 90%	-0.51	-0.87	-0.94	0.27	0.94	0.59		
MR 90%	-0.86	-0.86	-0.61	0.81	0.79			
α_1 100%	-0.66	-0.97	-0.89	0.57				
MR 100%	-0.64	-0.67	-0.32					
FEV ₁ %	0.57	0.82						
FEV ₃ %	0.72							

Table 4.2

Of note is that α_1 100% has a 0.78 correlation with α_1 75% but retains a -0.89 correlation with FEV₁ % which is almost the same as the correlation of α_1 75% with FEV₁ %. So with later truncation α_1 retains a very high correlation with FEV₁ %. For MR the correlation

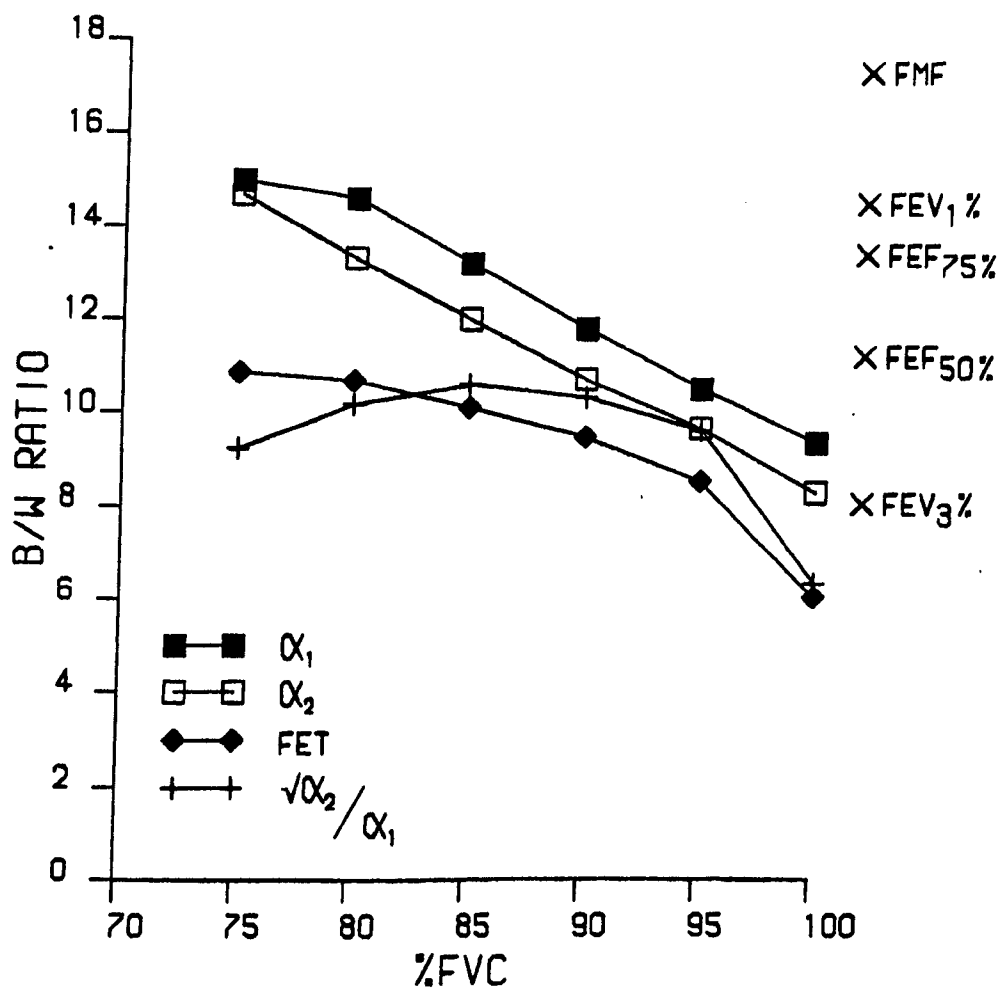


Figure 4.2 Mean discriminatory ability (B/W) of the sequentially derived spirometric indices.

with $FEV_1\%$ progressively falls with later truncation but its correlation with $FEF_{75\%}$ and $FEV_3\%$ is maximal at 90% FVC truncation.

DISCUSSION

These results indicate that the reproducibility and discriminatory ability of the moments are progressively improved by earlier truncation. With MR the reproducibility is improved by earlier truncation but the discriminatory ability shows a peak at 85% FVC. These findings mean that the increased within subject variability of the moments with later truncation is not matched by a commensurate rise in between subject variation. With earlier truncation the moments have a higher degree of reproducibility, and yet an important degree of between subject variability must also be present to account for the higher B/W ratio. For MR the balance seems to be optimal in the region of 85% of FVC expired.

It can be appreciated that the early part of an MFEM does contain discriminatory information by looking at the sequential moments and MR for several individuals. The sequential α_1 , $\sqrt{\alpha_2}$ and MR for a young normal subject, an older normal subject, a young asthmatic and a man with disabling chronic airflow limitation are shown in figures 4.3, 4.4, 4.5 and 4.6 respectively.

It is evident that in each of the 4 subjects the moments and MR are especially sensitive to the terminal part of the MFEM. However, earlier within the manoeuvre, differences between the subjects are still evident, albeit less dramatically. If all the valuable information

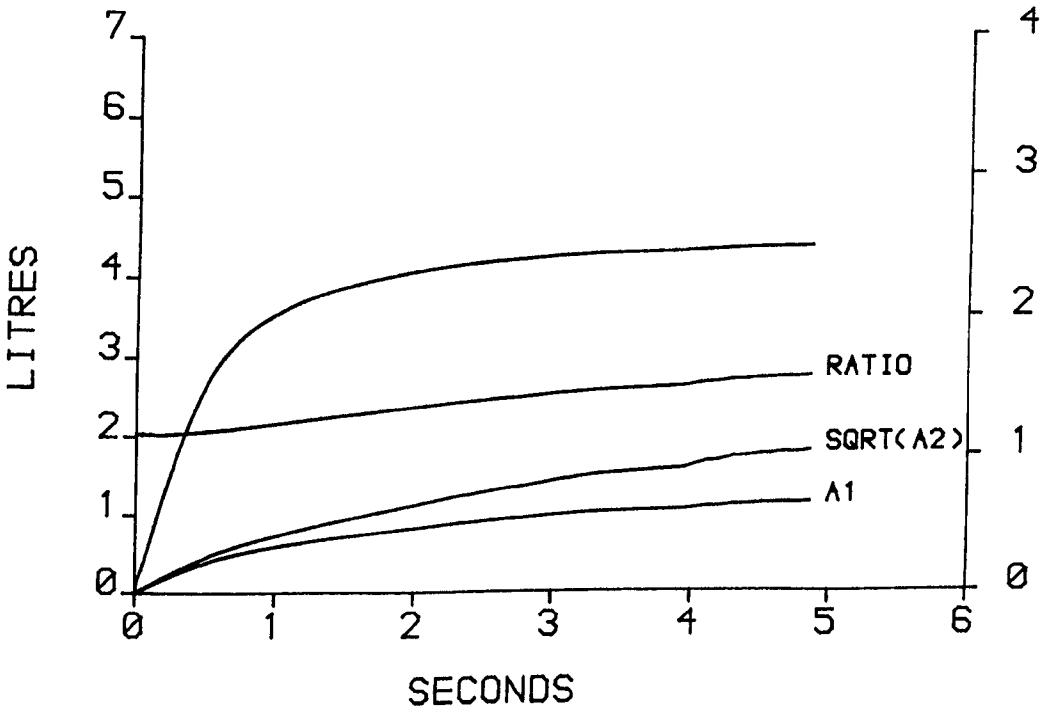
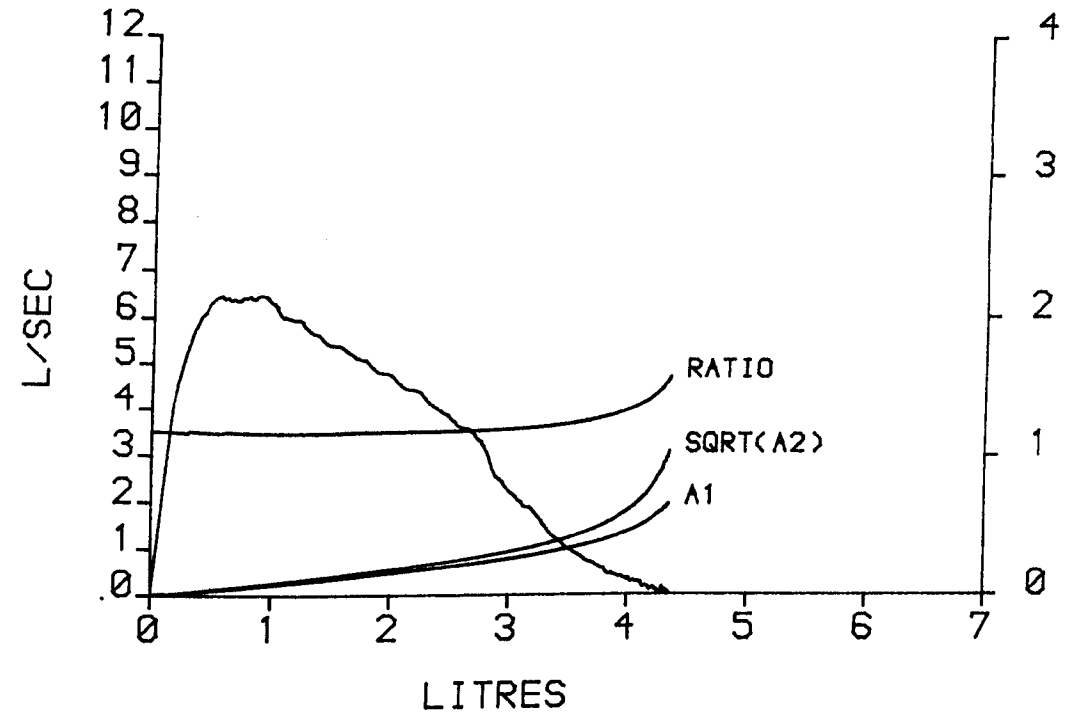


Figure 4.3 The sequential moments and moment ratio for a normal subject, aged 23, height 1.59m , plotted with the right hand ordinate scale.

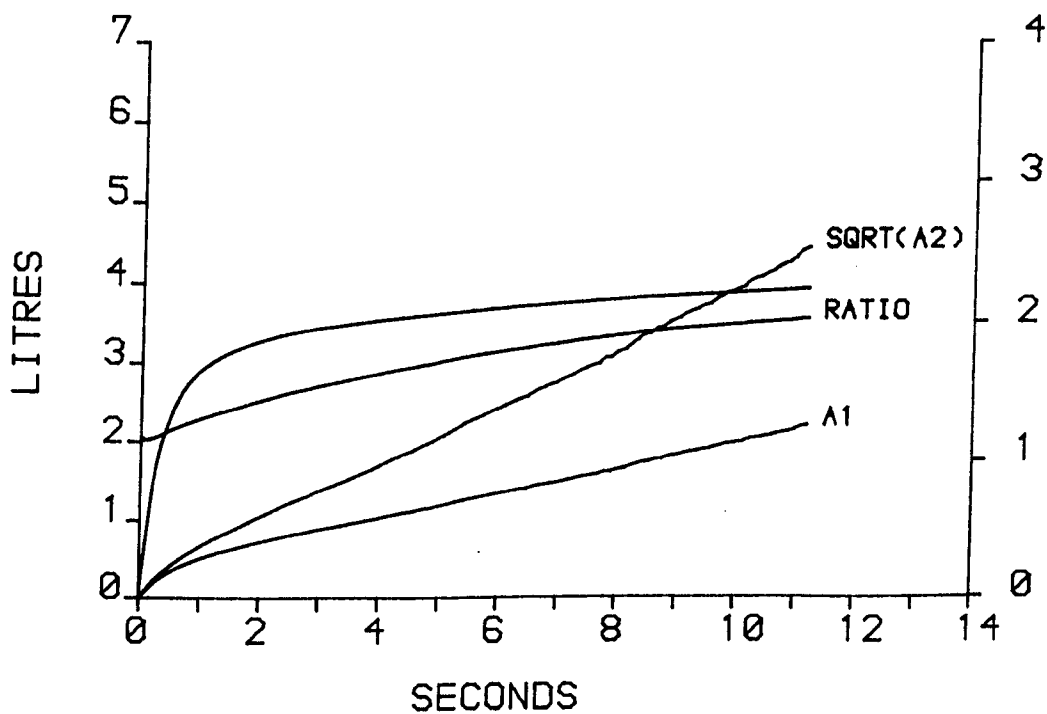
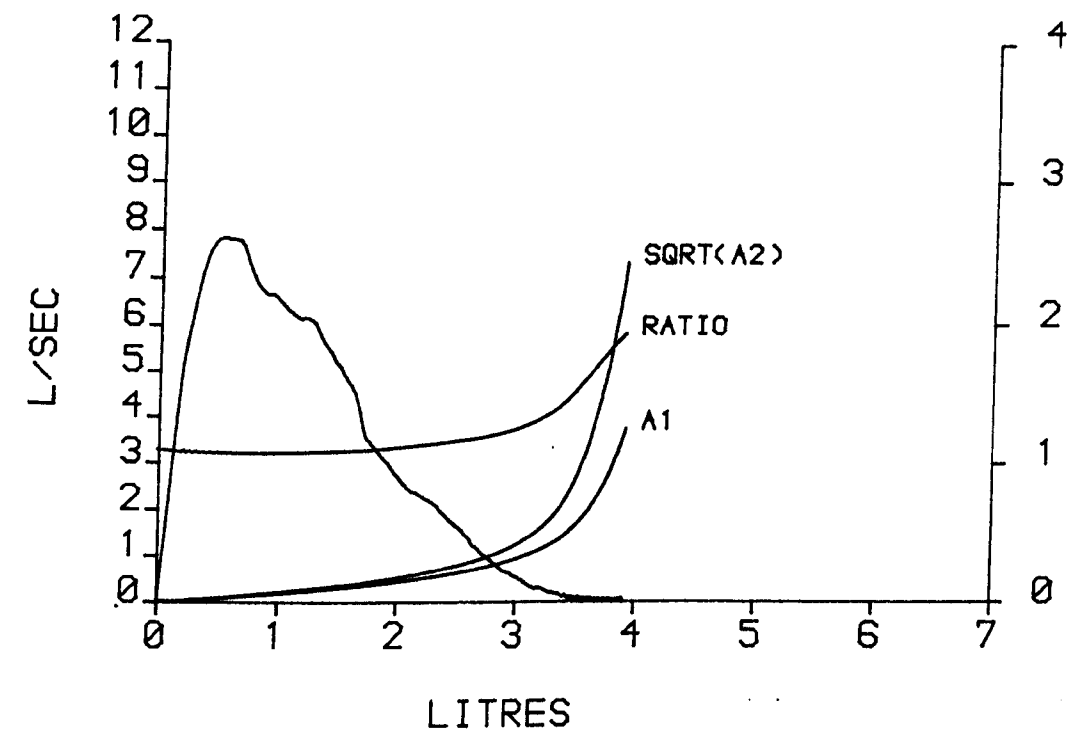


Figure 4.4 The sequential moments and moment ratio for a normal woman, aged 52, height 1.65m, plotted with the right hand ordinate scale.

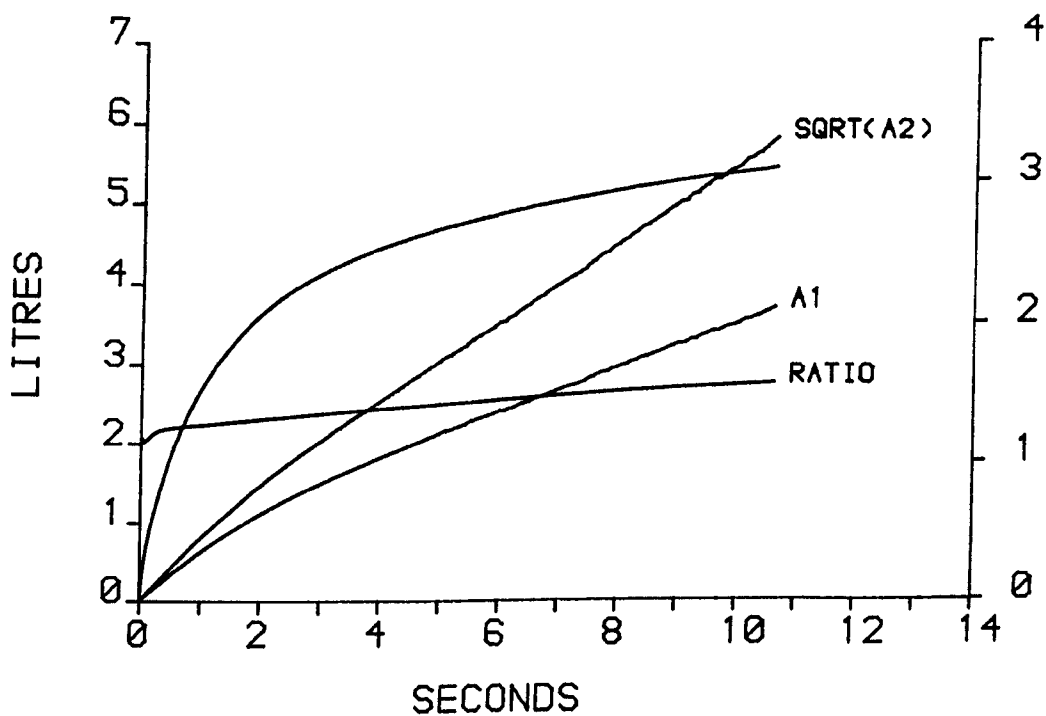
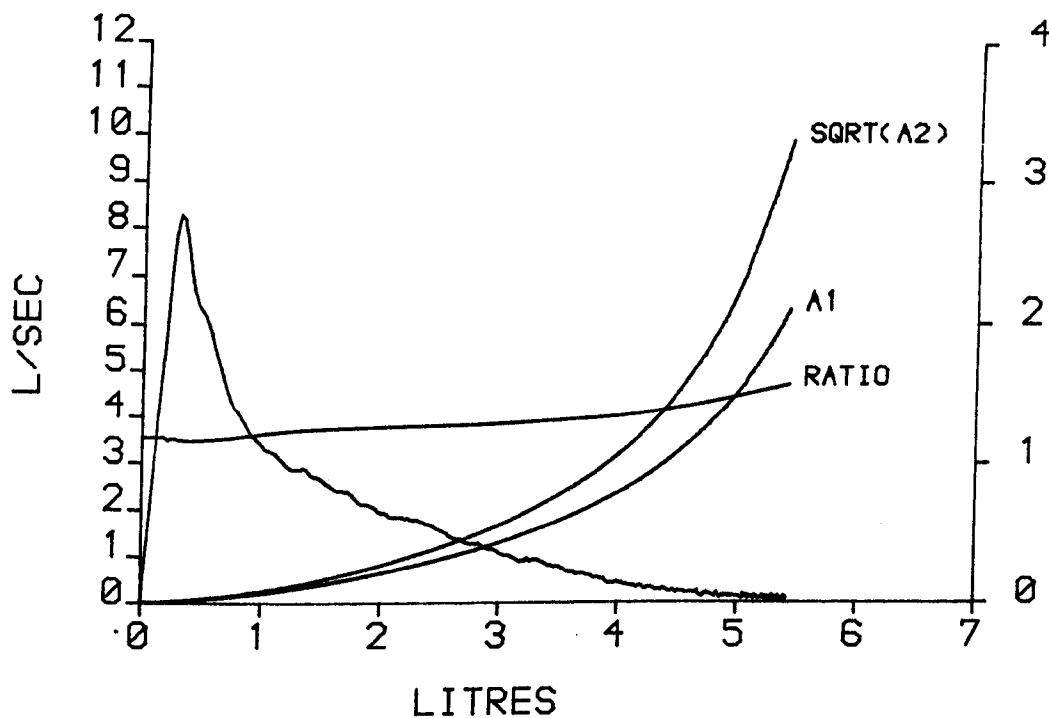


Figure 4.5 The sequential moments and moment ratio for a stable asthmatic man, aged 23, height 1.79 m, plotted with the right hand ordinate scale.

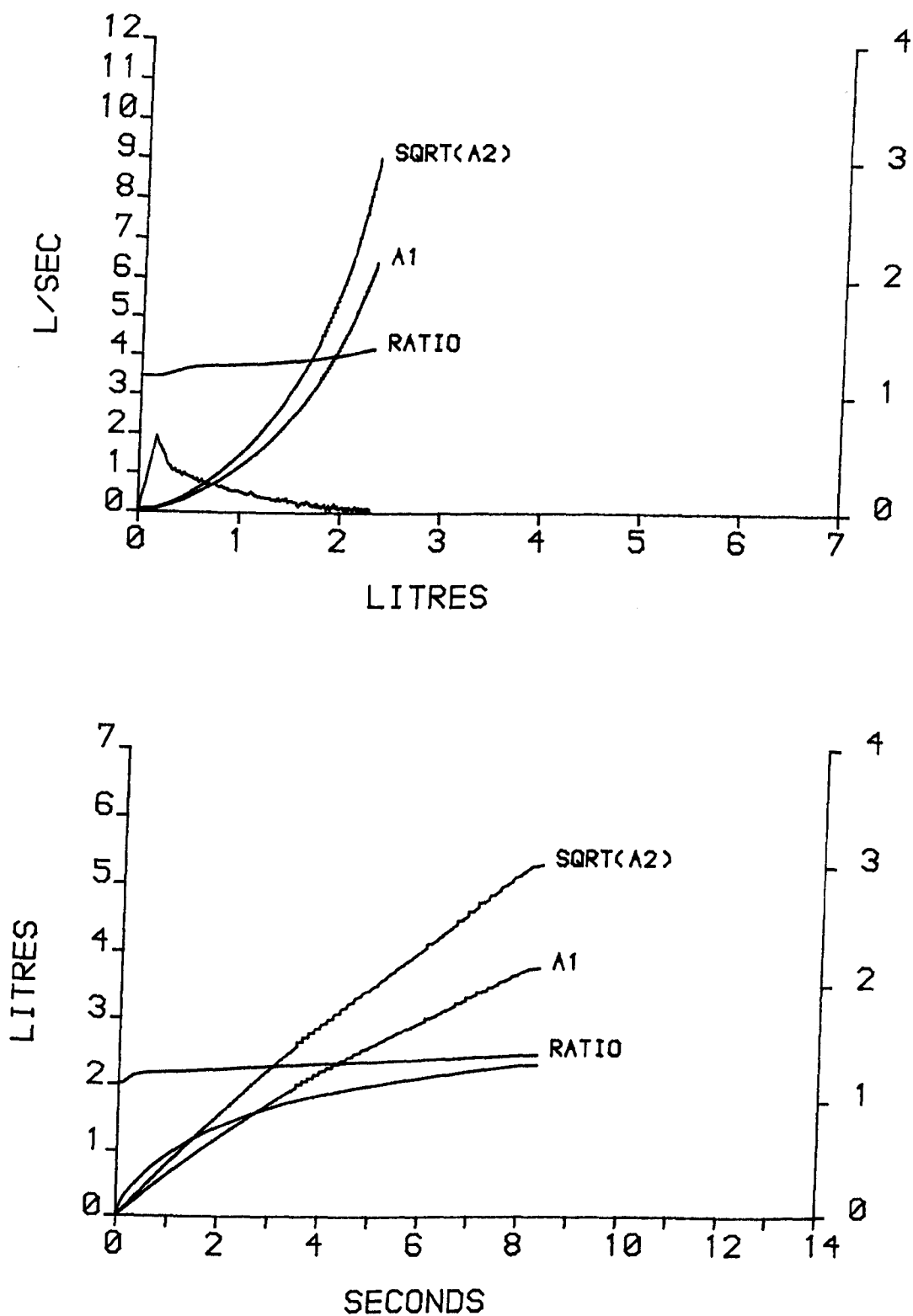


Figure 4.6 The sequential moments and moment ratio for a man with chronic obstructive lung disease, aged 53, height 1.85m, plotted with the right hand ordinate scale.

from an MFEM was contained in the last 5% in volume then moment analysis of spirograms would probably be as unhelpful as FET because of the poor reproducibility, in the time domain, of the end of an MFEM. Fortunately the slow emptying areas of the lungs do not solely express themselves during the end of an MFEM. They contribute throughout the manoeuvre and the proportion their contribution makes to the total contribution from the lungs at any instant is small early in the manoeuvre and large towards the end. Therefore with earlier truncation, to reduce inevitable truncation errors and to improve reproducibility, it may still be possible to detect the presence of areas in the lungs which are emptying slowly.

From figure 4.2 it can be seen that the discriminatory ability of the moments and MR in the group of subjects tested was comparable to conventional spirometric indices such as $FEV_1\%$, $FEF_{75\%}$, $FEF_{50\%}$ and $FEV_3\%$, and was inferior to that of FMF. This may have reflected special aspects of the differences within the group of subjects which may not be common to all subjects tested. Also the flow indices have been found to be dependent on age and size (63) whereas the moments and MR are volume standardised, unlike the flow indices, and the effect of age on the moments and MR was not yet determined. So at this stage it was not possible to draw any conclusions from the comparison of the B/W ratio of the moments and MR with conventional indices.

CHAPTER 5

A MULTI EXPONENTIAL MODEL OF THE FORCED EXPIRATORY SPIROGRAM

INTRODUCTION

The limitation of moment analysis of the spirogram is that the inevitable truncation of recorded spirograms means that the recorded α_1 is an unknown underestimate of the α_1 which would be achieved if the spirogram was perfectly asymptotic and continued to infinite time. It is not possible to predict what α_1 would be at infinite time without making certain assumptions. (65) Jordanoglou et al have proposed that the recorded α_1 should be adjusted by multiplying by the ratio of predicted FVC divided by recorded FVC. However, this ratio has no bearing whatsoever on the degree of truncation. A subject with a restrictive ventilatory defect may have a recorded FVC half that predicted and yet the spirogram may have no truncation, i. e. it is perfectly asymptotic. Conversely an asthmatic subject might have marked truncation of the spirogram but with a proportionately smaller difference between predicted and observed FVC. The manipulation proposed by Jordanoglou is clearly wrong and unhelpful.

Prompted by the problems of truncation Permutt and Menkes (39) proposed a mathematical model of the forced expiratory spirogram (FES) which made assumptions as to how a spirogram would continue to infinite time and could give an estimate of TTV and the moments at infinite time.

A model which describes an observed event has several attractions. If the model is based on known factors which influence the event, the

manner and magnitude of the influence of each factor on the event can be determined and also hitherto unknown influences may become apparent. Several approaches along these lines have been attempted.

Fry⁽⁶⁶⁾ derived a complicated mathematical model to explain the mechanical behaviour and flow characteristics of an arborized conduit system carrying gas from alveoli to trachea. The model was unwieldy with 45 parameters, the majority of which could not be verified experimentally. More recently Lambert, Hyatt and others⁽⁶⁷⁾ have proposed a model for determining maximal flow from the lungs but many aspects of their model were not open to experimental confirmation and like Fry's model it was not suitable for complete description of the maximal forced expiratory manoeuvre. Clement and Van de Woestijne⁽⁶⁸⁾ tried to fit the effort independent portion of the maximal expiratory flow volume curve by various equations relating flow to driving pressure, resistance and lung volume. Their simplest model relating flow linearly with volume could not fit a curvilinear flow volume curve. When their more complicated models, which could account for curvilinearity, were applied to real flow volume curves, they yielded solutions for the parameters of the model which were not physically interpretable e. g. negative resistances.

Permutt and Menkes⁽³⁹⁾ adopted an alternative approach by considering the spirogram in the time domain and deriving an empirical model based on the observation made many years earlier⁽⁶⁹⁾ that a spirogram approximates to a single exponential. They proposed a model which allowed for non-uniformity of lung emptying by invoking a distribution of time constants for lung emptying. Such a model does

not allow an easy interpretation in terms of the mechanics of emptying but it may have merit by reducing the vast amount of information from a spirogram into essentially two indices. There are a limitless number of spot indices that can be derived from a maximal forced expiratory manoeuvre which are all related to one another to a certain extent and the condensation of data by the model may lead to a better understanding of influences on the manoeuvre. Furthermore, because a spirogram is another way of presenting the information contained in an MEFV curve the model offers descriptors of the shape of MFEV curves.

THE MODEL

In this thesis the model first proposed by Permutt and Menkes has been studied and this model comprises a mixture of an infinite number of single exponentials of the form $V = 1 - e^{-t/D}$ (where V is the volume expired by time t and D is the time constant) whose time constants are lognormally distributed. μ , the mean of the log of the time constants, and σ , the standard deviation of the time constants, describe this distribution and from them theoretical spiograms can be constructed. Figure 5.1 shows theoretical spiograms with constant μ and increasing σ . It can be seen that increasing the dispersion of time constants (σ) is associated with a flattening of the tail of the spiogram relative to the beginning. Figure 5.2 shows theoretical spiograms with constant σ and increasing μ . Lengthening all the time constants with no change in dispersion results in a dramatic fall in FEV_1 with no flattening of the tail of the spiogram relative to the beginning.

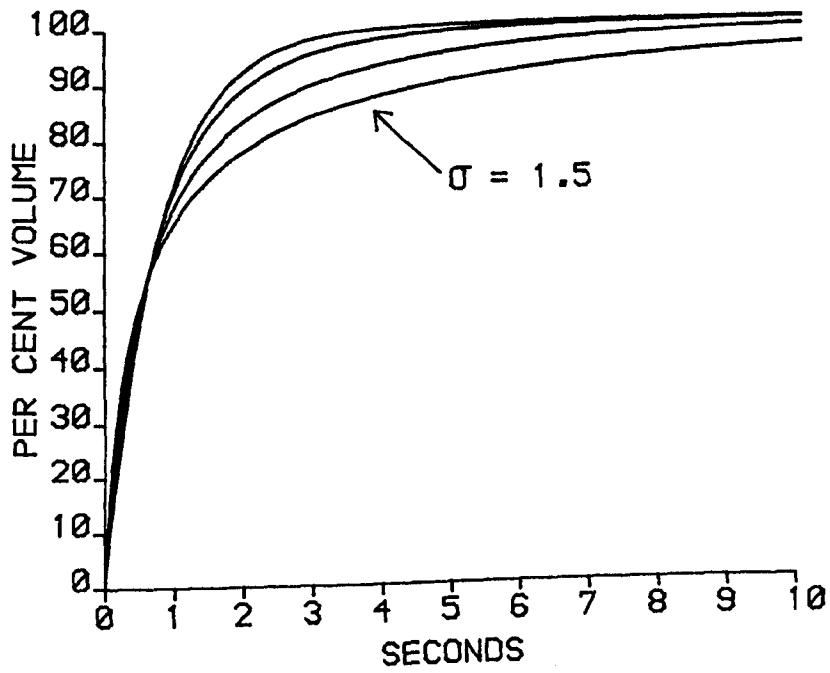
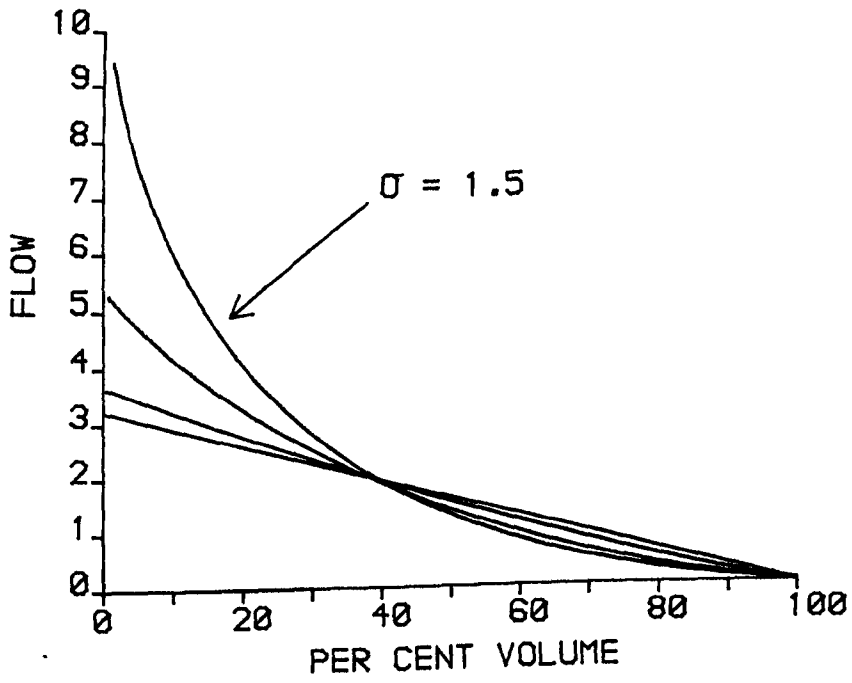


Figure 5.1 Theoretical spiograms and flow-volume curves with constant μ and sigma of 0.0, 0.5, 1.0 and 1.5.

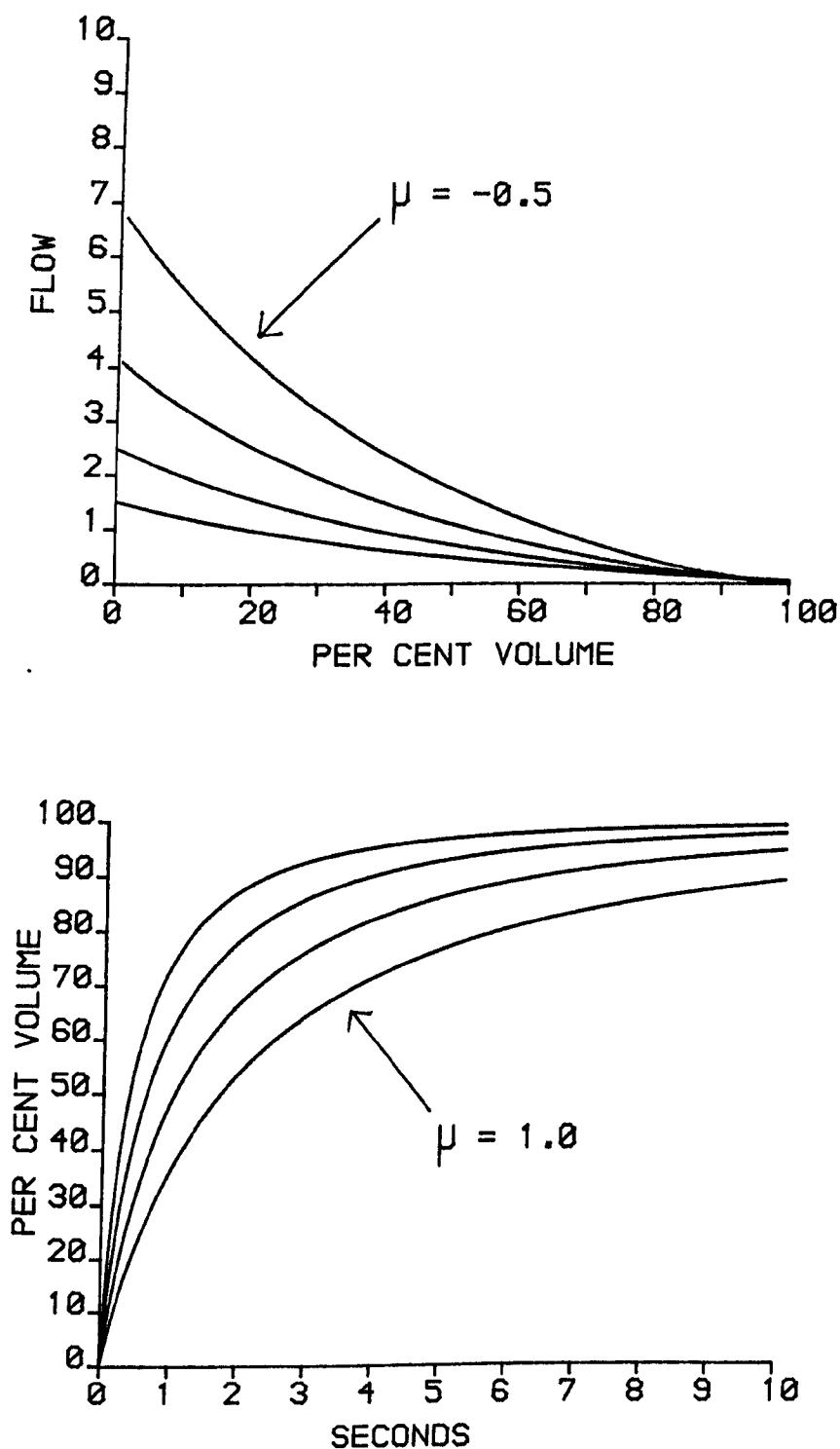


Figure 5.2 Theoretical spiograms and flow-volume curves with constant sigma and mu of -0.5, 0.0, 0.5 and 1.0.

The mathematical derivation of the model is expressed fully in Appendix B. However, two points should be emphasised. Firstly, when the model is applied to describe real spiograms it does not demand that the expression of gas from anatomically small units of the lungs should necessarily be exponential in form. The model is applied to fit the expression of gas from the mouth without reference to where within the lungs the gas comes from. For example, if a spiogram could be perfectly described by a mixture of two exponentials of time constants C_1 and C_2 then there is no constraint that the time constant C_1 necessarily represents the performance of one lung and C_2 represents the other lung. Secondly, because the model is defined in the time domain it implicitly can take truncation into account thus overcoming the limitations of using the moments and moment ratio to describe the spiogram.

The lognormal distribution disperses with a proportionately greater increase in the long time constants than the short time constants and this smaller increase in short time constants can be seen in figure 5.1 as a rise in peak flow with increase in sigma. A normal distribution would not be satisfactory since with increasing dispersion the short time constants would increase in the same proportion as the long time constants; Permutt and Menkes tried a normal distribution and were unable to fit
(39)
spiometric data. Ideally one would like a distribution which disperses in one direction only, but there is no such distribution. The only other suitable distribution, that is one which disperses with greater increase in the proportion of long time constants, is the inverse gaussian distribution but the parameters describing this distribution are not familiar and are cumbersome. Therefore in this thesis the lognormal distribution was used.

FITTING THE MODEL TO SPIROGRAMS

In order to fit the model to real spirograms an algorithm was derived which when supplied with the observed first and second moments of a real spirogram at a specified time could solve for the indices of the model.

(i) The Algorithm

The algorithm used an iterative optimisation routine following a modified method due to Marquardt⁽⁷⁰⁾. For given start values of mu and sigma at the specified time t the first and second moments were computed αC_1 , αC_2 and compared with the original recorded moments αO_1 and αO_2 . The sum of the square of the discrepancies between the original and computed moments can be considered as a residual R where

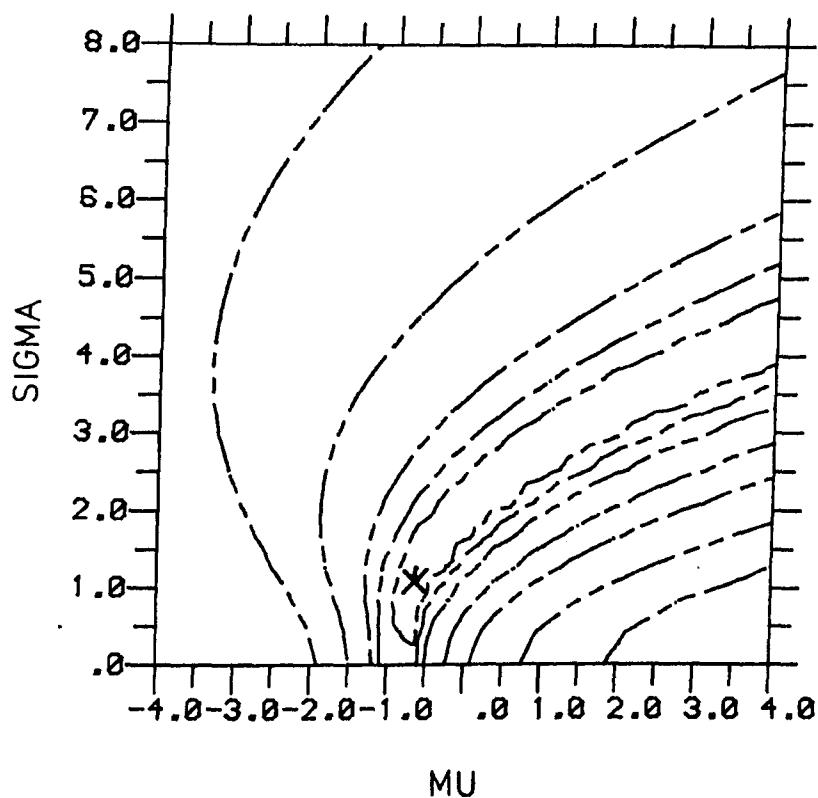
$$R_1 = \alpha O_1 - \alpha C_1$$

$$R_2 = \alpha O_2 - \alpha C_2$$

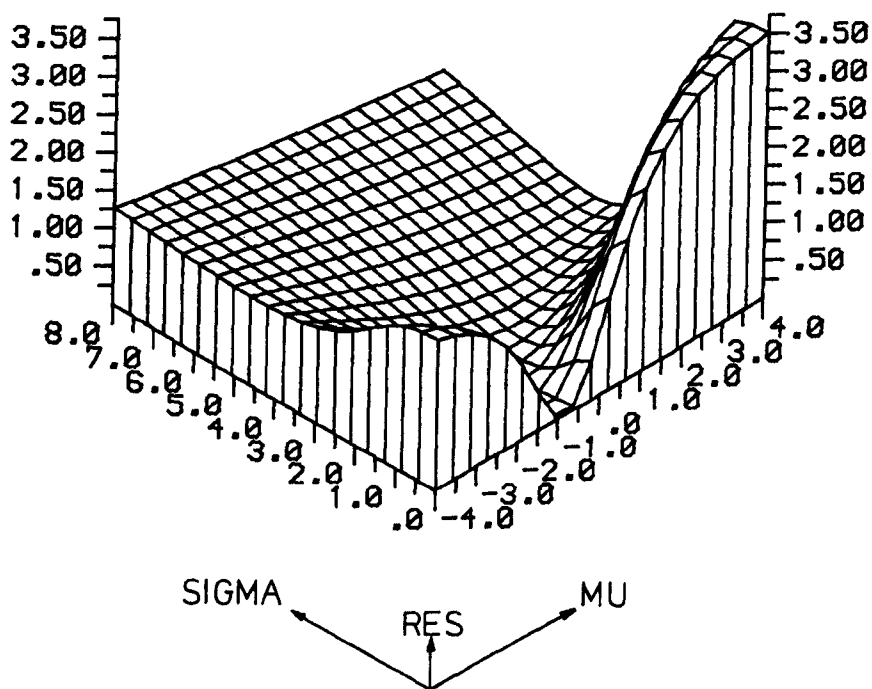
and
$$R = R_1^2 + R_2^2$$

The residual R is that function which the optimisation routine had to minimise by manipulating the mu and sigma values at each iteration. The optimisation procedure stopped when the residual could no longer be minimised and the optimal mu and sigma values returned together with the residual for each of the two moments.

Figure 5.3 shows a three dimensional plot of the residual R on the Z axis against mu and sigma when the supplied data from the recorded spirogram was $t = 1.485$, $\alpha_1 = 0.387$ and $\alpha_2 = 0.253$. It can be seen that the solution, i. e. $R = \text{zero}$ (identified by an X), lies on the floor of a valley which has a shallow gradient floor and steeper sides. Hence



A



B

Figure 5.3 Relationship between residual and changes in mu and sigma.
A) Contour plot B) Three-dimensional plot.

for the given start values of $\mu = 0$, $\sigma = 1$ the quickest direction to the solution would follow the steepest slope down to the valley floor.

The modified Marquardt optimisation method used combines a bias towards following the steepest descent together with a Gauss Newtonian method (or generalised least squares method). The steepest descent method is usually convergent but slow, whereas the Gauss-Newton method is rapid but has less reliable convergence ⁽⁷¹⁾. When a Gauss-Newtonian method alone was applied to solve for μ and σ there was a very strong tendency for each iteration to diverge from the true solution. At each iteration the μ and σ values would increase while the residual fell with the iterative journey gradually coming down the sides of the valley (figure 5.3) but at the same time travelling towards the horizon. The iterative journey would eventually join the floor of the valley with μ and σ values greater than 20 and then follow a multi-iterative tedious route down the floor of the valley towards the solution. With many examples the solution would not be found, with the optimisation procedure terminating a long way up the valley floor. If the correct solution could be found the procedure was lengthy because of the 100 or more iterations required. This problem with the Gauss-Newton method could not be overcome by constraining the algorithm with bounds for μ and σ , by limiting the maximum displacement of μ and σ per iteration, or by choice of start values that would suit all cases.

This sort of behaviour has been found previously with similarly shaped problems ⁽⁷¹⁾ and the modified Marquardt method which uses a bias towards steepest descent reaches the floor of the valley very

quickly and invariably converges rapidly on the solution. This method on average requires about 5 to 10 iterations to find the solution.

Sensible start values are essential for these iterative optimisation procedures. A good algorithm should not be perturbed by different start values; the correct answer should be returned irrespective of start values. Obviously the closer the start values are to the solution the quicker the solution is obtained. Arbitrary start values of $\mu = 0$ and $\sigma = 1$ were chosen as being within that range which yields theoretical spiograms within the bounds found in clinical practice.

The algorithm which used only a Gauss-Newton optimisation procedure was found to be sensitive to start values, whereas the modified Marquardt method was not perturbed by extreme start values. It was concluded that the modified Marquardt method was superior, demonstrating rapid convergence on the solution even when faced with an extreme solution or extreme start values.

The algorithm was written using an optimisation subroutine from the Numerical Algorithm Group library Mark 7 called EQ4GAF which uses the modified Marquardt method. During the course of this work this subroutine was withdrawn when the library Mark 8 was introduced. This involved extensive evaluation of other routines to see if they could be used. Although correct solutions can be achieved using other routines none was as robust or as efficient as the modified Marquardt method. Therefore source code for the routine was obtained by special arrangement so that use of this routine could be continued.

(ii) Testing the Algorithm

The algorithm can be tested by supplying α_1 and α_2 for a curve known to fit the model precisely. An α_1 and α_2 generated from the model could be used but a more rigorous test is to supply the moments of a single exponential which can be derived precisely from definite integrals. A single exponential is a special instance of a lognormal distribution with a sigma of zero.

The first two moments of a single exponential of time constant 0.6065 s ($\log_e 0.6065 = -0.5$) were derived every 0.1 s from definite integrals and supplied to the algorithm. The mu and sigma values returned are plotted in figure 5.4 using the right hand ordinate scale, together with the first one second of the single exponential. By 0.3 s the correct mu value was identified and was constant thereafter to infinite time; by the same time the sigma value was within 0.1 of the correct value which was identified at 0.7 s and was constant thereafter. The correct mu and sigma values cannot be determined from the earlier moments as they cannot be supplied with sufficient precision. Because of these findings this form of analysis on real spiromograms was started after 0.3 s had elapsed. The algorithm was tested with moments generated from the model with a non-zero sigma value and the same pattern of results was found.

In order to work with precision the algorithm requires the moments and elapsed time to be supplied precise to three decimal places. Although elapsed time can fulfil this requirement the earlier experiments using the pump to determine the effects of temperature demonstrated that the moments were not precise to three decimal places.

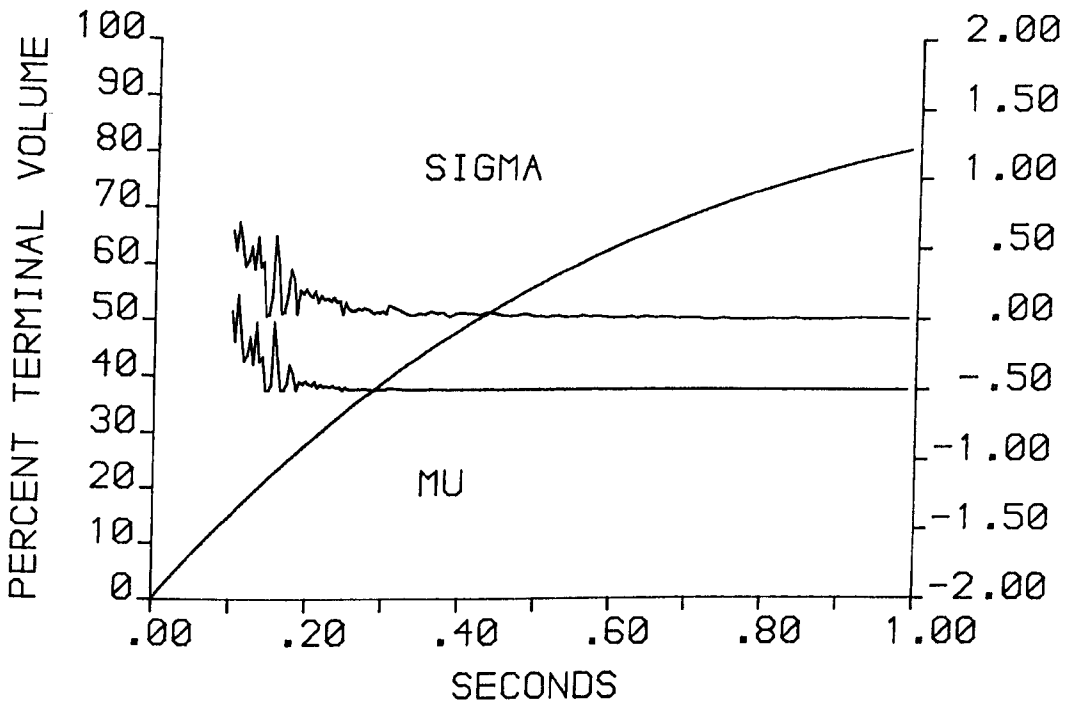


Figure 5.4 Testing the algorithm: sequential mu and sigma for a single exponential of time constant 0.6065 s ($\log_e 0.6065 = -0.5$) Mu and sigma plotted with the right hand ordinate scale.

This is therefore a limitation of this algorithm which only uses three indices α_1 , α_2 and elapsed time to solve for mu and sigma.

The algorithm was not run on the microcomputer in the laboratory but on the University of Birmingham Computer Centre's DEC 20-60 computer. On this large computer there was the necessary library of integration and optimisation routines which facilitated writing the algorithm. Furthermore, the DEC 20-60 was able to perform the integration and optimisation with astonishing speed. The algorithm used by Permutt and Menkes⁽⁷²⁾ employed a crude optimisation sequence. When their algorithm was tried on the DEC 20-60 computer it performed with tolerable efficacy when supplied with the moments towards the end of a spirogram, but was not so precise or as robust as the algorithm used in this study when tested with extreme examples (i. e. with the moments early on in a spirogram or with spirograms with extreme mu and sigma values)

Work is proceeding to establish the algorithm used in this study on a microcomputer as this would facilitate its use. All the work presented in this thesis used the algorithm on a DEC 20-60 computer.

SEQUENTIAL MU AND SIGMA FOR REAL SPIROGRAMS

When real spirograms were analysed in this way the volume, flow and time arrays of the recorded spirogram were sent to the University of Birmingham's DEC 20-60 computer via the computer interface. From the flow and time arrays the moments were derived sequentially by numerical integration after a back extrapolation procedure had been performed to find a new time zero.⁽³⁷⁾

For all data points from the arrays with elapsed time, t , greater than or equal to 0.3 s, the α_1 , α_2 and t were sequentially passed to the algorithm and the returned mu, sigma and residual values stored. This procedure took 30 to 90 seconds to derive the 100 to 250 sequential mu and sigma values for average spiograms. The residuals are not subsequently mentioned in this text unless they exceed 0.001, the maximum precision likely for the moments.

Figures 5.5a) and b) show a real spiogram and flow volume curve respectively for a normal subject together with the sequential mu and sigma values plotted with the right hand ordinate scale. The first observation is that the sequential mu and sigma values are not constant and show no ultimate tendency to constancy which was seen in figure 5.4 for curves known to fit the model. Therefore this spiogram is not a perfect mathematical fit for the model. This has been found to be true for each of over 700 spiograms subsequently tested. Secondly there is an early phase where sigma is zero followed by a steady rise in sigma and mu to terminal values of $\mu = -0.59$ and $\sigma = 0.93$. Where sigma is zero it means that a single exponential is the best fit for the spiogram and this agrees with the flow-volume curve during this phase which approximates to a straight line.

Another way of presenting this data is to compare the original spiogram with theoretical spiograms derived from the mu and sigma values obtained. As there are 107 sequential mu and sigma values for the subject only a chosen 3 theoretical spiograms are shown in figure 5.5c) together with the original spiogram identified with crosses. These 3 spiograms demonstrate the trend over the 107 theoretical spiograms.

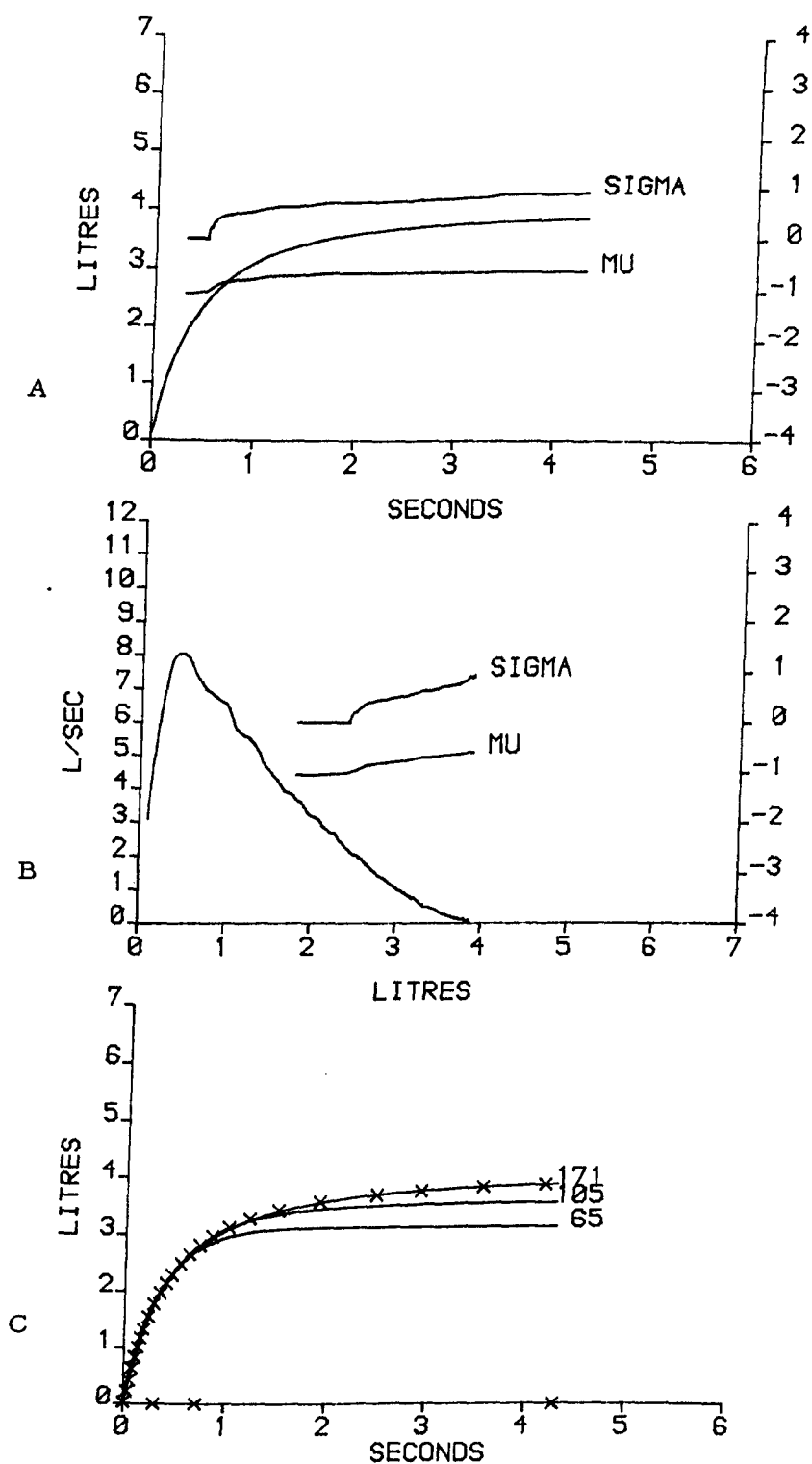


Figure 5.5 Normal female subject, aged 28, height 1.64m.
Sequential mu and sigma, plotted with the right hand ordinate scale,
and theoretical spirograms:

No. 65	$v = 1.8 \text{ L}$	$t = 0.30 \text{ s}$	$\mu = -1.05$	$\sigma = 0.0$
No. 105	$v = 2.8 \text{ L}$	$t = 0.72 \text{ s}$	$\mu = -0.82$	$\sigma = 0.46$
No. 171	$v = 3.9 \text{ L}$	$t = 4.30 \text{ s}$	$\mu = -0.59$	$\sigma = 0.93$

Theoretical spirogram 65 is derived from the sequential μ and σ values at 0.3 s (which correspond to the 65th triplet of volume flow and elapsed time stored for this spirogram). It is a close fit for the early part of the spirogram but undershoots the FVC with a TTV of only 3.0 L. The model predicts that from the data up to 0.3 s it expects the TTV to be 3.0 L. It can be seen from the flow volume curve that when the expired volume is 1.8 L ($t = 0.3$ s) an extrapolation of the flow-volume curve as a single exponential i.e. a straight line, would intersect the volume axis at about 3.0 L. A later μ and σ yield theoretical spirogram 105 which undershoots to a lesser extent and the last μ and σ derived from this spirogram yield theoretical spirogram 171 which is a tolerably good fit.

It can be seen from this progression that later μ and σ values represent an updated prediction of the ultimate form of the spirogram based on the additional information received from the later moments. This can be appreciated from the flow volume curve; as the minimal degree of curvilinearity in this example is encountered so the μ and especially σ values are adjusted.

Figures 5.6 a), b) and c) show similar plots for an older subject. It is evident that the model is sensitive to terminal curvilinearity of the flow volume curve and that it interprets this as principally an increased dispersion of time constants (high σ value). As before, there is an early phase with zero σ but in this subject there is a very steep rise in σ to a value of 2.93 with terminal $\mu = -0.24$. In this subject at the end of the spirogram the residuals from the algorithm reach importance at an absolute value of 0.001 for each of the moments.

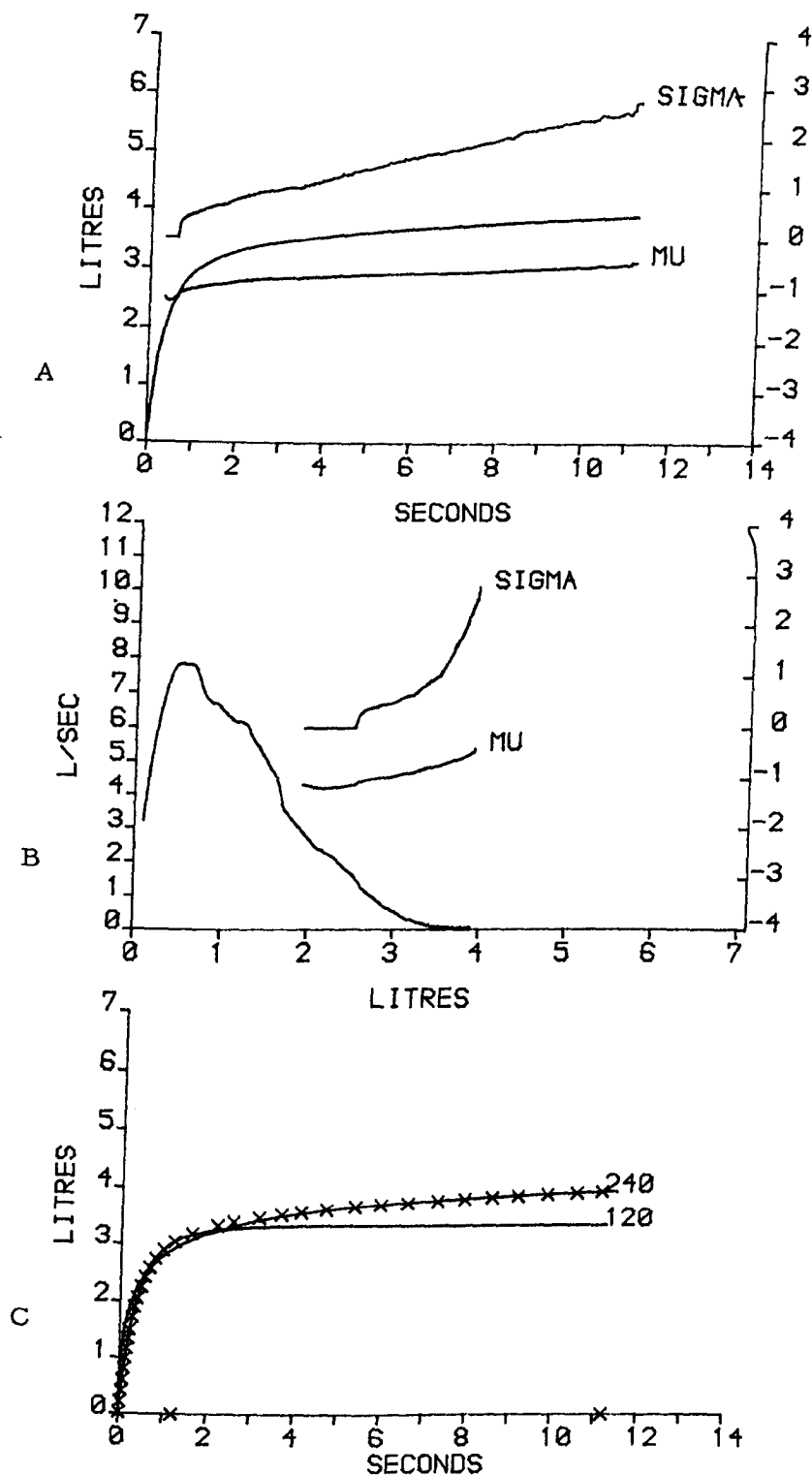


Figure 5.6 Normal female subject, aged 52, height 1.65 m.
Sequential mu and sigma, plotted with the right hand ordinate scale,
and theoretical spiograms:

No. 120	$v = 3.0 \text{ L}$	$t = 1.21 \text{ s}$	$\mu = -0.92$	$\sigma = 0.54$
No. 240	$v = 3.9 \text{ L}$	$t = 11.20 \text{ s}$	$\mu = -0.24$	$\sigma = 2.93$

This means that the model is having difficulty fitting the first two moments. The magnitude of this difficulty is apparent in figure 5.6c). An early theoretical spirogram 120 is a good fit for the early part of the spirogram and undershoots the FVC as can be deduced from the flow volume curve. A later theoretical spirogram 240 is a good fit for the tail of the spirogram but is a poor fit early on. In this subject the model can precisely fit each half of the spirogram separately but not the whole spirogram.

The above two subjects demonstrate the configuration of sequential mu and sigma found in 8 of the 21 subjects in the repeatability study. Figures 5.7 a), b) and c) show the configuration seen in 9 of the subjects, that is a changing mu and sigma with no period of zero sigma. In this subject the early theoretical spirograms ~~under~~^{over} shoot the true FVC but the ultimate degree of fit is very good with terminal sigma = 0.90 and mu = -0.16

The same configuration was seen in a young stable asthmatic subject while in remission, figure 5.8. However with the asthmatic subject the flows were generally lower, $FEV_1\%$ was lower at 55% and the flow volume curve was more curvilinear; this is reflected in the higher terminal mu = 1.14 and sigma = 1.93. This finding of high mu and sigma values in an asthmatic subject agrees with those of Permutt and Menkes⁽³⁹⁾.

A third configuration of sequential mu and sigma plot was found in 3 out of 20 normal subjects tested and is shown in figure 5.9. In this subject there is an early high plateau of mu and sigma values

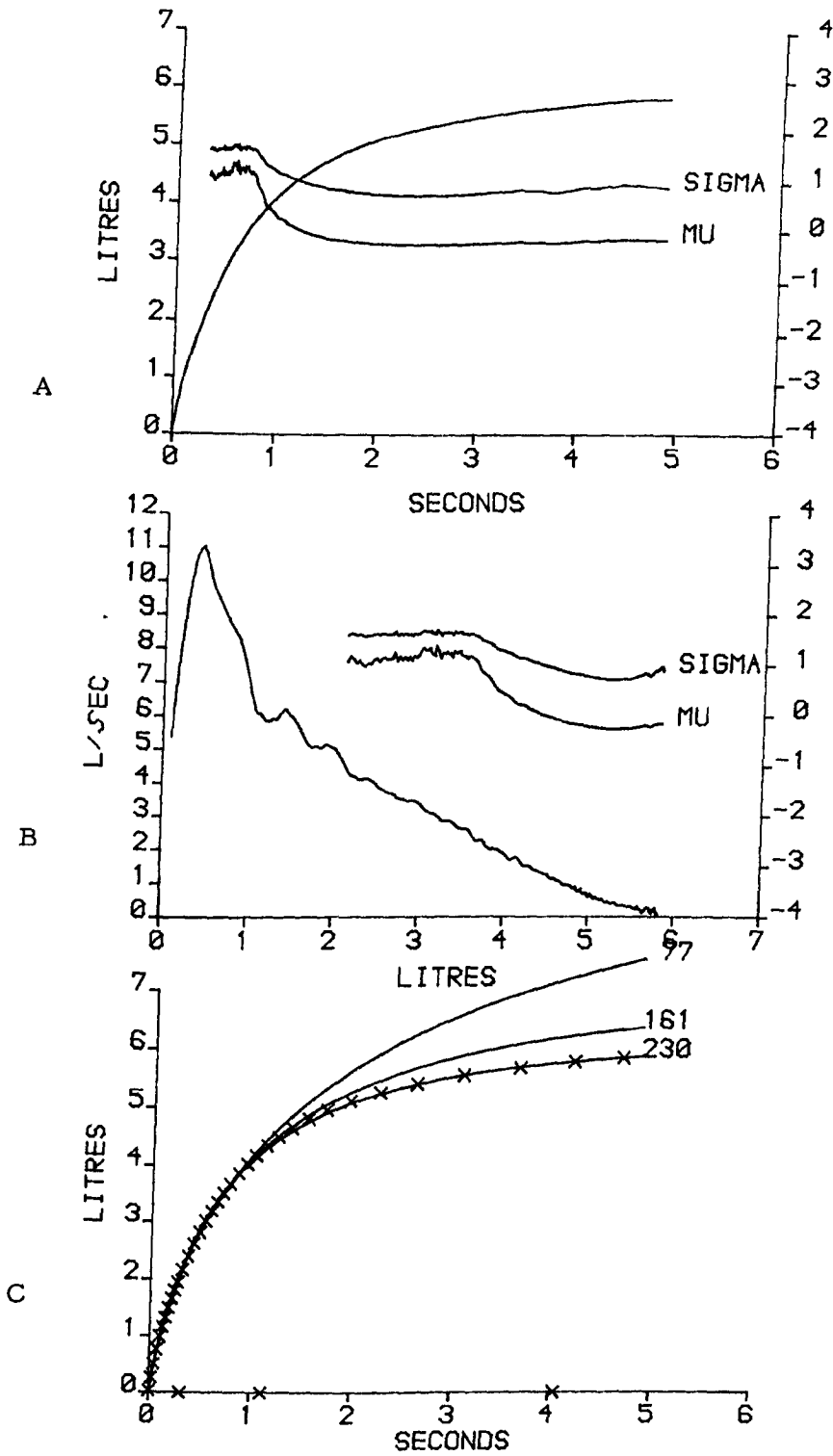


Figure 5.7 Normal male subject, aged 34, height 1.88m.
Sequential mu and sigma, plotted with the right hand ordinate scale,
and theoretical spirometrys:

No. 77	$v = 2.1 \text{ L}$	$t = 0.31 \text{ s}$	$\mu = 1.08$	$\sigma = 1.60$
No. 161	$v = 4.3 \text{ L}$	$t = 1.11 \text{ s}$	$\mu = 0.11$	$\sigma = 1.07$
No. 230	$v = 5.7 \text{ L}$	$t = 4.05 \text{ s}$	$\mu = -0.17$	$\sigma = 0.90$

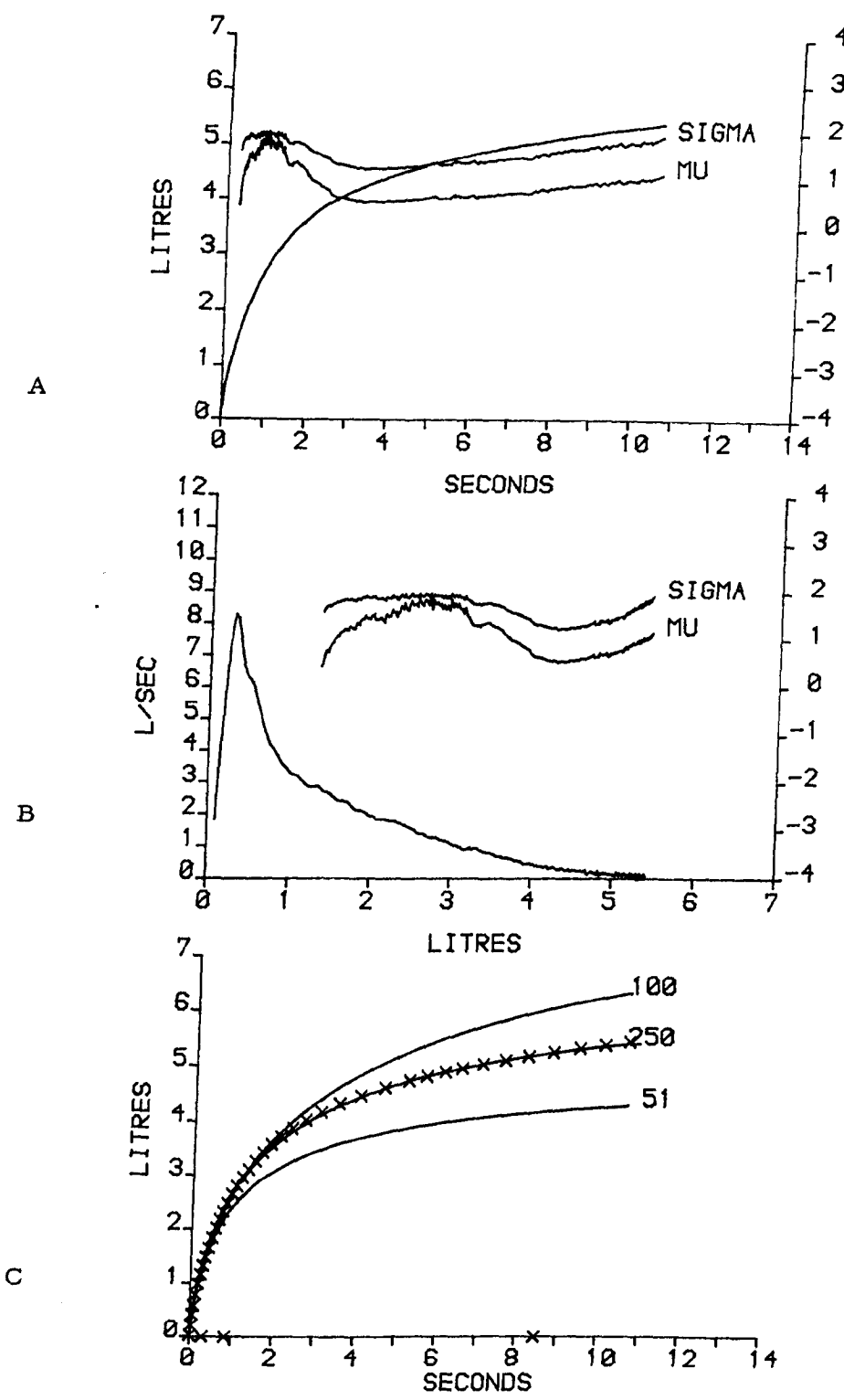


Figure 5.8 Male asthmatic, aged 23, height 1.79 m.
Sequential mu and sigma, plotted with the right hand ordinate scale,
and theoretical spirograms:

No. 51	$v = 1.4 \text{ L}$	$t = 0.30 \text{ s}$	$\mu = 0.44$	$\sigma = 1.58$
No. 100	$v = 2.5 \text{ L}$	$t = 0.86 \text{ s}$	$\mu = 1.69$	$\sigma = 1.89$
No. 250	$v = 5.2 \text{ L}$	$t = 8.48 \text{ s}$	$\mu = 0.90$	$\sigma = 1.66$

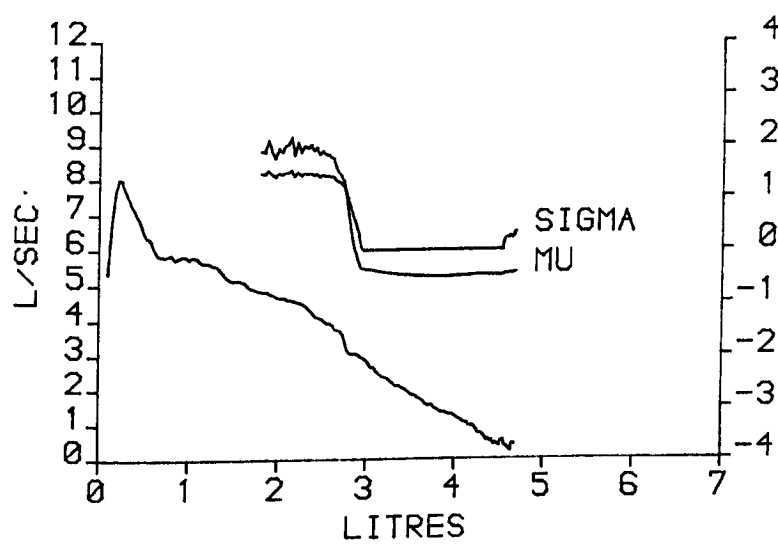


Figure 5.9 Sequential mu and sigma for a young normal subject.

which are not completely stable followed by a sharp fall to the more usual configuration of zero sigma followed by a terminal rise in mu and sigma. The sharp fall in this subject coincides with a small inflexion on the flow volume curve. A more dramatic example of this configuration is seen with subjects who have a fixed upper airway obstruction. Figure 5.10 a) shows the flow volume curve and sequential mu and sigma for a man with a goitre impinging on his trachea and b) shows the configuration after surgical removal of the obstruction.

The model has difficulty in fitting the spirogram which corresponds to the flow-volume curve in figure 5.10 a) and this is reflected in the residuals which reach importance at an absolute value of 0.002 for each of the moments. Where flow is constant with respect to volume the spirogram is a straight line and so cannot be fitted by a mixture of exponentials. This third configuration is seen whenever the MEFV curve is concave towards the volume axis and therefore implies difficulty in fitting the data.

SELECTION OF A MU AND SIGMA TO DESCRIBE A SPIROGRAM

The purpose of the model is to derive a single mu and sigma value to describe a subject's spirogram. It is evident from the foregoing that there are many pairs of mu and sigma values to choose from for a given spirogram and the mu and sigma values derived from the moments towards the end of the spirogram tend to give a theoretical spirogram which more closely fits the original spirogram than do earlier mu and sigma values.

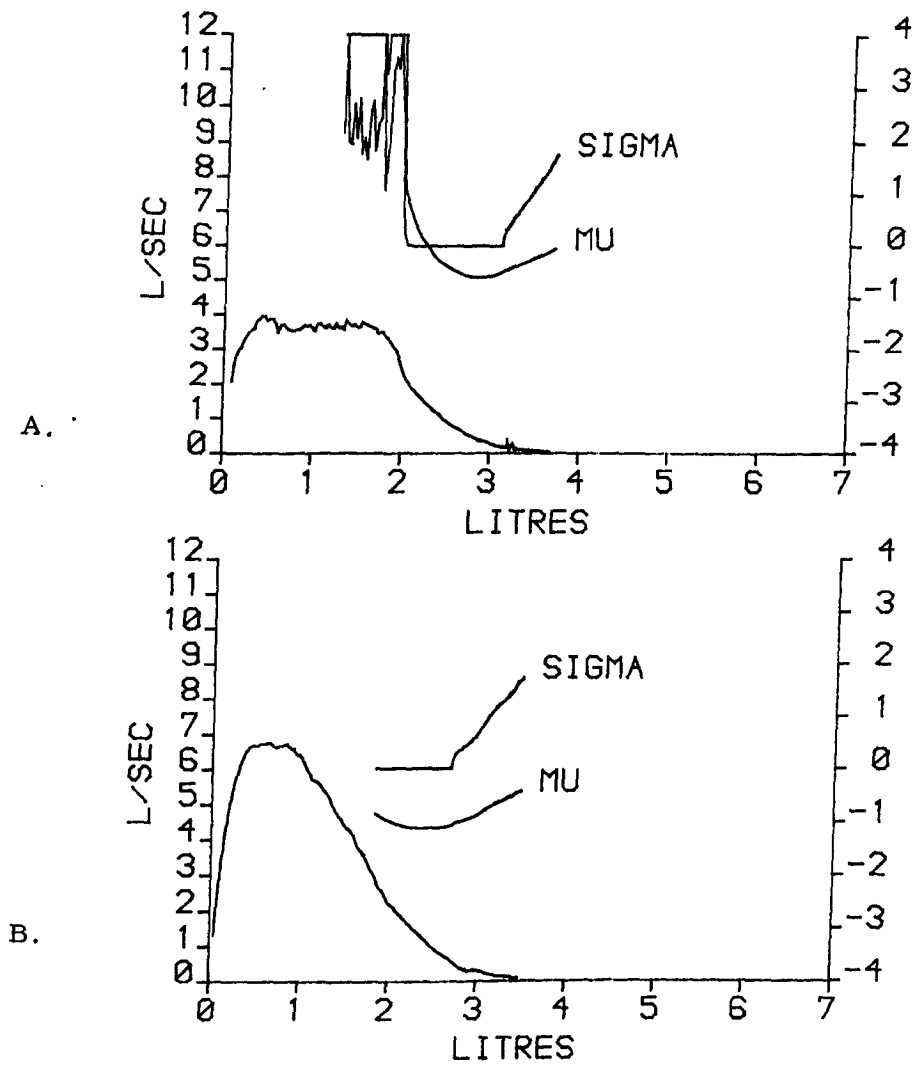


Figure 5.10 Sequential mu and sigma for a man with an extrathoracic airway obstruction.

A. before operation and B. after operation.

One option is to use the μ and σ derived from the moments up to the end of the spirogram, thus utilising data from the whole spirogram (subsequently referred to as Method A). However, this does not always give the closest fit between theoretical and original spirograms. Figure 5.11 shows an original spirogram identified with crosses and two theoretical spirograms. Theoretical spirogram 197 derived from the last μ and σ values does not give as good a fit as those taken at 4.1 s yielding theoretical spirogram 182. It is not entirely clear whether Permutt and Menkes used Method A or the μ and σ values at 6 s when the forced expiratory time exceeded 6 s. In the data presented with details of their programme ⁽⁷²⁾ all the examples showed that the moments at 6 s were used. Just as there is no reason why Method A should necessarily give the best fit, similarly the μ and σ values from the moments at 6 s have no special call to give the best fit. A further problem is demonstrated in figure 5.12 where two theoretical spirograms cannot be separated by eye and give an equally good fit for the original spirogram and yet the μ and σ values for each are slightly different.

It was therefore necessary to test other options for the selection of a μ and σ value to describe a given spirogram. One option was to select from amongst all the sequential μ and σ values derived for a subject that pair which gave the minimum sum of squared volume differences between the theoretical spirogram and the original data points stored in the computer (subsequently referred to as Method B). Method B is necessarily tedious in having to evaluate the sum of squared differences for over 100 theoretical spirograms.

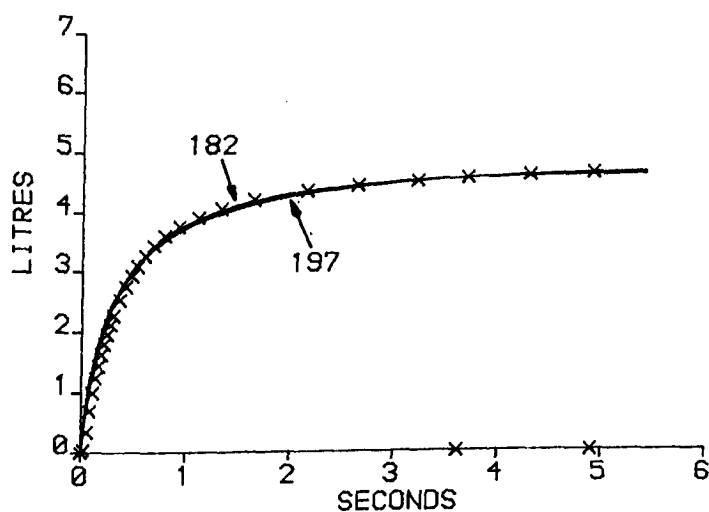


Figure 5.11 Two theoretical spirometers and the original. A better fit from an earlier mu and sigma value.

No. 182	$t = 4.10 \text{ s}$	$\mu = -0.82$	$\sigma = 1.03$
No. 197	$t = 5.38 \text{ s}$	$\mu = -0.80$	$\sigma = 1.28$

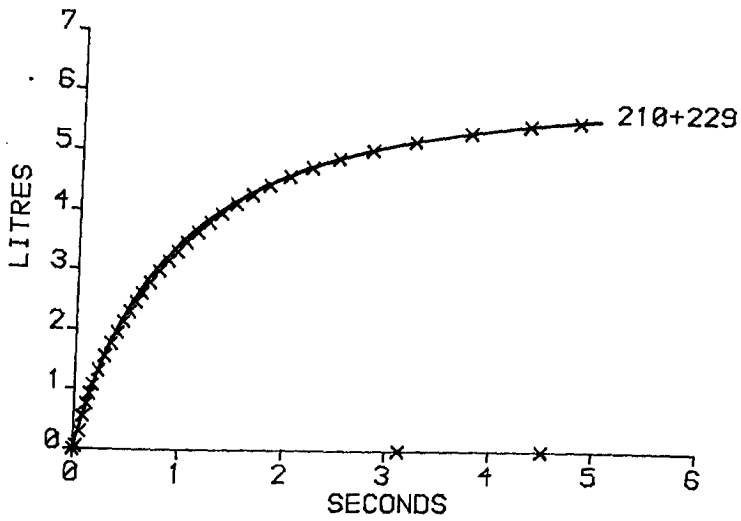


Figure 5.12 Two theoretical spiograms and the original. Equally good fit yet different mu and sigma values.

No.210	$t = 3.54 \text{ s}$	$\mu = 0.12$	$\sigma = 0.90$
No.229	$t = 4.94 \text{ s}$	$\mu = 0.08$	$\sigma = 0.81$

An additional method was devised by constructing an algorithm which optimised for μ and σ in the first instance by matching theoretical and original spiograms using a least squares method with no reference to the moments (subsequently referred to as Method C). This curve-fitting algorithm was tested in a similar way to the moment algorithm with single exponentials. The curve-fitting algorithm was found to be superior to the moment algorithm; when it was supplied with only the first 0.1 s of a single exponential it identified the correct μ value and was within 0.001 of the correct σ value. This superior performance is to be expected since this curve-fitting algorithm is supplied with considerably more data than the moment algorithm upon which to base the optimisation procedure. Furthermore, because more data is supplied to the algorithm the precision required of the volume measurements for satisfactory working of the algorithm is readily attainable, unlike the moment algorithm which required an unachievable precision in the moments. The curve-fitting algorithm was tried with several optimisation routines and again the modified Marquardt method was found to be the best. This was expected as the plot of residuals for changes in μ and σ was identical to that seen for the moments in figure 5.3.

The three methods A, B and C all yield the same solution for 'spiograms' which are a perfect fit for the model. Because spiograms recorded from subjects are not a perfect fit for the model, different solutions are obtained with the different methods. Amongst 20 normal subjects the largest absolute differences between the methods were 0.5 for μ and 1.6 for σ , and the largest differences expressed as a percent of the largest value obtained were

50% for mu and 100% for sigma. Thus it was necessary to establish which method was the most suitable for selecting a mu and sigma to describe a spirogram.

To determine which of the three methods (A B or C) was the most satisfactory each method was used to determine a mu and sigma value for each of 20 of the normal subjects used previously. For each subject six spirometric indices (FVC, FEV₁, FEV₃, FEF_{50%}, FEF_{75%} and FMF) were computed from the mu and sigma found by each method and these results were compared with the original recorded results. Table 5.1a shows the results for the volume indices expressed as percent of the original with all 20 subjects considered together. Method C is overall superior to the other two methods for these volume indices and is precise to within the tolerance of the original measurements. Table 5.1b shows the results for the three flow measurements. The degree of fit for early events such as FEF_{50%} and FMF was not so good as that for later events, FEF_{75%}, FEV₁ and FEV₃. This can be appreciated from previous examples (figures 5.5, 5.6, 5.7, 5.8) where the theoretical spirograms fit the tail of the spirogram well but tend to overestimate expired volume early on i. e. overestimate the flows. In Table 5.1b it is evident that Method A was not as good as either Methods B or C. Therefore it was concluded that Method C was overall the best method.

THE MODEL AND RECOGNISED VENTILATORY ABNORMALITIES

Before proceeding with the use of the model it was first necessary to see if the model correctly reflected the abnormalities of well

		A	B	C
		Last μ σ from moments	Best fit μ σ from moments	Curve fitting
FVC				
	Mean % of original	100.0	99.6	100.0
	SD from mean	0.0	2.0	0.0
	Mean % deviation from original	0.0	1.4	0.0
FEV ₃				
A	Mean % of original	99.6	101.1	100.9
	SD from mean	0.9	2.1	1.3
	Mean % deviation from original	0.5	1.3	1.2
FEV ₁				
	Mean % of original	98.3	99.8	99.3
	SD from mean	1.7	1.7	1.5
	Mean % deviation from original	1.9	1.4	1.1
		A	B	C
		Last μ σ from moments	Best fit μ σ from moments	Curve fitting
FEF ₅₀				
	Mean % of original	90.9	94.5	92.4
	SD from mean	8.7	6.1	7.3
	Mean % deviation from original	10.7	6.6	8.8
B	FEF ₇₅			
	Mean % of original	88.4	105.3	101.9
	SD from mean	10.0	11.0	9.1
	Mean % deviation from original	12.9	9.4	7.4
FMF				
	Mean % of original	74.0	80.4	78.7
	SD from mean	12.4	8.4	9.4
	Mean % deviation from original	26.1	19.6	21.4

Table 5.1. Comparison of recorded spirometric indices and those predicted by the model using 3 methods for selecting mu and sigma.

recognised spirographic abnormalities. A few pronounced examples of airflow limitation due to asthma, chronic bronchitis and upper airway obstruction and an example of a restrictive ventilatory defect were chosen and the model used to describe their spirograms. Table 5.2 below presents a few recorded spirometric indices and the mu and sigma derived by curve-fitting (method C) for the representative examples and two normal subjects.

Table 5. 2						
	FVC litres	FEV ₁ %	PFR L/s	FET secs	mu	sigma
1. female 28 yrs. never smoked	3.9	80	8.0	4.4	-0.61	0.79
2. male 34 yrs never smoked	5.8	71	11.0	4.9	-0.20	0.84
3. male 23 yrs stable asthma	5.4	50	8.3	10.8	0.86	1.55
4. male 53 yrs smoker, chronic bronchitis	2.3	42	2.4	8.5	1.48	1.49
5. female 47 yrs pulmonary fibrosis	1.9	99	6.4	2.1	-1.33	0.50
6. male 64 yrs a. goitre pre-op	3.7	70	4.0	9.0	-0.13	0.92
b. post-op	3.5	78	6.7	5.4	-0.59	1.08

The spirograms, flow volume curves and sequential mu and sigma from the moments for subjects 1, 2 and 3 in table 5. 2 have been shown in figures 5. 5, 5. 7 and 5. 8 respectively. The mu value for subject 2 is higher (less negative) than that of subject 1 which means that the average time constant ($= e^{\text{mu}}$) is longer for subject 2 which is in keeping with the lower FEV₁% for subject 2. In the asthmatic subject and in the man with chronic bronchitis the FEV₁% is lower still and this

is reflected not only in a markedly higher μ (very long average time constant) but also with an increased σ value. Subject 5 who had pulmonary fibrosis and marked restrictive ventilatory defect has a very low μ value (i. e. very short average time constant) which is in keeping with the high $FEV_1\%$ and short FET. In subject 6 removal of this man's upper airway obstruction is reflected by a marked reduction in μ (average time constant fell from 0.88 s to 0.55 s, a 38% reduction) with little change in σ . Despite the difficulty the model has in fitting spiograms such as that for subject 6a (Figure 5.10) the model correctly reflects that the reduction of early flows due to upper airway obstruction increases the average time constant of the manoeuvre. With the latter part of his flow volume curve and spiogram undisturbed the σ value is essentially unchanged. This presents an example of how μ is very sensitive to changes in the early part of the spiogram and σ is more sensitive to changes in the tail of the spiogram (see figures 5.1 and 5.2)

DISCUSSION

Although the proposed model is an attractive concept it has inherent deficiencies. The first relates to the methods of optimisation used within the algorithms. It is apparent from the foregoing that the results of the model depend on the efficacy of the algorithms used and that if the model was applied in various centres using different algorithms different answers might be obtained. It is comforting that the quoted results from Permutt and Menkes' algorithm⁽⁷²⁾ can be reproduced exactly by the independent and different algorithm used in this study. However, the potential for divergence from the true

solution using certain optimisation routines could be a source of confusion. There is no similar weakness when using the moments alone as descriptors of the spirogram. The only problem with the moments is due to inevitable truncation, and if this problem could be independently overcome the model would be irrelevant. For instance, if the exact degree of true truncation of a spirogram is known (e. g. if $FVC = 95\%$ of TTV) then sigma can be deduced directly as there is a unique sigma value corresponding to a given MR at specified percent of TTV. However, the truncation problem appears insurmountable without the help of assumptions such as those used in the model.

The second weakness of the model is that it clearly does not precisely fit all spirograms. In the majority of normal spirograms and those with airflow limitation the degree of fit has been found to be quite good; in older normal subjects who have a normal $FEV_1\%$ but long tail to the spirogram i. e. long FET, the model has difficulty fitting the data e. g. figure 5. 6.

The lack of fit in some cases may be due to the lognormal distribution being unsatisfactory and one approach to the problem would be to try a different distribution as has already been discussed. Following the observation that the model can usually precisely fit the early and late parts of the spirogram separately it was decided to try to fit spirograms in two parts. This invokes that at a certain point during an MFEM there is a dramatic change in the dynamics of the manoeuvre which alters events. This could be the onset of dynamic collapse of airways. Preliminary studies were undertaken to evaluate

the technique and it was possible to reduce substantially the residuals with a curve-fitting technique.

It was also appreciated that the model does not anticipate closing volume except inasmuch as the termination of the contribution of areas with short time constants may take this into account. By applying the curve-fitting algorithm to fit small regions of a spirogram and then by gradually extending the region to be fitted, it was possible by observing any increase in residual accrued to determine whether there were any regions in the spirogram which the model had particular difficulty in fitting. In the small number of normal spiograms analysed this way there were a few that showed a point towards the end of the spirogram beyond which the model had increasing difficulty in fitting the data.

This above approach may have important applications but it increases both the complexity of the model and the number of indices to describe a spirogram. The moments and moment ratio represent the simplest descriptors of the spirogram and the model was derived in order to overcome the errors associated with the inevitable truncation of the moments. Because the errors with the moments can be reduced by considering them with earlier truncation, as discussed in Chapter 2, it was decided to evaluate the model using curve-fitting for the whole spirogram and compare this with the moments before embarking on a more complex application of the model.

The three shapes to the sequential μ and σ values derived from the moments are demonstrated in figures 5.5, 5.7 and 5.9. These 3 shapes correspond to the early part of the flow volume curve either

approximating to a straight line (figure 5.5b), or being convex (figure 5.7b) or concave (figure 5.10a) to the volume axis. However, when the model is applied to fit the whole spirogram (and flow volume curve) the resulting sigma value predominantly reflects the curvilinearity of the terminal part of the flow-volume curve. This curvilinearity has received attention as a possible means of identifying the early onset of disabling chronic airflow limitation (CAL) and the moment ratio (MR) and sigma are separate but related descriptors of this curvilinearity.

MR is highly reproducible within subjects whereas in the 20 subjects tested with curve-fitting the mean within day within person co-efficient of variation for sigma was 10% versus 4% for MR 100%. Therefore full evaluation of both indices was necessary to establish if either or both are useful for the early detection of CAL.

The model does not readily translate into variables that define the mechanics of the forced expiratory manoeuvre. The product of airway resistance and lung compliance has the units of time and is akin to a time constant of emptying for the lungs. In electrical circuits the analogy is the product of resistance and capacitance. If a small subunit of the lungs is considered then if its airway resistance was reduced it would speed up its emptying and so shorten its time constant of emptying. Similarly a reduced compliance would shorten the expiration and time constant, since the collapse of the unit for a given driving pressure would be diminished. Increased resistance and compliance would have the opposite effect. The model considers the spirogram as the amalgamation of the contribution of many lung

units which empty exponentially. The lung unit so considered does not necessarily have to conform to any defined anatomical unit although this eventuality is not precluded.

If the model is to be interpreted by physiological alterations within the lungs then changes in μ may reflect changes in resistance and/or compliance which affect the lungs overall, and changes in σ may reflect changes in resistance and/or compliance which affect the lungs in a patchy way or with differing severity throughout the lungs. The distinction between generalised and patchy effects on the lungs is not clear, but some processes do tend to favour one of these. The ageing of the lungs is associated with loss of elastic recoil^(73, 74), reduced terminal flows and increased curvilinearity of the flow volume curve⁽²²⁾ with relative preservation of FEV₁%. Histologically the effects of age tend to be patchy so one might expect a greater change in σ with age than for μ . Asthma affects the airways generally but not necessarily with the same severity which may explain why Permutt and Menkes⁽³⁹⁾ found both μ and σ to be higher in asthmatics than normals. Interestingly they found that bronchial challenge caused changes mainly in μ and not σ .

Therefore the model can be interpreted in terms of generalised or patchy effects but cannot on its own resolve whether an effect is principally on large airways (i. e. greater than 3 mm diameter) or small airways (i. e. less than 2 mm diameter).

CHAPTER 6

POPULATION SURVEY

INTRODUCTION

Before it is possible to use a test for diagnostic purposes the range of normal values must be determined. This involves measuring the values for the test in a population defined as being normal. Predicted values for conventional spirometric indices have been published, but some workers did not separate smokers from non-smokers^(75, 76) because they found little difference arose in the predictions if smokers and non-smokers were considered together.

It has been recognised that the majority of cigarette smokers have little diminution in their ventilatory function when compared with non-smokers and only about 10% of all smokers⁽⁷⁷⁾ appear susceptible to developing disabling chronic airflow limitation⁽³⁴⁾. The early identification of these susceptible smokers would increase the understanding of the development of chronic airflow limitation, it would facilitate research into the putative mechanisms behind this susceptibility and it may help preventative measures. Therefore if a test is to be applied to detect this small proportion of smokers it is sensible to derive normal values for the test from a non-smoking population and then determine which smokers do not conform to this normal range.

Evidence has been presented^(78, 79) that the early pathological changes due to cigarette smoking occur predominantly in 'small' airways (< 2mm internal diameter) and that similar changes are present in patients with chronic obstructive lung disease⁽⁸⁰⁾.

Macklem and Mead⁽⁸¹⁾ demonstrated that the performance of these 'small' airways is predominantly reflected in the terminal 30% in volume of the vital capacity and so there has been considerable interest in this region of MEFV curves and spiograms^(24, 26, 29, 83, 84), and other tests thought to reflect the performance of small airways^(24, 29, 83-85) as a means for identifying susceptible smokers. Moment analysis of spiograms offers a means for critically analysing the terminal part of a maximal forced expiratory manoeuvre (MFEM) and some workers have found it to be sensitive in detecting changes due to smoking^(24, 29). However, these workers all looked for differences between groups of non-smokers and smokers. Identifying differences on this basis may afford little information about susceptibility to developing disabling chronic air-flow limitation (CAL). For example, the most discriminating test for the criterion of distinguishing smokers from non-smokers is the question 'Do you smoke cigarettes? '.

In this study it was decided to perform a cross-sectional survey of a working population to establish normal values for the conventional and time domain spirometric indices and then apply these to identify those smokers in the population with abnormalities. The choice of population to sample is important. It is very difficult to obtain an ideal normal population and sometimes unrepresentative populations, such as medical staff, have been used. Any survey which only samples volunteers, such as in this study, may be sampling a motivated and thus biased population. However, this criticism cannot be avoided because compulsory participation is unethical, undesirable and

unsatisfactory for tests such as these which require a subject's complete co-operation.

SAMPLE POPULATION

The work force of the Cadbury Schweppes Ltd., Bournville factory was chosen as the sample population for several reasons. Sampling a working population reduces the exclusion rate due to illness and major diseases which may be prevalent in surveys of residential areas. The Bournville factory was chosen because of (i) its proximity to the Department of Medicine, Queen Elizabeth Hospital, (ii) the known concern of the Cadbury Schweppes management for the well being of its workforce which is manifest in their excellent medical facilities on site and their keen interest in programmes which may improve the health of the workforce, (iii) the lack of exposure to dusts or chemicals at the factory which are known to be injurious to the lungs and (iv) the size and composition of the workforce which comprises approximately 4000 men and 4000 women with the male workforce including all grades from senior management to unskilled manual labour.

The survey was carried out with the full agreement and co-operation of the Cadbury Schweppes management, the Trades Unions and the site medical staff. Volunteers were asked to return a brief questionnaire about their age and smoking habits, and whether they had ever suffered with any of the following - asthma, heart trouble, chest deformity or chest operation. All subjects returning questionnaires were sampled.

PROCEDURE

Prior to testing their lung function all subjects answered a modified MRC questionnaire with the help of a skilled interviewer. The subjects were asked about the presence of existing serious disease or past history of such disease and their smoking habit was recorded. The questions in Appendix C were used to assess symptoms of cough, wheeze, breathlessness and chest illnesses. All subjects were measured for standing height and their weight, both without shoes.

Each subject had three MFEM recorded using a heated PT, as previously described, with the subject seated wearing a nose clip. The PT was calibrated morning and afternoon and evening prior to each recording session. The three blows were recorded onto computer disk for subsequent reference. Each subject had one or two test blows as necessary to familiarise them with the procedure before recording commenced. A blow was rejected as unsatisfactory if time to peak flow exceeded 300 msec, if the subject coughed during the manoeuvre or if the FVC was more than 5% below that of a previous blow. Of the 265 men sampled all were able to perform three satisfactory maximal forced expiratory manoeuvres. All day workers were tested between the hours of 0930 to 1215 and 1400 to 1500 and evening shift workers were sampled between 1900 and 2100 hrs., thus avoiding the extremes of diurnal variation in performance⁽⁸⁶⁾. All cigarette smokers were asked to refrain from smoking for 2 hours prior to testing⁽⁸⁷⁾. Compliance with this request was facilitated by the fact that smoking was not permitted within the factory complex. Any subject who was suffering from or was convalescent from a

respiratory tract infection had their test deferred until they were well and 3 weeks had elapsed. ⁽⁸⁸⁾

ANALYSIS OF RECORDED MFEM

From the three blows recorded the data for statistical analysis were identified in the following way. The largest PFR, FVC, FEV₁ and FEV₃ were identified even if they occurred from different blows ⁽⁵¹⁾. The largest FVC was divided into the volumes V₂₅, V₅₀, V₇₅, V₈₅ corresponding to 25%, 50%, 75% and 85% of the largest FVC. Each of the recorded blows was scanned to determine the maximal instantaneous flow achieved when the volumes V₅₀ and V₇₅ had been expired and these flows were identified as FEF_{50%} and FEF_{75%}. In a similar way the maximal mean flows over the range V₂₅ to V₇₅ and V₇₅ to V₈₅ were determined and identified as FMF and FEF₇₅₋₈₅ respectively. In this way spuriously high values for these flow measurements due to a shortfall in FVC on one blow was avoided. The maximal forced expiratory time was identified as FET.

Of the 3 blows recorded that which had the largest sum of FEV₁ and FVC was used for moment analysis and application of the model. This follows the procedure suggested by the Snowbird Workshop ⁽⁵¹⁾ for selecting a 'best' blow. For moment analysis it is necessary to choose one blow that is a compromise between analysing that blow which demonstrates the performance of as much of the lungs as possible (i. e. largest FVC) and the blow with the fastest delivery. For example, neither a fast blow with a small FVC nor a slow blow with the largest FVC would be completely satisfactory. From the

best blow selected this way α_1 and MR were determined at 75%, 80%, 85%, 90%, 95% and 100% of the FVC of that blow and mu and sigma were found by the curve fitting algorithm.

NORMAL VALUES FOR MEN

Out of the 265 men sampled 83 were selected as normal subjects because they fulfilled the following criteria

- 1) white caucasian
- 2) smoked less than a total of 100 cigarettes in their life and had never smoked cigars or a pipe
- 3) never had any of the following - asthma, tuberculosis, heart disease, chest deformity, chest operation, bronchiectasis, treatment with any drug known to influence pulmonary function, rheumatoid arthritis or other connective tissue disease, ankylosing spondylitis, pulmonary fibrosis or sarcoidosis.
- 4) were symptom free on the questionnaire i. e. had a total aggregate symptom score of zero.

3 subjects were included in the 83 who fulfilled the first 3 criteria but each had a solitary symptom as shown below -

subject 1 - mild breathless walking up slight hills

subject 2 - produced phlegm from the throat in winter without
a cough

subject 3 - had one period of cough and sputum in the last 3 years
which lasted for 3 weeks or more.

Of the remaining 182 subjects, 29 were excluded because of ethnic origin or because of past or present disease (10 with asthma), 6 had never smoked but had significant symptoms and 147 were current or ex-smokers. These 147 men were the population used to detect abnormalities due to smoking.

The age and height distribution of the 83 men in the 'normal' population is shown in figure 6.1. Multiple linear regression of conventional and time domain spirometric indices was performed with age, height, weight and surface area as possible predictors. Surface area was not significant ($p > 0.05$) for any variable. Only for FET was weight a significant predictor. Height was not a significant predictor ($p > 0.05$) for any of the flow indices. Two subjects were excluded from the regression analysis for $FEF_{75\%}$. Figure 6.2 shows the relationship between $FEF_{75\%}$ and age. It can be seen that two young subjects have an unusually high $FEF_{75\%}$ and this is because their MFEM terminated abruptly probably due to chest wall mechanics⁽³⁸⁾. These two subjects disproportionately influenced the regression line and were therefore excluded. The regression equations for the conventional spirometric indices are shown in Table 6.1 and the multiple correlation co-efficients and residual standard deviations (RSD) are in broad agreement with those found by other workers^(63, 89, 90).

Figure 6.3 shows the relationship between age and mu and sigma. Linear regression is satisfactory for both indices. For mu the 3 subjects with extremely low mu values were excluded from the regression because of their disproportionate influence on the regression.

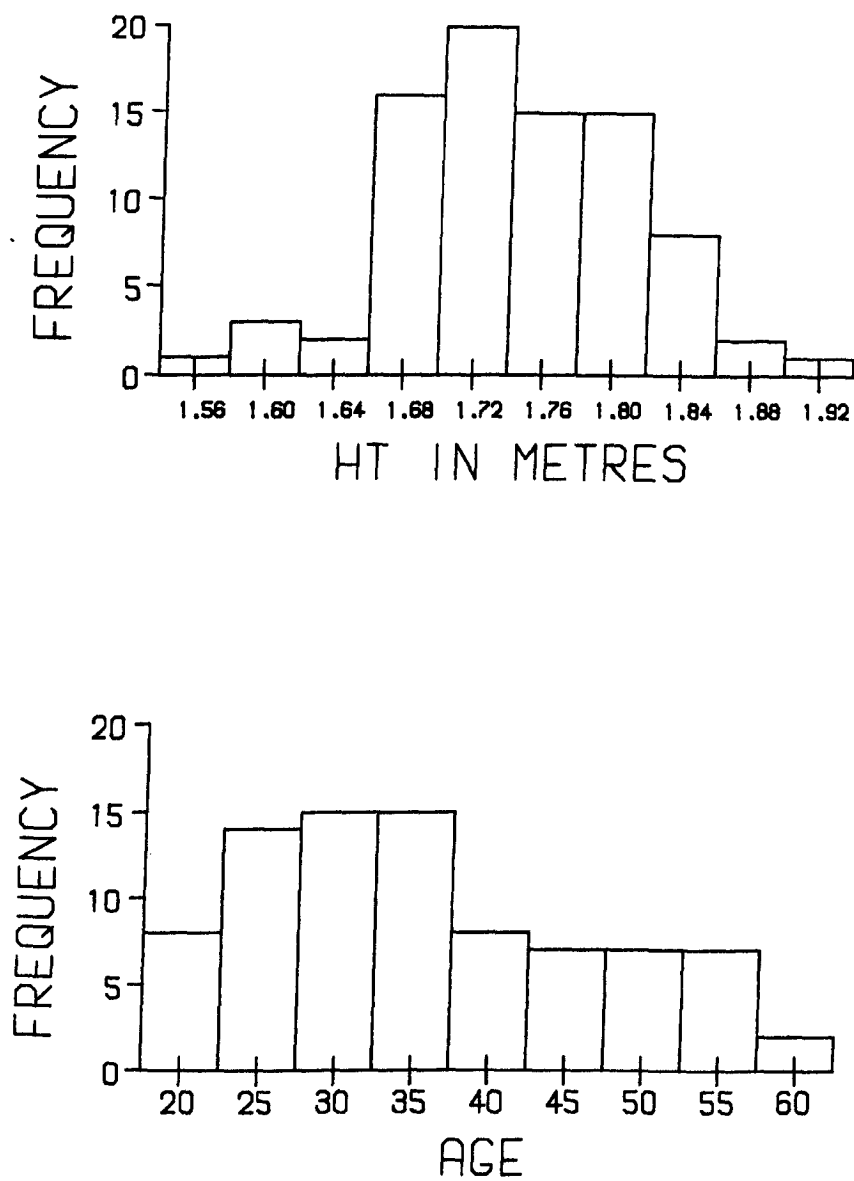


Figure 6.1 Age and height distribution for the 'normal' men.

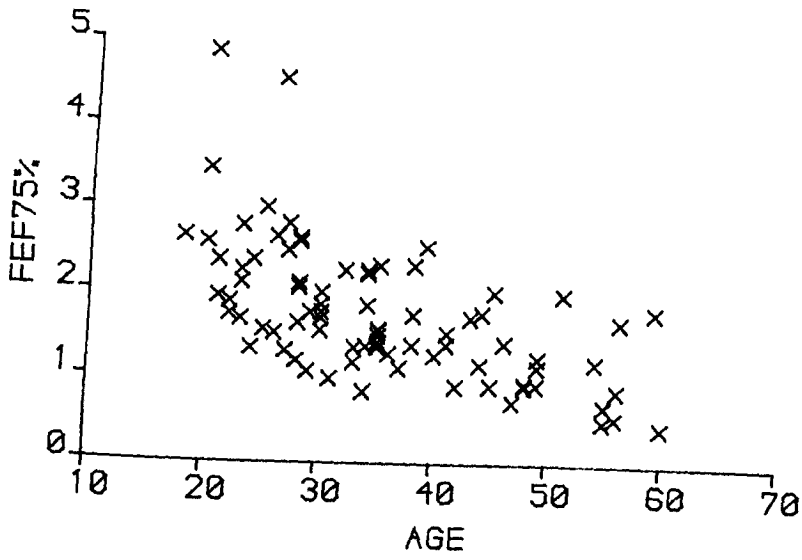


Figure 6.2 Relationship between $FEF_{75\%}$ and age for the 'normal' men

Table 6.1

Regression Equations from 83 men who had never smoked for predicting conventional spirometric indices

RSD = Residual Standard Deviation

R = Multiple Correlation Co-efficient

Height in Metres

NS = Not Significant at 5% level

Variable	Age Co-eff	Height Co-eff	Constant	RSD	R ²
FVC	-0.018	6.12	-5.16	0.47	0.56
FEV ₃	-0.031	5.63	-4.01	0.44	0.64
FEV ₁	-0.030	4.19	-2.28	0.42	0.58
PFR	-0.040	NS	11.59	1.62	0.08
FEF _{50%}	-0.050	NS	6.38	1.12	0.20
FEF _{75%}	-0.038	NS	3.03	0.50	0.42
FMF	-0.056	NS	5.84	0.93	0.31
FEV ₃ %	-0.163	-6.72	113.0	2.93	0.25
FEV ₁ %	-0.320	-20.1	128.2	5.99	0.17
FET	0.092	0.052*	-1.98	1.93	0.28

* weight co-efficient
(wt. in kgs.)

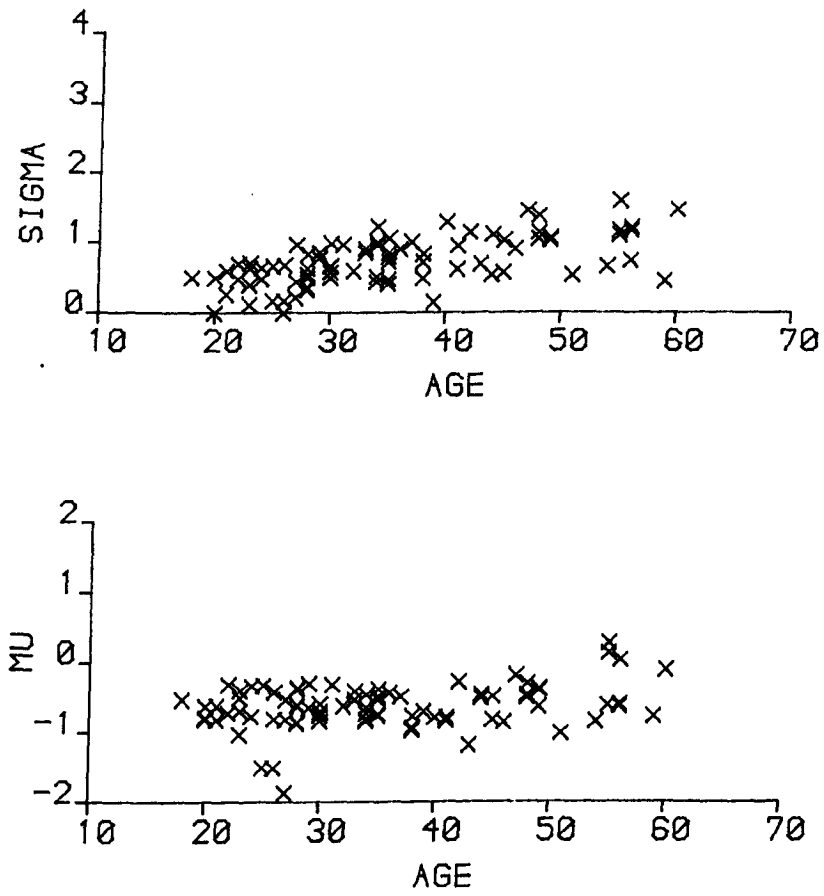


Figure 6.3 Plot of mu and sigma versus age for the 'normal' men.

These three subjects with extremely short time constants all had severely truncated spiograms and flow-volume curves with a sudden cessation of flow. These subjects probably reflect those young subjects who have their MFEM terminated by chest wall mechanics⁽³⁸⁾; two of these three subjects were those that were excluded from the FEF_{75%} regression for the same reason. Their FET values were between 1.1 and 1.4 s. All moment ratio values were satisfactory for linear regression.

For α_1 and $\sqrt{\alpha_2}$ linear regressions were not felt to be satisfactory. Figure 6.4 shows the relationship between $\alpha_1 100\%$ and age ; having performed linear regression with age and height as predictors the relationship between the predicted value and standardised residual (difference between actual result and predicted, divided by RSD) is also shown. It is evident that with increasing age the range of $\alpha_1 100\%$ found increases. This relationship is not ideal for a linear regression and this is demonstrated in the standardised residual versus predicted plot. In this plot the data should fall in a parallelogram if a linear model is satisfactory, which is not the case.

Various manipulations of the data were tried and a natural log transformation was found to be most satisfactory. Figure 6.5 shows the equivalent plots for $\log_e (\alpha_1 100\%)$ and the result is more satisfactory. $\alpha_1 100\%$ has been used to demonstrate this problem which was common to $\sqrt{\alpha_2}$ and found at all levels of truncation. The regression equations for the time domain indices are shown in tables 6.2 and 6.3. For α_1 and $\sqrt{\alpha_2}$ the multiple correlation co-efficient

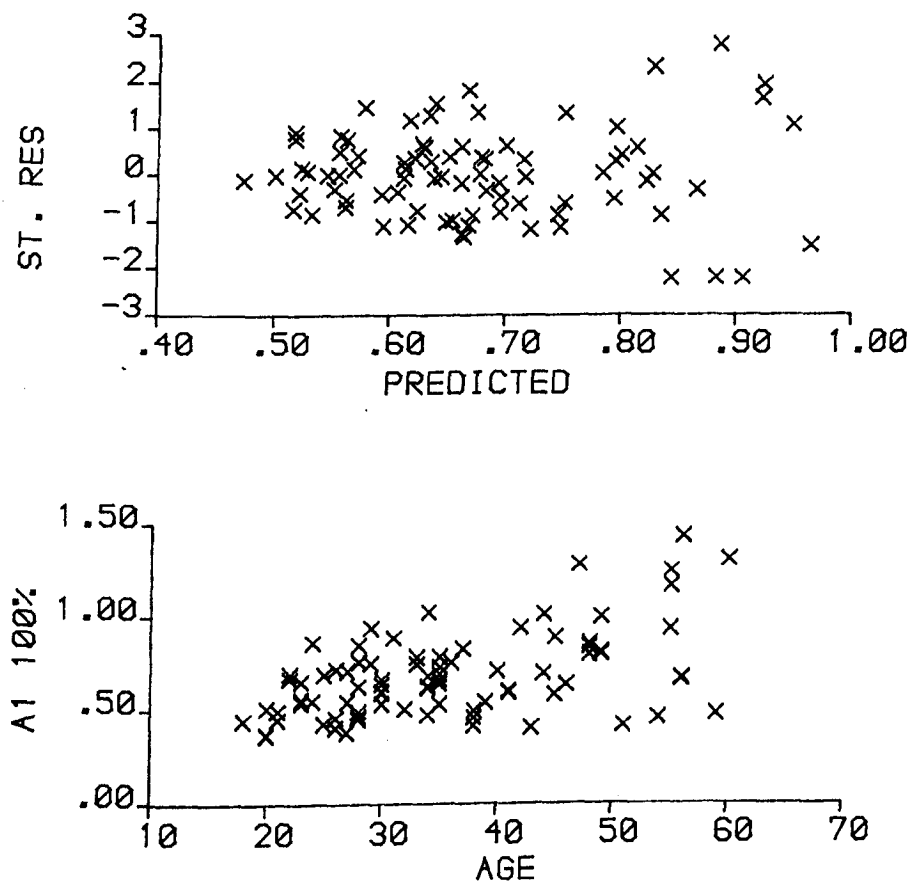


Figure 6.4 Plot of $\alpha_1 100\%$ versus age and the standardised residual versus predicted $\alpha_1 100\%$ for the 'normal' men.

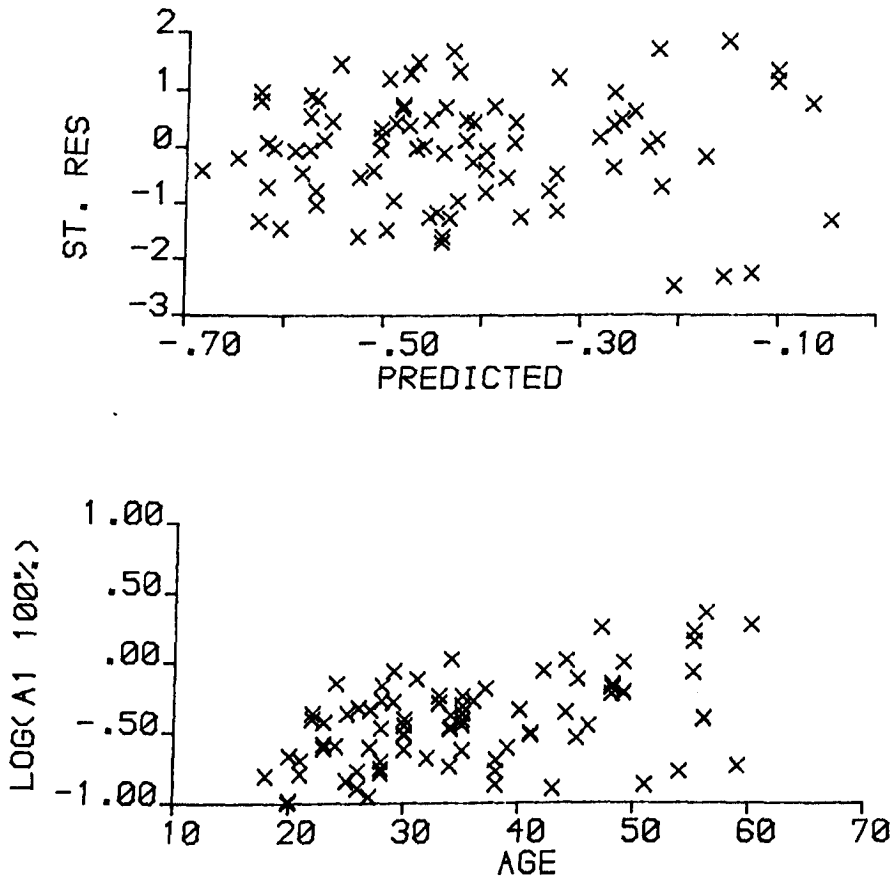


Figure 6.5 Plot of $\log_e (\alpha_1 100\%)$ versus age and the standardised residual versus predicted $\log_e (\alpha_1 100\%)$ for the 'normal' men.

Table 6.2

Regression equations from 83 'normal' men for predicting the natural log of α_1 and $\sqrt{\alpha_2}$

RSD = Residual Stand Deviation

R = Multiple Correlation Co-efficient

Height in metres

<u>Log variable</u>	<u>Age co-eff</u>	<u>Height co-eff</u>	<u>Constant</u>	<u>RSD</u>	<u>R²</u>
α_1 75%	0.005	1.15	-3.46	0.21	0.14
α_1 80%	0.006	1.15	-3.38	0.22	0.15
α_1 85%	0.008	1.13	-3.27	0.22	0.17
α_1 90%	0.010	1.10	-3.14	0.23	0.20
α_1 95%	0.012	0.97	-2.80	0.25	0.23
α_1 100%	0.014	0.72	-2.18	0.27	0.24
$\sqrt{\alpha_2}$ 75%	0.006	1.17	-3.33	0.22	0.15
$\sqrt{\alpha_2}$ 80%	0.008	1.16	-3.23	0.23	0.17
$\sqrt{\alpha_2}$ 85%	0.011	1.13	-3.09	0.25	0.20
$\sqrt{\alpha_2}$ 90%	0.013	1.07	-2.90	0.26	0.24
$\sqrt{\alpha_2}$ 95%	0.016	0.84	-2.35	0.29	0.27
$\sqrt{\alpha_2}$ 100%	0.018	0.38	-1.27	0.33	0.27

Table 6.3

Regression equations from 83 'normal' men for predicting moment (MR), mu and sigma

RSD = Residual Standard Deviation

R = Multiple Correlation Co-efficient

Height in metres

NS = Not Significant at the 5% level

<u>Variable</u>	<u>Age Co-eff</u>	<u>Height Co-eff</u>	<u>Constant</u>	<u>RSD</u>	<u>R²</u>
MR 75%	0.002	NS	1.19	0.04	0.29
MR 80%	0.003	NS	1.19	0.04	0.34
MR 85%	0.004	NS	1.19	0.05	0.38
MR 90%	0.005	NS	1.20	0.07	0.40
MR 95%	0.006	NS	1.23	0.09	0.38
MR 100%	0.006	-0.54	2.32	0.14	0.27
mu	0.008	1.39	-3.30	0.24	0.19
sigma	0.019	NS	0.07	0.28	0.37

- 140 -

increased with later truncation, but for MR this fell off after 90% truncation.

ABNORMALITIES IN MALE SMOKERS

(i) Identification of abnormal smokers.

The age and height distributions of the 147 smokers are shown in figure 6.6. Using the regression equations from the 'normal' subjects predicted values for each index were determined for the 147 male smokers. Any smoker who had a recorded index value that was more than 2 RSD outside the abnormal end of the predicted values was identified. By 'abnormal end' is meant low values for volumes and flows and high values for all the time domain indices. The same procedure was applied to the 'normals' for comparison. For a normally distributed population, one expects 2.5% of the population to lie more than 2 RSD abnormal for any test. Therefore one could expect to identify 2 'normals' and 3 to 4 smokers abnormal by these criteria for any test. The number of subjects so identified for each test is shown in table 6.4.

It is evident from this table that of conventional indices $FEV_3\%$ and $FEV_1\%$ were the most sensitive to abnormalities in individual smokers and that the flow indices were not so rewarding. μ , α_1 and $\sqrt{\alpha_2}$ detected more subjects as abnormal than did sigma and MR; α_1 and $\sqrt{\alpha_2}$ and MR were less rewarding with later truncation. It may be argued that the moments at the end of the spirogram are identifying a smaller but more important group of abnormalities. However, only 3 individuals had an abnormal α_1 100% but were normal

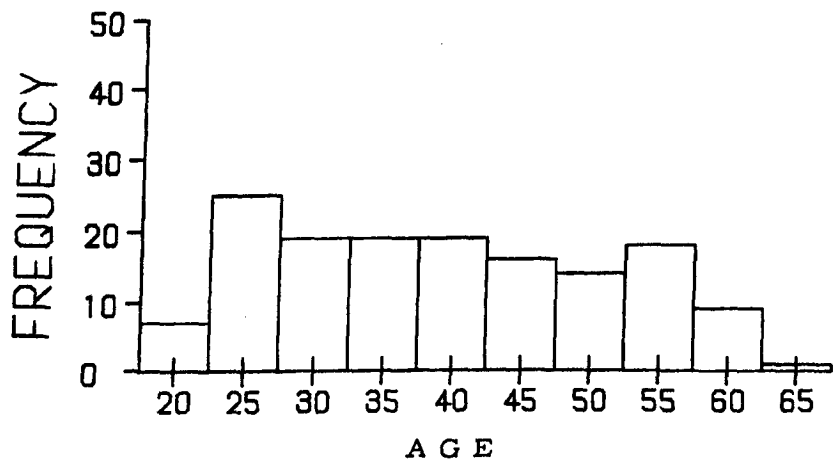
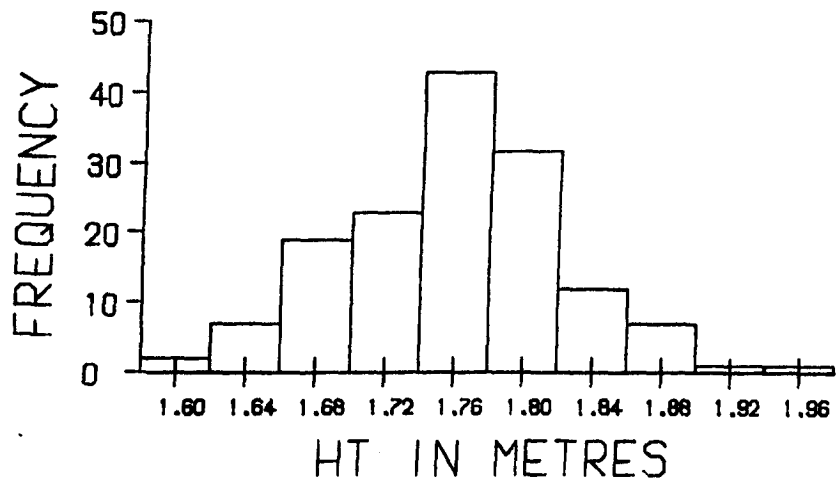


Figure 6.6 Age and height distribution of the male smokers

Table 6.4

The number of subjects more than 2 RSD 'abnormal' for each test, the number more than 3 RSD shown in brackets.

The expected number for a normal distribution would be 2 Non-Smokers and 3-4 Smokers.

	NON-SMOKERS	SMOKERS	
FVC	3	2	
FEV	2	5	
FEV ₃ ^{3%}	3	16	(9)
FEV ₃ ^{1%}	2	5	(1)
FEV ₁ ^{1%}	0	13	(3)
FET ₁	4	14	(5)
FMF	1	4	
PFR	3	6	
FEF ₅₀	1	6	
FEF ₇₅	0	1	
mu	4	17	(8)
sigma	0	7	(3)
α_1 75%	4	19	(5)
α_1 80%	3	17	(5)
α_1 85%	2	16	(4)
α_1 90%	1	15	(4)
α_1 95%	1	17	(3)
α_1 100%	0	12	(2)
$\sqrt{\alpha}_2$ 75%	3	17	(5)
$\sqrt{\alpha}_2$ 80%	2	16	(4)
$\sqrt{\alpha}_2$ 85%	1	13	(4)
$\sqrt{\alpha}_2$ 90%	0	16	(4)
$\sqrt{\alpha}_2$ 95%	0	12	(2)
$\sqrt{\alpha}_2$ 100%	0	8	(1)
MR 75%	2	12	(5)
MR 80%	3	10	(6)
MR 85%	3	10	(5)
MR 90%	4	7	(4)
MR 95%	1	7	(1)
MR 100%	1	2	

up to and including $\alpha_1 90\%$, and these 3 subjects also had the most extreme abnormalities found for MR90%. All the remaining subjects with abnormal $\alpha_1 100\%$ had an even more abnormal $\alpha_1 75\%$. The 3 subjects with the most extreme abnormalities in MR90% were showing an altered dispersion of time constants at a point in the manoeuvre when α_1 and $\sqrt{\alpha_2}$ on their own were not abnormal. It is evident that the last 10% in volume contributed nothing to the identification of abnormal subjects in smokers. All the smokers with abnormalities in the time domain had declared themselves abnormal by the time 90% of the FVC had been expired.

(ii) Patterns of Abnormality

Many of the subjects identified as abnormal by one test were also identified as abnormal by other tests. Therefore all the individuals with any test > 2 RSD abnormal had their pattern of abnormality demonstrated graphically. As there were 10 stable asthmatics sampled and coded for separately, the 7 asthmatic subjects with abnormalities had their pattern of spirogram abnormality demonstrated in figure 6.7, as a guide to the interpretations of the patterns. The height of the histograms in figure 6.7 and the subsequent figures represents the magnitude of the abnormality above 2 RSD, with the dots each representing 0.5 RSD increments to a maximum of 4 RSD. Any abnormality of more than 4 RSD was plotted as 4 RSD for simplicity as these all represent extreme abnormalities. Those tests with overall the highest number of subjects abnormal were placed to the left with decreasing order to the right.

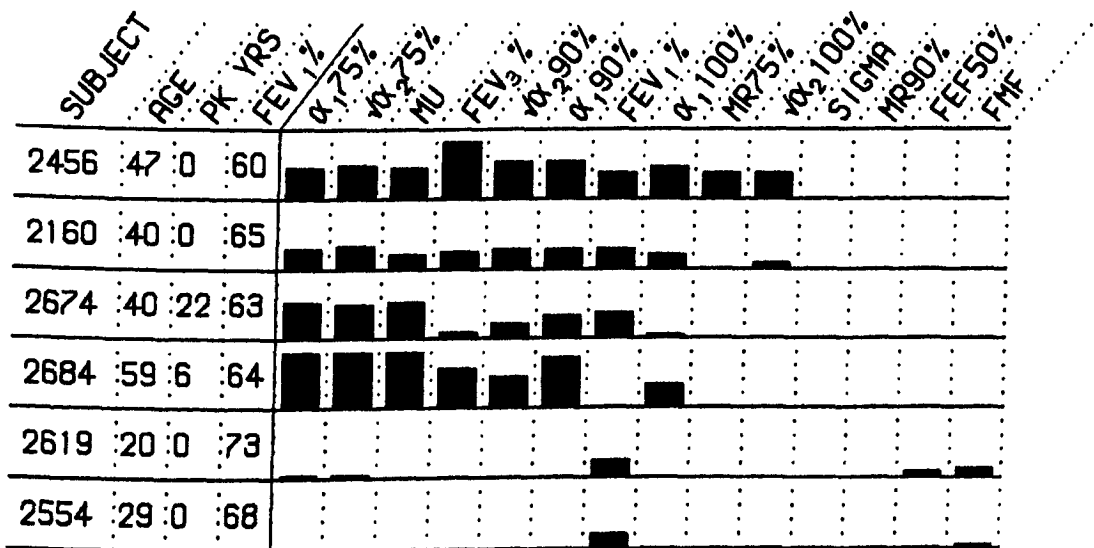


Figure 6.7 Patterns of spirometric abnormalities in the asthmatics.

Details of subject number, age, pack years smoking exposure and recorded FEV₁% are to the left. Histograms indicate the magnitude of the abnormality for each spirometric index expressed in terms of the number of RSD above 2 RSD. Each dot represents 0.5 RSD increments above 2 RSD. Any index abnormal by more than 4 RSD has been plotted as 4 RSD for simplicity.

A. Asthmatics

The pattern of abnormality found in the asthmatics is shown in figure 6.7. These subjects who had mild asthma, had never required admission and who were in remission at the time of the test showed a pattern with abnormalities in α_1 , $\sqrt{\alpha_2}$, μ and $FEV_1\%$ but with normal σ and MR 90% (MR 75% abnormal in one subject). The flow indices were poor in identifying abnormalities. The normal MR and σ with high α_1 and μ is consistent with a generalised effect over the lungs slowing the delivery of gas in a roughly uniform manner throughout the lungs. In more marked asthma the σ value has been found to be high but this change was not as marked as the change in μ ⁽³⁹⁾.

B. 'Normal' subjects

The pattern of abnormalities in the normal subjects is shown in figure 6.8. Seven subjects have only 1 test abnormal, 4 subjects have abnormalities in μ and α_1 75% and 2 subjects have abnormalities in MR 90% and $FEV_3\%$ only. These 2 subjects have abnormalities consistent with a difference only in the latter part of the spirogram whereas the group of 4 have abnormalities in the early part of the spirogram.

C. Smokers

Thirty smokers were found to have abnormalities which could be grouped into three patterns:

Pattern I is shown in figure 6.9 and was found in 17 smokers. This pattern was typified by abnormalities in α_1 75%, $\sqrt{\alpha_2}$ 75% and μ .

The pattern was similar to that seen in the asthmatics. Only 4 of these subjects had abnormal σ values and those 4 were among the most

SUBJECT	AGE	PK	YRS	FEV ₁ %	$\alpha_{175\%}$	$\alpha_{75\%}$	MU	FEV ₉ %	$\alpha_{90\%}$	$\alpha_{90\%}$	FEV ₁ %	$\alpha_{100\%}$	MR75%	$\alpha_{100\%}$	SIGMA	MR90%	FEF50%	FHF
243	56	0	66															
272	30	0	76															
447	55	0	66															
439	55	0	64															
143	55	0	72															
669	47	0	71															
135	56	0	75															
598	48	0	76															
595	34	0	77															
223	40	0	82															
548	38	0	88				*											
398	57	0	75				*											
206	31	0	73						*									

Figure 6.8 Patterns of spirometric abnormalities in the 'normal' men.

* indicates the abnormality was only in the absolute FEV_n and not in FEV_n%.

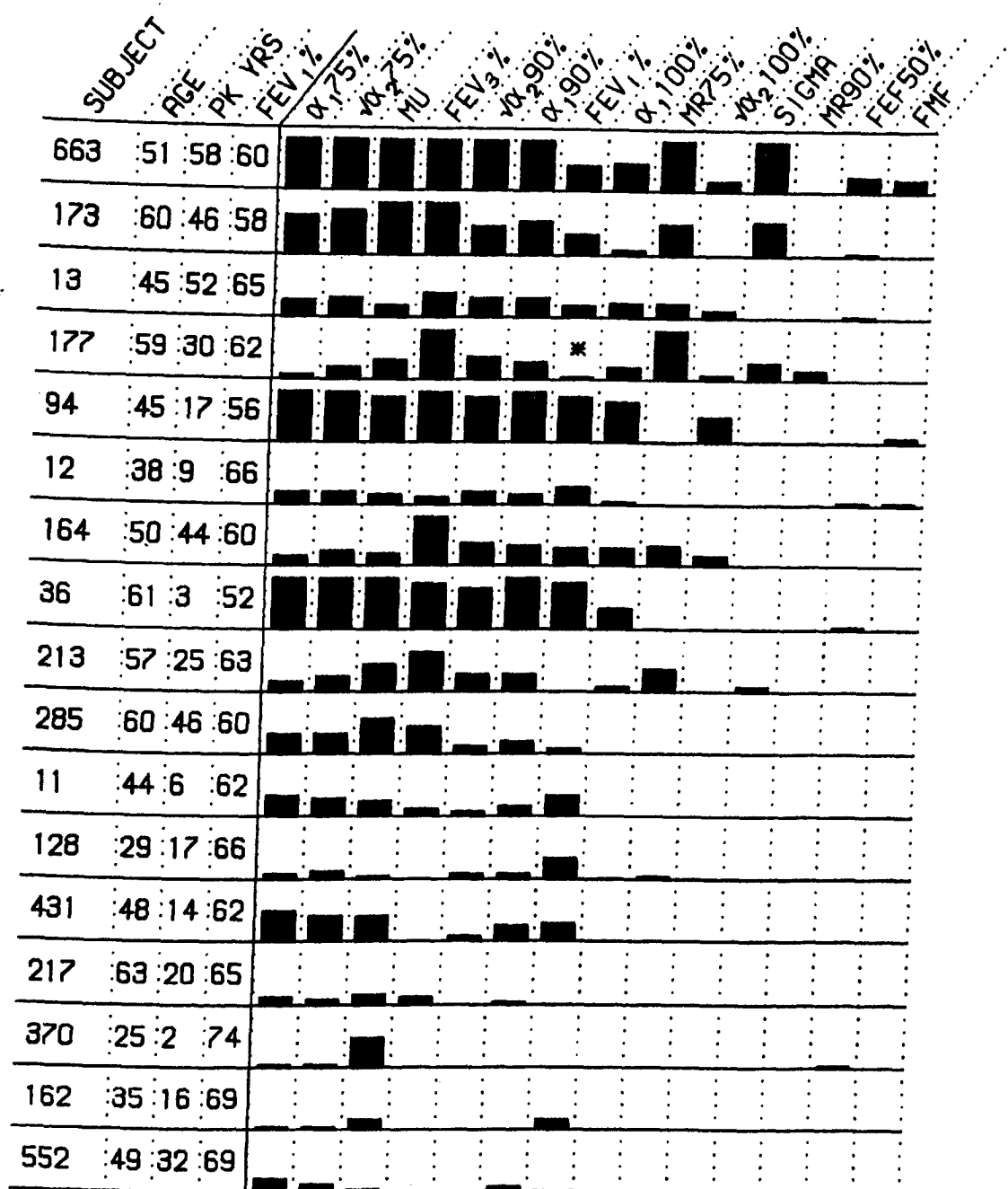


Figure 6.9 Pattern I of spirometric abnormality in the male smokers.

* indicates the abnormality was only in the absolute FEV_n and not in $FEV_n\%$.

abnormal subjects. Only one of these 4 had an abnormal MR 90%, although all had abnormal MR 75%. For all the 256 subjects sampled in the study the correlation between sigma and MR was highest for MR 85% ($r = 0.96$). The lack of agreement between the abnormalities in sigma and MR 90% in these 3 smokers probably reflects truncation errors reducing MR 90% and thus making them fall within normal limits. Whereas for MR 75% the truncation errors were smaller and hence it was a better reflection of the abnormal dispersion.

Pattern II is shown in figure 6.10 and was typified by abnormalities in $FEV_3\%$ and/or MR 90% without abnormalities in μ , $\alpha_1 75\%$ and $\sqrt{\alpha_2} 75\%$. 6 smokers had this type of abnormality which represents an abnormality only in the tail of the spirogram, the early part being normal.

Pattern III is shown in figure 6.11 and represents the 7 smokers with isolated abnormalities and these subjects can be regarded as normal.

From inspection of the data in figures 6.9 and 6.10 it appears that the degree of exposure to cigarette smoke in terms of pack years is comparable for the smokers who had Pattern I and Pattern II, and there was no statistically significant difference between them ($p > 0.05$). The mean exposure for all the smokers was 16.5 pack years with a standard deviation of 17.3 and range of 0.05 to 110.2.

A comparison of symptoms recorded for the smokers with Patterns I and II is shown in table 6.5

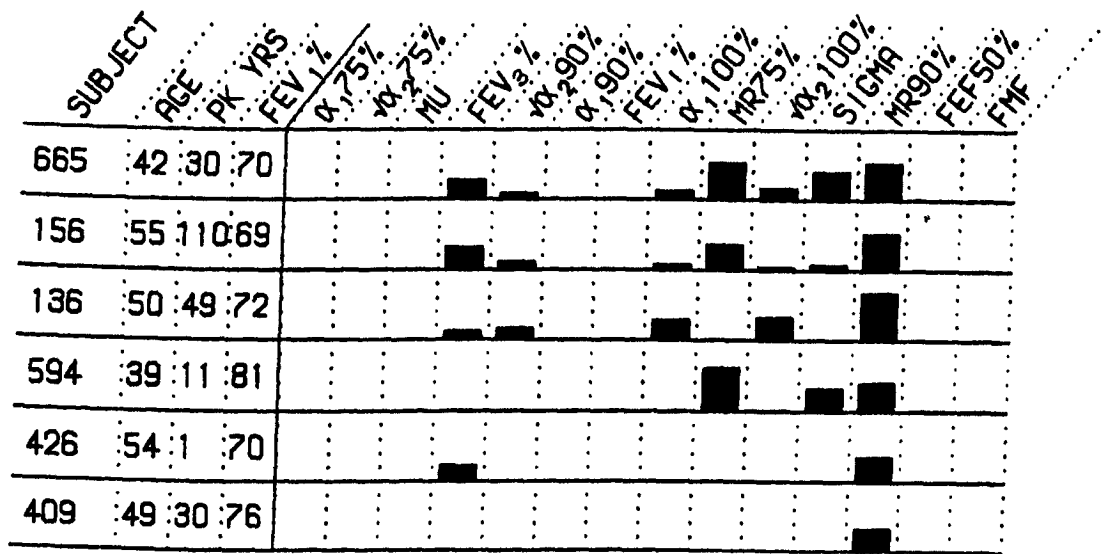


Figure 6.10 Pattern II of spirometric abnormality in the male smokers.

SUBJECT	AGE	PK	YRS	FEV ₁ %	$\alpha_{1.75\%}$	$\alpha_{2.75\%}$	MU	FEV ₃ %	$\alpha_{2.90\%}$	$\alpha_{1.90\%}$	FEV ₁ %	$\alpha_{1.100\%}$	MR75%	$\alpha_{2.100\%}$	SIGMA	MR90%	FEF50%	FME
413	47	55	78															
582	27	3	73															
519	23	7	73															
535	33	28	71															
356	54	13	69															
100	32	6	69															
70	30	12	78				*											

Figure 6.11 Pattern III of spirometric abnormality in the male smokers.

* indicates the abnormality was only in the absolute FEV_n and not in FEV_n%.

Table 6.5

The number of smokers with Pattern I and Pattern II with specific groups of symptoms (Appendix C)

<u>Symptom</u>	<u>Pattern I</u>		<u>Pattern II</u>	
	7 current	10 ex-smokers	3 current	3 ex-smokers
Wheeze		8		3
Cough		5		0
Phlegm		3		0
Breathlessness		3		1
Periods of cough		4		1
Chest illnesses		0		1
No symptoms		8		2

The only apparent difference between the groups was that Pattern I had a greater proportion of subjects with cough and phlegm and these subjects had very high cough and phlegm scores (Appendix C).

DISCUSSION

Disabling chronic airflow limitation (CAL) has been found to occur in only a minority of smokers^(34, 94) and chronic bronchitics⁽⁹⁵⁾ and there is an increased morbidity and mortality in those subjects with the most severe reduction in FEV_1 ⁽⁹⁶⁾ and those who continue to smoke^(94, 95). A low FEV_1 and/or $FEV_1\%$ are the hallmarks of clinically significant CAL being related to both a patient's and a clinician's perception of disease⁽⁹⁷⁾. It has been recognised that changes in FEV_1 occur late in the process of lung damage due to smoking and so attention has turned to the early identification of those

smokers who will later develop disabling CAL.

The present study has explored a more rigorous analysis of the spirogram to determine the natural history of the spirogram from health to disease (figure 2.1). This approach does not directly investigate the mechanism or site of lung damage due to smoking but seeks to improve the clinically useful information from a relatively simple test of ventilatory performance which remains the mainstay of diagnosis and prognosis of CAL. However, time domain analysis of spirograms does afford indirect evidence to test the current hypothesis concerning the development of CAL due to smoking.

Dosman and Macklem⁽⁹⁸⁾ hypothesised that there is a sequential progression of abnormalities which begins with obstruction of small airways. After an unspecified time changes occur in the mechanical properties of alveoli and ultimately there is a loss of elastic recoil of the lungs. Finally the FEV_1 diminishes and clinically recognisable lung disease ensues. It is pertinent to review some of the evidence leading to this hypothesis before discussing the present survey in this context.

A wealth of evidence has accumulated implicating abnormalities of small airways in smokers. Qualitative changes in regional gas exchange were found in subjects who had mild chronic bronchitis and minimal spirometric abnormalities⁽⁹⁹⁾. Those changes were attributed to abnormalities in small airway performance. Using retrograde intrabronchial techniques it was found that airways of

less than 2mm internal diameter (ID) contributed little to overall lung resistance^(81, 100) and could harbour marked abnormalities in chronic obstructive lung disease with little change in overall ventilatory performance⁽¹⁰¹⁾.

As interest in small airways performance developed the frequency dependence of compliance⁽¹⁰²⁾ and closing volume⁽¹⁰³⁾ were proposed as tests sensitive to small airway function. Frequency dependence of compliance did not lend itself as a useful test because of the difficulty in performing and recording the manoeuvres required. Furthermore, both large and small airways defects can cause frequency dependence of compliance⁽¹⁰⁰⁾ and the degree of collateral ventilation present may to a large extent determine the frequency dependence.

Buist et al^(104, 105) measured closing volume on a large number of selected smokers. The percentage of their smokers with abnormal tests was, 44% for closing capacity, 47% for slope of alveolar plateau, 21% for FMF and 11% for FEV₁, where abnormality was defined as more than 1.65 residual standard deviations above normal. However, this proportion of smokers with abnormal 'small airways' tests suggests that these tests may not be useful in detecting the smaller percentage of smokers who later develop CAL. A similar percentage of smokers had abnormal closing capacity in a less selected group of subjects⁽⁸⁵⁾. No long term prospective studies have yet been completed which demonstrate the predictive value of closing volume and the slope of alveolar plateau. The possibility remains that they may only

be sensitive to relatively non-specific effects of smoking, for instance, mucus plugging of small airways.

Several indices from the maximal forced expiratory manoeuvre (MFEM) have been proposed as tests of small airways function although there is little evidence to substantiate this claim. Macklem and Mead⁽⁸¹⁾ in animal experiments found that airways of less than 2mm ID only began to contribute significantly to overall lung resistance at lung volumes of less than 30% of vital capacity. Therefore interest has been shown in indices from the terminal part of the MFEM. FEF_{75%} was thought to be a promising index⁽⁸³⁾ although its wide range of normal values limits its usefulness in individuals^(22, 63). McFadden et al⁽¹⁰⁶⁾ found FMF to be abnormal in smokers when FEV_{1%} was normal and also found it to be more often abnormal than closing volume⁽¹⁰⁷⁾. However, they defined abnormal as less than 80% of predicted value and this definition has no physiological or statistical basis for defining abnormality⁽¹⁰⁸⁾. If the lower 95% confidence limit for a test is expressed as a percentage of predicted value it can vary widely according to the relationship between the residual standard deviation (which is constant) and the predicted value being considered. This would lead to more 'abnormalities' being defined for FMF than for FEV_{1%} because the above relationship varies more for FMF than for FEV_{1%}.

In the study presented here FEF_{75%} and FMF were not as sensitive as FEV_{1%} in detecting individuals with abnormalities. The influence of the use of percent of predicted value can be appreciated

from figure 6.2. The variability of $FEF_{75\%}$ at any age is roughly the same (apart from the two young subjects excluded) so 95% confidence limits can be clearly defined. 80% of predicted $FEF_{75\%}$ for the older age groups would leave many of the normal group below this limit. The poor showing of flow indices in this survey may be because the influence of the blow to blow variability of FVC on the flow indices ⁽¹⁰⁹⁾ was taken into account ⁽⁶³⁾. The chosen $FEF_{75\%}$ was the highest flow recorded at an expired volume equal to 75% of the largest recorded FVC.

Evidence that tests such as closing volume truly reflect the performance of airways of less than 2mm ID was presented by Cosio et al ⁽⁷⁸⁾. They examined lungs resected for localised pulmonary lesions in subjects who had previously performed detailed lung function tests. They found that only closing volume and slope of alveolar plateau distinguished between their mildest grades of small airway pathology, whereas $FEV_1\%$ and FMF could not. However all their data on pulmonary function was expressed as percent of predicted and this could have led to substantial errors when defining abnormalities of closing volume and slope of alveolar plateau ⁽⁸⁴⁾.

It was with this background that alternative ways of extracting information from the MFEM were explored. Increasing curvilinearity of flow-volume curves has been noted to accompany chronic airflow limitation and several methods for describing this have been tried ⁽²²⁻²⁵⁾. None have found wide acceptance and Mead's slope ratios ⁽²⁵⁾ have been found to lack reproducibility ⁽²⁶⁾. Moment analysis of spiograms

was proposed as a different approach to analysis of the MFEM.

Early studies^(24, 29) confirmed that it was as sensitive to smoking damage as both conventional indices from the MFEM and other tests deemed sensitive to small airways disease.

Moment analysis and the model described in this thesis allow the hypothesis proposed by Dosman and Macklem⁽⁹⁸⁾ to be tested indirectly. If small airways disease gradually progresses until eventually FEV_1 is diminished then the first changes in the spirogram should be manifest in the terminal part of the manoeuvre. Therefore one would expect abnormalities in sigma, moment ratio (MR) and $\sqrt{\alpha_2}$ rather than in α_1 to be the early signs of this progression.

The findings of the survey presented in this thesis do not fulfil this expectation. Sigma and MR detected fewer abnormal subjects than did mu and α_1 . Furthermore, α_1 75% detected more abnormal subjects than did the later moments and α_1 was slightly more sensitive than $\sqrt{\alpha_2}$. Webster et al⁽²⁴⁾ also found α_1 more discriminatory than α_2 .

One explanation for this unexpected finding is that the terminal 30% in volume of the spirogram is known to be less reproducible than the earlier part and it is more susceptible to changes in a subject's effort. This variability was noted in the repeatability study presented in Chapter 4 and might lead to difficulty in distinguishing signal from noise in the tail of the spirogram. However, if this were the case one would expect that the multiple

correlation coefficient of the regression would be smaller for the later moments and that the residual standard deviation would increase dramatically in relation to the predicted value of the later moments. Neither of these expectations was found. Although the variability of any given truncated moment increases with age, thus necessitating the log transformation, this variability was not especially worse for later truncation.

The moments were able to identify some subjects whose abnormalities were restricted to the tail of the spirogram. Three smokers were normal up to and including $\alpha_1 85\%$ but had abnormal $\alpha_1 95\%$ and $\alpha_1 100\%$. These 3 subjects also had extreme abnormalities of MR90% and thus fulfil the expectation of Dosman and Macklem's hypothesis. These abnormalities are consistent with a patchy small airways abnormality. A further 3 smokers had similar abnormalities and together they comprise the group with Pattern II abnormalities (figure 6.10). These all had normal $\alpha_1 75\%$, μ , FEV_1 and $FEV_1\%$. Thus despite the greater variability of the tail of the spirogram the moments were able to identify subjects with abnormalities only in this region. However, this variability probably accounted for the lower number of smokers with abnormal $\alpha_1 100\%$, compared with the earlier moments.

A much larger group comprising 17 smokers was identified with abnormalities in the early part of the MFEM i. e. with abnormal $\alpha_1 75\%$ and μ (Pattern I, figure 6.9). The expectation from the hypothesis is that there should be more smokers found with Pattern II

than Pattern I and this discrepancy requires explanation. If the transition phase from a predominantly small airways abnormality to more generalised disease and diminished FEV_1 was short then a cross-sectional survey would catch only a few subjects in this transition phase. If this were true then the subjects in this short transition might be expected to be younger and lighter smokers whereas the age and pack-years exposure of the subjects with Pattern II is not dissimilar from those with Pattern I. Furthermore, other evidence suggests that the transition phase is long rather than short, although it is conceivable that the transition from spirometrically detectable 'small airways' disease to diminishing FEV_1 may be short.

If the subjects with Pattern II are in transition to the group with Pattern I then one would expect some overlap. Two subjects with Pattern I (numbers 177 and 213, figure 6.9) look as if they may have arisen from the group with Pattern II. However, it seems just as probable that there are two separate patterns of response. One is manifest as abnormalities only in the tail of the spirogram. The other shows abnormalities early on in the MFEM, which in this cross-sectional survey seem to have a gradation suggesting a progression to those abnormalities recognised as CAL. Within this progression abnormalities also become evident in the tail of the spirogram, just as they are in some smokers without any abnormalities early on in the manoeuvre. This sort of interpretation is conjectural but the demonstration by moment analysis of two hitherto undescribed patterns of abnormality offers a possible means

for testing the Dosman and Macklem hypothesis in a prospective survey.

Several factors may confound such interpretations. Inadvertent inclusion of asthmatic subjects would lead to a bias towards Pattern I abnormalities. Great care was taken with the questionnaire to ensure that subjects with a diagnosis of asthma, or who had had wheeze at a young age, or who showed marked day to day or within day variation in wheeze were all coded as asthma. The cumulative prevalence of asthma for the men in this survey was 3.8%. This is of the right order⁽¹¹⁰⁾ confirming that this method of coding was satisfactory. Wheeze as a symptom was equally common in smokers with Pattern I and Pattern II which also suggests that inadvertent inclusion of asthmatics did not account for the difference in numbers with the two patterns. Recent upper respiratory tract infections could not have accounted for these differences as all subjects with symptoms suggesting such an infection in the three weeks prior to testing were deferred for the appropriate time and none of the smokers with Patterns I and II were so deferred.

Comparison of the survey presented here with other surveys using moment analysis is difficult for several reasons. This thesis has outlined several sources of important errors in the work of others. These include incorrect truncation at 6 seconds^(24,28-30,91), inappropriate analysis about the mean for the higher moments^(26,30,31,33,91,92) and the use of spirometers to record the spiograms^(24,29-31,33,65,91-3). Furthermore, the computation

of the moments by many groups of workers included substantial quantitising errors which would vary with the shape of spirogram analysed (26, 28, 29, 32, 33, 93).

The limit of normality for the tests in this survey was defined as a 98% one-sided confidence interval i. e. 2 RSD on the appropriate side of the mean. Some studies have used a 95% one-sided confidence interval^(84, 85, 104, 105). If the object of new tests of ventilatory performance is to identify with certainty individuals with abnormalities early on in the disease process and then try to relate these to outcome it seems sensible to adopt the higher confidence interval so that interpretation is not confounded by too many false positives in the smoking group. Reducing the one-sided confidence interval from 98% to 95% increases the percentage of smokers in this study defined as abnormal from 3.4% to 6.8% for FEV₁, from 8.8% to 13.6% for FEV₁% and from 12.9% to 17% for α_1 75%. This change in definition of abnormality would add one smoker to the group with Pattern II and five smokers to Pattern I.

The smokers in this survey have been generally lighter smokers than in other surveys with mean pack years of 16.5 with SD = 17.3. The smokers studied by Nemery et al⁽⁸⁵⁾ had a mean pack years exposure of 32.0 ± 14.2 and 35% of these smokers had an FEV₁% outside the one-sided 95% confidence limit defined from their non-smokers, whereas only 13.6% of the smokers in this study were similarly abnormal. Therefore this study is not biased

towards the more severe ventilatory abnormalities which were found in a more heavily exposed group.

If the results from this survey do not concur with the expectations from Dosman and Macklem's hypothesis then two premises relating to their hypothesis must be questioned. The first premise is that the terminal part of the MFEM especially reflects the performance of small airways. Although Macklem and Mead⁽⁸¹⁾ found that in animals the resistance of airways of less than 2mm ID only began to rise over the lower 30% of lung volume, this resistance rose to only 20% of total resistance because of the concomitant rise in central airway resistance. These experiments were not conducted with the airways dynamically collapsed as they would be during an MFEM. Macklem et al⁽¹¹¹⁾ recorded intra-bronchial pressures in patients with emphysema and chronic obstructive lung disease under conditions of maximum flow. They found in all subjects that as lung volume decreased from 75% of VC to 25% of VC the resistance distal to the segmental bronchi increased by approximately 50% whereas the central resistance increased by 600%. This distribution of resistance was similar to that of the animal work. Hence the premise that the terminal part of the MFEM is especially sensitive to small airways performance depends on which size of airways at a particular lung volume are limiting flow.

In normal subjects flow limitation is thought to be between segmental bronchi and trachea⁽¹¹²⁾. Out of 9 subjects with chronic obstructive lung disease Macklem et al⁽¹¹¹⁾ found that in two subjects

flow limitation at 50% VC occurred in airways distal to segmental bronchi. In 5 subjects lobar bronchi were flow limiting at 50% of VC and in the remaining 2 subjects flow limitation appeared to be from both peripheral and central airways. These latter 2 subjects showed no evidence of central airway limitation at a higher lung volume (75% of VC). Thus despite all evidence suggesting the presence of small airways disease in smokers the majority of the subjects they tested with CAL seemed to have large airway flow limitation evident. Interestingly the 2 subjects with airflow limitation distal to the segmental bronchus were demonstrating this at 50% VC i. e. quite early on in the manoeuvre. Therefore, it is difficult to be certain that the terminal part of the MFEM is in any way specifically sensitive to small airways disease.

The second premise relating to the hypothesis is that small airways disease is an important determinant of susceptibility to developing CAL. Only long term prospective studies will answer this point.

The author has reservations about interpreting any tests from an MFEM in terms of large and small airways effects. However if small airways effects are assumed to be dominant in the group of smokers in this survey then the following interpretation can be made. Pattern II abnormalities are consistent with a patchy small airways effect causing a relatively small proportion of the lungs to empty as a slow space. Pattern I abnormalities would have to be caused by a diffuse small airways effect making the whole of the lungs

empty as a slow space. This implies that each of over 2000 airways of 1 mm diameter would have to be uniformly affected whereas post-mortem studies suggest that the changes in such airways are patchy in severity and distribution⁽⁷⁹⁾. However, if only a few small airways are diseased the functional effect of this may spread to adjacent airways because the pressure that cannot be dissipated by displacing gas down the diseased airways may adversely affect adjacent airways. Also the mechanical properties of adjacent airways may be influenced by the presence of compressed trapped gas upstream (distal) to diseased airways.

An alternative explanation for Pattern I abnormalities is that it is large and not small airways that are flow limiting in these subjects. Pathological studies⁽¹¹³⁻¹¹⁵⁾ of bronchi in subjects with chronic obstructive lung disease have shown loss of bronchial cartilage predominantly in segmental and subsegmental bronchi and these airways were more compliant than those of non-smokers. What was less clear was whether the affected bronchi were flow limiting. The work of Macklem et al⁽¹¹¹⁾ suggests that major bronchi can be a site of limitation in chronic obstructive lung disease.

The use of breathing 80% helium and 20% oxygen (He-O₂) has been suggested as a means of determining whether flow limitation is in small or large airways. Despas et al⁽¹¹⁶⁾ found that in smokers FEF_{50%} did not increase as much with He-O₂ as it did in normal subjects. They attributed this to the fact that the density dependent increase in flow expected with He-O₂ breathing will only occur if flow limitation occurs in regions of turbulence

where flow depends on both gas viscosity and density. Laminar flow is dependent on viscosity and not density so they suggested that in their subjects with chronic obstructive lung disease $FEF_{50\%}$ was flow limited in regions of laminar flow i. e. small airways. Added to this was the evidence that density dependence of flow declined with age in smokers but did not in non-smokers⁽¹¹⁷⁾. The above interpretation of density dependence has recently been questioned by evidence⁽¹¹⁸⁾ that in animal experiments the expected full density dependence was not observed because with $He-O_2$ increased frictional losses in small airways caused equal pressure points and the flow limiting segment to move upstream into smaller airways. Thus diminished density dependence of flow using $He-O_2$ may not allow a simple interpretation about the site of flow limitation on air.

From the evidence presented in this thesis it is not possible to resolve where the site of flow limitation is in smokers. However, the results suggest that the current idea that small airways flow limitation is dominant may not be correct.

Clearly not all of the many moment analysis indices are necessary to detect the patterns of abnormality described. The most discriminatory of these indices would seem to be $\alpha_{175\%}$ and $MR_{90\%}$ which agrees with the findings of the repeatability study. μ and σ from the model appeared no better than these two indices and this relates to the fact that in this population survey the spiograms obtained were essentially asymptotic. Thus truncation errors were minimal and therefore the model has little advantage over the moments

of the spirogram. The discordance between sigma and MR90% in the two most abnormal smokers with Pattern I suggests that truncation errors in these subjects limited the efficacy of MR90%. It is interesting that in these two subjects MR75% was markedly abnormal substantiating the argument that with early truncation the inevitable truncation errors are reduced. Hence the model appears only necessary when truncation errors become important. However, mu and FEV₃% were the indices with the most subjects more than 3 RSD above normal and mu showed the greatest extremes of abnormality with 1 subject 9 RSD and 2 subjects 6 RSD above normal.

Of the conventional indices FEV₁% and FEV₃% were more sensitive than FEV₁ and FEV₃ in detecting abnormalities. FEV₁ divided by the cube of height in metres did not remove the strong correlation of FEV₁ with height so this manipulation of the data was not pursued. Although FEV₃% and FEV₁% detected many abnormal smokers they were not able to distinguish any patterns of abnormality. Although an abnormal FEV₃% with normal FEV₁% suggested a Pattern II abnormality there were some exceptions such as subject 217 with Pattern I and most notably asthmatic subject 2684 (figure 6.7). The problems associated with defining the lower limit of normality for absolute volumes FEV_n may be to some extent answered by FEV_n% and the moment indices. In Figure 6.8 3 subjects have an abnormal FEV₃ or FEV₁ but are normal on all other indices and conversely subject 177 in figure 6.9 has a normal FEV₁% and minimal abnormality in FEV₁ but is clearly abnormal on the time domain indices. The conventional time domain

index FET identified 14 smokers as abnormal but for more than half of these this was their only abnormality. Thus FET has again been confirmed to be unhelpful.

CONCLUSIONS

Several aspects concerning the recording and analysis of spirograms have been discussed in this thesis. In this chapter the implication of these findings will be briefly discussed.

RECORDING SPIROGRAMS

Data has been presented in this thesis indicating that cooling errors when recording an MFEM with a spirometer are substantial and that a simple BTPS correction factor does not correct the distortion due to cooling. The experiments conducted here suggest that for the spirometers tested only 95% of the true BTPS correction factor needs to be used for FEV_1 . As the cooling characteristics of spirometers are time dependent a time array of factors would have to be stored which express the proportion of the relevant BTPS correction factor required to make an accurate correction for the whole spirogram. This array would be a representation of the spirometer's thermal time constant. However, any change in spirometer configuration, such as a change in deadspace due to failure to expel all the air from the spirometer prior to the blow, would alter the cooling characteristics of the device and invalidate the array of factors. An alternative to this would be to heat spirometers to an appropriate temperature.

Although clinical errors of judgement are unlikely to be caused by these cooling errors it is disconcerting that much epidemiological and other research work on spirometric lung function includes these errors.

The temperature experiments presented here were conducted with the pump temperature at 37°C . Estimates of mouth temperature suggest that it is approximately 33°C ^(56, 57) so the errors when recording subjects may be smaller than those presented here. The spirograms recorded from subjects in this study by the pneumotachograph were standardised to 33°C saturated. Gas in the alveoli is at approximately 37°C and static lung volumes are appropriately standardised to this temperature. During an MFEM the time course of the cooling of gas within the airways is not known and this raises the question as to what is the relevant temperature for standardisation of indices of an MFEM. The choice of 33°C in this study did not influence the time domain indices which are volume standardised, and conventional spirometric indices quoted in this thesis can be easily converted to a 37°C standardisation if required.

The heated PT fulfilled current guidelines for precision of recording an MFEM whereas the spirometers tested did not. The use of a PT requires careful attention to choice of transducer, amplifiers, upstream configuration, calibration procedure and control of PT temperature and these have limited its widespread use for recording the MFEM. The non-linearity of PT response can be corrected within the computer thus improving its characteristics. This was not performed in this study but deserves consideration. The main problem encountered with using a heated Fleisch PT was that the amount of heating and consequent expansion of gas passing through the PT varied at a specified PT temperature according to whether the PT head was cooling from a higher temperature, heating

up from a lower temperature or in a steady state. The total heat content of the PT was the important determinant of the gas expansion and not the temperature at any point within the PT assembly. In this study the PT was always used with the PT head temperature rising through 40°C . The temperature of 40°C was chosen arbitrarily and a lower temperature of 35°C (still above mouth temperature of 33°C) might reduce this problem. However, the design of the Fleisch PT is bad in this respect because of its large heat capacity. The use of a fine mesh screen PT with its smaller heat capacity would reduce this effect. If a mesh screen PT can be engineered to give satisfactory linearity it is likely to prove superior to the Fleisch.

TIME DOMAIN ANALYSIS

Substantial deficiencies and errors in the work of others concerning time domain analysis of spiograms have been exposed in this study. This has limited the interpretation of their results in the context of those presented here.

The moments of the spiogram appear to be a useful adjunct to conventional spirometric indices in defining abnormalities in a population of smokers. They are also efficient in detecting abnormalities in mild asthmatic subjects. The indices of the model of the spiogram were not found to be superior to the moments in the population sampled in this survey. This can be anticipated as the spiograms obtained from this population were all essentially asymptotic and so inevitable truncation errors in the moments would

be minimal. For assessing subjects with marked chronic airflow limitation by time domain analysis of their spiograms the use of the model would be necessary. Assessment of reversibility of airflow limitation using the moments of the spiogram is likely to be fruitless because of the changes in degree of truncation that may occur. Application of the model in this context deserves attention.

The natural history of the shape of spiograms in chronic obstructive lung disease can now be determined by time domain analysis of spiograms. The results of such analysis need to be compared and interpreted with the results from the same subjects of other tests which are thought to reflect certain aspects of airway performance. In this way hypotheses concerning smoking damage to lungs can be verified and translated into changes within the spiogram.

APPENDIX A

Consider a single exponential of the form

$$v = 1 - e^{-kt}$$

where v is the volume expired expressed as a fraction of unity

terminal volume, t is the elapsed time and k is the reciprocal of the time constant C

The ' r 'th moment at time T when expired volume is V_T is given by

$$\alpha_r^T = \int_0^{V_T} t^r dv = \int_0^T \frac{dv}{dt} \cdot t^r dt$$

since $\frac{dv}{dt} = k e^{-kt}$

then $\alpha_r^T = \int_0^T k t^r e^{-kt} dt$

This can be integrated in parts, giving

$$\alpha_1^T = \frac{1}{k} - e^{-kT} \left(T + \frac{1}{k} \right)$$

and $\alpha_2^T = \frac{2}{k^2} - e^{-kT} \left(T^2 + \frac{2T}{k} + \frac{2}{k^2} \right)$

for $T = \infty$

$$\alpha_1 = \frac{1}{k} \quad \text{and} \quad \alpha_2 = \frac{2}{k^2}$$

for $T = \infty \quad \sqrt{\alpha_2/\alpha_1} = \sqrt{2} \quad \text{irrespective of time constant}$

APPENDIX B

Consider a theoretical spiogram characterised by a single exponential of time constant D where by time t seconds a volume V is expired (V is expressed as a fraction of unity terminal volume at infinite time)

$$\text{then} \quad V = 1 - e^{-t/D} \quad (1)$$

Equation (1) can be regarded as the cumulative distribution function of transit times for this theoretical spiogram.

Differentiating equation (1) with respect to t yields an expression of the instantaneous flow at time t ,

$$dV/dt = \frac{e^{-t/D}}{D} \quad (2)$$

In order to make equation (2) a probability density function of transit times, $f(t)$, for a theoretical spiogram truncated at the time T seconds, i. e. it does not continue to infinite time, it is necessary for the integral of $f(t)$ to equal unity at time T

$$\text{So} \quad \frac{f(t)}{V_T} = \frac{dV/dt}{D(1 - e^{-T/D})} = \frac{e^{-t/D}}{D(1 - e^{-T/D})} \quad (3)$$

where V_T is the volume expired by truncation time T

The moment generating function, M , of any probability density function $f(t)$ is given by

$$M = \int_{-\infty}^{\infty} e^{st} f(t) dt$$

where s is that point within the distribution about which the moments are generated.

Hence the moment generating function for equation (e) is

$$M = \int_0^T \frac{e^{-t(1/D - s)}}{D(1 - e^{-T/D})} dt$$

Therefore

$$M = \left[\frac{1}{1 - SD} \right] \left[\frac{1 - e^{-T(1/D - s)}}{1 - e^{-T/D}} \right] \quad (4)$$

To obtain from M the 'r'th moment about the origin, $\alpha_r(D)$, at truncation time T for the theoretical single exponential spiogram of time constant D equation (4) is differentiated r times with respect to s and then s set to zero. This yields:

$$\alpha_r(D) = D^r r! \left[\frac{1 - e^{-T/D} \sum_{n=1}^r \left[\frac{T^n}{D^n n!} \right]}{1 - e^{-T/D}} \right] \quad (5)$$

as T tends to ∞ so $\alpha_r(D) = r! D^r$

Hence for any time constant D, $\sqrt{\alpha_2} / \alpha_1 = \sqrt{2}$

A single exponential theoretical model of the spiogram cannot adequately fit real spiograms so the model was expanded to comprise a mixture of an infinite number of single exponentials of the type in equation (1) whose time constants were defined by a continuous distribution function h(D).

Then h(D) dD is the fraction of unity terminal volume expired by infinite time contributed by the portion with time constant in the range D to D + dD

Therefore $\int_0^{\infty} h(D) dD = \text{unity by definition of a probability density function.}$

The volume, V_p , expired from the portion with time constant

D to $D + dD$ up to time T is given by

$$V_p = h(D) dD (1 - e^{-T/D}) \quad (6)$$

So the total volume V_T from all portions up to time T is given by

$$V_T = \int_0^{\infty} h(D) (1 - e^{-T/D}) dD \quad (7)$$

Integrating equation (7) by parts yields:

$$V_T = \int_0^{\infty} h(D) dD - \int_0^{\infty} e^{-T/D} h(D) dD$$

$$\text{Therefore} \quad V_T = 1 - \int_0^{\infty} e^{-T/D} h(D) dD \quad (8)$$

Hence from equations (6) and (8) the fraction of the total volume, V_f , contributed by the portion with time constant D to $D + dD$ up to time T is given by

$$V_f = \frac{h(D) dD (1 - e^{-T/D})}{1 - \int_0^{\infty} e^{-T/D} h(D) dD} \quad (9)$$

Let $\alpha_r(D)$ be the ' r 'th moment about the origin of the theoretical spirogram with single time constant D . Since the ' r 'th moment about the origin of the whole spirogram at time T , α_r^T , is equal to the sum of the compartmental moments $\alpha_r(D)$ mixed appropriately according to their contribution, then

$$\begin{aligned} \alpha_r^T &= \int_0^{\infty} \alpha_r(D) V_f \\ \alpha_r^T &= \frac{\int_0^{\infty} \alpha_r(D) h(D) (1 - e^{-T/D}) dD}{1 - \int_0^{\infty} h(D) e^{-T/D} dD} \end{aligned} \quad (10)$$

$\alpha_r(D)$ in equation (10) can be substituted for by equation (5).

Following this substitution, α_r^T can be computed for any given time T by numerical integration routines if the distribution function $h(D)$ is defined. Similarly the fractional volume expired by given time T can be computed from equation (9) if $h(D)$ is defined.

APPENDIX C

Aggregate scores for each of the following 6 groups of questions were obtained.

		SCORE	
Q1.	COUGH	NO	YES
	a) Do you USUALLY cough first thing in the morning in the winter (with first smoke or on first going out)?	0	1
	b) Do you USUALLY cough during the day or night in the winter ? (6 coughs/day)	0	2
	If NO, go to Q2		
	c) Do you cough like this on most days for as much as 3 months per year?	0	4
Q2	PHLEGM		
	a) Do you USUALLY bring up phlegm from your chest first thing in the morning in winter (not phlegm from nose)?	0	1
	b) Do you USUALLY bring up phlegm from your chest during the day or night in winter?	0	2
	If NO, go to Q3		
	c) Do you bring up phlegm like this on most days for as much as 3 months/year?	0	4
Q3	PERIODS OF COUGH		
	a) In the past 3 years have you had a period of (increased) cough and phlegm lasting for 3 weeks or more?	0	1
	If NO, go to Q4		
	b) Have you had more than one such period?	0	2

Q 4 BREATHLESSNESS

a) Do you have any difficulty in walking?

NO
0

YES
9

If the subject is disabled from walking by
any condition other than heart or lung disease
enter 9 and go to Q5

b) Are you troubled by shortness of breath
when walking quickly on level ground or
walking up a slight hill?

0

1

If NO, go to Q5

c) Do you get short of breath walking with
people of your own age on level ground?

0

2

d) Do you have to stop for breath when
walking at your own pace on level ground?

Q5 WHEEZING

a) Does your chest ever sound wheezing or
whistling?

0

1

If NO, go to Q6

b) Do you get this on most days or nights?

0

2

c) Have you ever had attacks of shortness
of breath when wheezing?

0

4

d) Is/ Was your breathing absolutely normal
between attacks?

0

1

Q6 CHEST ILLNESSES

NO

YES

a) During the last 3 years have you had any

0

1

chest illnesses which have kept you from your

usual activities for as much as 1 week?

if NO, go to end

b) Did you bring up more phlegm than usual

0

2

in these illnesses?

c) Have you had more than one illness like

0

4

this in the past 3 years?

REFERENCES

1. HUTCHINSON J. On the capacity of the lungs, and on the respiratory function, with a view to establishing a precise and easy method of detecting disease by the spirometer. Medico-chirurgical transactions 1846; 29: 137-252
2. THACKRAH CT. The effects of arts, trades and professions and of civic states and habits of living on health and longevity. Longman. London 1831
3. BAIN WP. On a portable spirometer. Br Med J 1870; 1: 129
4. PEABODY FW. Clinical studies in respiration. 3. A mechanical factor in the production of dyspnoea in patients with cardiac disease. Arch Int Med 1917; 20: 433-42
5. PEABODY FW. Clinical studies in respiration. 4. The vital capacity of the lungs and its relation to dyspnoea. Arch Int Med 1917; 20: 443-67
6. DREYER G, BURRELL LST. The vital capacity constants applied to the study of tuberculosis. Lancet 1920; 1: 1212-6
7. DREYER G, BURRELL LST. The vital capacity constants applied to the study of tuberculosis. Lancet 1922; 2: 374-6
8. CAMERON C. The vital capacity in pulmonary tuberculosis. Tubercle 1922; 3: 353-62, 385-99
9. HERMANNSEN J. Untersuchungen über die maximale Ventilationsgrosse (Atemgrenzwert) Z Ges Exper Med 1933; 90: 130-7

10. TIFFENEAU R, PINELLI. Air circulant et air captif dans l'exploration de la fonction ventilatrice pulmonaire.
Paris Med 1947; 133: 624-8
11. GAENSLER EA. Analysis of the ventilatory defect by timed capacity measurements. Am Rev Tuberc 1951; 64: 256-78
12. DAYMAN H Mechanics of airflow in health and in emphysema.
J Clin Invest 1951; 30: 1175-90
13. FRY DL, EBERT RV, STEAD WW, BROWN CC. The mechanics of pulmonary ventilation in normal subjects and in patients with emphysema. Am J Med 1954; 16: 80-97
14. HYATT RE, SCHILDER DP, FRY DL. Relationship between maximum expiratory flow and degree of lung inflation.
J Appl Physiol 1958; 13: 331-6
15. FRY DL, HYATT RE. Pulmonary mechanics: a unified analysis of the relationship between pressure, volume and gas flow in the lungs of normal and diseased human subjects.
Am J Med 1960; 29: 672-89
16. LEUALLAN EC, FOWLER WS. Maximal midexpiratory flow.
Am Rev Tuberc 1955; 72: 783-800
17. HIGGINS ITT. Respiratory symptoms, bronchitis and ventilatory capacity in a random sample of an agricultural population. Br Med J 1957; 2: 1198-1203

18. WRIGHT BM, MCKERROW CB. Maximum forced expiratory flow rate as a measure of ventilatory capacity. Br Med J. 1959; 2: 1041-7
19. TINKER CM. Peak expiratory flow measured by the Wright peak flow meter. Br Med J 1961; 1: 1365-6
20. MEAD J, TURNER JM, MACKLEM PT, LITTLE JB. Significance of the relationship between lung recoil and maximum expiratory flow. J Appl Physiol 1967; 22: 95-108
21. PRIDE NB, PERMUTT S, RILEY RL, BROMBERGER-BARNEA B. Determinants of maximal expiratory flow from the lungs. J Appl Physiol 1967; 23: 646-62
22. GREEN M, MEAD J, HOPPIN F, WOHL ME. Analysis of the forced expiratory manoeuvre. Chest 1973; 63: 33S-36S
23. LANDAU LI, TAUSSIG LM, MACKLEM PT, BEAUDRY PH. Contributions of inhomogeneity of lung units to the maximal expiratory flow-volume curve in children with asthma and cystic fibrosis. Am Rev Respir Dis 1975; 111: 725-31
24. WEBSTER PM, ZAMEL N, BRYAN AC, KRUGER K. Volume dependence of instantaneous time constants derived from the maximal expiratory flow-volume curve. Am Rev Respir Dis 1977; 115: 805-10
25. MEAD J. Analysis of the configuration of maximal expiratory flow-volume curves. J Appl Physiol 1978; 44: 156-65

26. JANSSEN JM, PESLIN R, BOHADANA AB, RACINEUX JL.
Usefulness of forced expiration slope ratios for detecting mild
airway abnormalities. *Am Rev Respir Dis* 1980; 122: 221-30.
27. MILLER RD, HYATT RE. Evaluation of obstructing lesions of
the trachea and larynx by flow-volume loops.
Am Rev Respir Dis 1973; 108: 475-81
28. FISH J, MENKES H, ROSENTHAL R, SUMMER W, NORMAN P,
PERMUTT S. The effect of acute bronchospasm on the
distribution of transit times during forced expiration.
Am Rev Respir Dis 1974; 109: 700
29. TOCKMAN M, MENKES H, COHEN B, PERMUTT S, BENJAMIN J,
BALL WC, TONASCIA J. A comparison of pulmonary function
in male smokers and non-smokers. *Am Rev Respir Dis*
1976; 114: 711-22
30. LIANG A, MACFIE AE, HARRIS EA, WHITLOCK RML. Transit
time analysis of the forced expiratory spirogram during clinical
remission in juvenile asthma. *Thorax* 1979; 34: 194-9
31. NEUBERGER N, LEVISON H, BRYAN AC, KRUGER K. Transit
time analysis of the forced expiratory spirogram in growth.
J Appl Physiol 1976; 40: 329-332
32. JORDANOGLU J, KOURSUBA E, LALENSIS C, GOTSIS T,
KONTOS J, GARDIKAS C. Effective time of the forced expiratory
spirogram in health and airways obstruction. *Thorax* 1979; 34: 187-93

33. PARTRIDGE MR, WATSON AC, SAUNDERS KB. Moment analysis of the flow-time curve after breathing gases of different densities. *Thorax* 1981; 36: 38-44

34. FLETCHER C, PETO R. The natural history of chronic airflow obstruction. *Br Med J* 1977; 1: 1645-8

35. MACDONALD JB, COLE TJ, SEATON A. Forced expiratory time - its reliability as a lung function test. *Thorax* 1975; 30: 554-9

36. KENDALL MG. The advanced theory of statistics. Vol 1 Chapter 3. Moments and Cumulants. Charles Griffith & Co. 5th Ed. 1952 p57-96

37. SMITH AA, GAENSLER EA. Timing of forced expiratory volume in one second. *Am Rev Respir Dis* 1975; 112: 882-5

38. DAVIS C, CAMPBELL EJM, OPENSHAW P, PRIDE NB, WOODROOF G. Importance of airway closure in limiting maximal expiration in normal man. *J Appl Physiol* 1980; 48: 695-701

39. PERMUTT S, MENKES HA. Spirometry: analysis of the forced expiration within the time domain. The lung in transition between health and disease. In Macklem P, Permutt S eds. *Lung Biology in health and disease. Volume 12.* New York: Marcell Dekker 1979

40. MILLER MR, PINCOCK AC. Repeatability of the moments of the truncated forced expiratory spirogram. Thorax 1982; 37: 205-11
41. GARDNER RM, HANKINSON JL, WEST BJ. Evaluating commercially available spirometers. Am Rev Respir Dis 1980; 121: 73-82
42. BERGLUND E, BIRATH G, BJURE J et al. Spirometric studies in normal subjects. I. Forced expirograms in subjects between 7 and 70 years of age. Acta Medica Scand 1963; 173: 185-91
43. GLINDMEYER HW, ANDERSON ST, DJIEM JE, WEILL H. A comparison of the Jones and Stead-Wells spirometers. Chest 1978; 73: 596-602
44. PERKS WH, SOPWITH T, BROWN D, GREEN M. Should values obtained with a bellows spirometer be converted to BTPS? Thorax 1981; 31: 225
45. TASHKIN DP, PATEL A, DEUTSCH R, PETERSON E, CALVARESE B. Is standard ATPS to BTPS correction of volumes and flow rates measured with a volumetric spirometer valid? Am Rev Respir Dis 1980; 121 suppl: 412
46. FINUCANE KE, EGAN BA, DAWSON SV. Linearity and frequency response of pneumotachographs. J Appl Physiol 1972; 32: 121-6

47. HUDSON LD, PETTY TL, BAIDWAN B, STARK K. Clinical
evaluation of a new office spirometer. JAMA; ^{1978:} 240: 2754-5
48. SHANKS DE, MORRIS JF. Clinical comparison of two electronic
spirometers with a water-seal spirometer. Chest 1976; 69: 461-6
49. GLINDMEYER HW, ANDERSON ST, KERN RG, HUGHES J.
A portable adjustable forced vital capacity simulator for routine
spirometer calibration. Am Rev Respir Dis 1980; 121: 599-602
50. BERNSTEIN L, D'SILVA JL, MENDEL D. The effect of the
rate of breathing on maximum breathing capacity determined
with a new spirometer. Thorax 1952; 7: 255-62
51. ATS STATEMENT - Snowbird workshop on standardisation of
spirometry. Am Rev Respir Dis 1979; 119: 831-8
52. STATEMENT of the Committees on Environmental Health and
Respiratory Physiology. American College of Chest Physicians.
The assessment of ventilatory capacity. Chest 1975; 67: 95-7
53. FLEISCH A. Der Pneumotachograph - ein Apparat zur
Geschwindigkeitsregistrierung der Atemluft. Pflügers Arch
Ges Physiol 1925; 209: 713- 22
54. LILLY JC. Flow meter for recording respiratory flow of human
subjects. In - Methods in medical research. Chicago. Year
Book Publishers Inc. 1950. Vol 2 pp 113-21.

55. FRY DL, HYATT RE, MCCALL CB, MALLOS AJ. Evaluation^{-186 -}
of three types of respiratory flowmeter. *J Appl Physiol*
1957; 10: 210-4
56. COLE P. Recording of respiratory air temperatures.
J Laryng 1954; 68: 295-307
57. LIESE W, WARWICK WJ, CUMMING G. Water vapour pressure
in expired air. *Respiration* 1974; 31: 252-61
58. KAYE GWC, LABY TH. Tables of physical and chemical
constants and some mathematical functions. Longmans, London,
9th ed. 1944. pp 40-1
59. GRENVIK A, HEDSTRAND U, SJÖGREN H. Problems in
pneumotachography. *Acta Anaesth Scand* 1966; 10: 147-55
60. VON DER HARDT H, ZYWIETZ C. Reliability in pneumo-
tachographic measurements. *Respiration* 1976; 33: 416-24
61. GULESIAN PJ. Design and calibration of sampled-data
system for the measurement of airway dynamics.
J Appl Physiol 1971; 31: 616-9
62. GILL PE, MILLER GF. An algorithm for the integration of
unequally spaced data. *The Computer Journal* 1972 ; 15: 80-3
63. KNUDSON RJ, SLATIN RC, LEBOWITZ MD, BURROWS B.
The maximal expiratory flow-volume curve. Normal standards,
variability and effects of age. *Am Rev Respir Dis* 1976; 113:
587-600.

64. MACDONALD JB, COLE TJ, SEATON A. Forced expiratory time - its reliability as a lung function test.
Thorax 1975; 30: 554-9
65. JORDANOGLOU J, HADJISTAVROU C, TATSIS G, ANEVLAXIS E MELISSINOS C. Total effective time of the forced expirogram in disease: sources of error and a correction factor.
Thorax 1982; 37: 304-8
66. FRY DL. A preliminary lung model for simulating the aerodynamics of the bronchial tree. Comp Biomed Res 1968; 2: 111-34
67. LAMBERT RK, WILSON TA, HYATT RE, RODARTE JR. A computational model for expiratory flow. J Appl Physiol 1982; 52: 44-56
68. CLEMENT J, VAN DE WOESTIJNE . Validity of simple physical models in interpreting maximal expiratory flow-volume curves. Respiration Physiology 1972; 15: 70-86
69. LOWELL FC, SCHILLER IW. Significance of changes in the expiratory rate observed during measurement of the vital capacity in asthma. J Allergy 1953;24: 492-8
70. FLETCHER R. A modified Marquardt subroutine for non-linear least squares. United Kingdom Atomic Energy Authority Research Group report. AERE - R6799 HMSO 1971

71. FLETCHER R. A review of methods for unconstrained optimization. In: Optimisation. Ed. R. Fletcher. Academic Press Inc., London 1969 pp 1-12
72. EISNER A, EBERT WL. Evaluation of lognormal parameters for the distribution of time constants in spirometry. The Johns Hopkins University Applied Physics Laboratory Report Oct. 1976
73. COHN JE, DONOSO HD. Mechanical properties of lung in normal men over 60 years old. J Clin Invest 1963; 42: 1406-10
74. TURNER JM, MEAD J, WOHL ME. Elasticity of human lungs in relation to age. J Appl Physiol 1968; 25: 664-71
75. COTES JE, ROSSITTER CE, HIGGINS ITT, GILSON JC. Average normal values for the forced expiratory volume in white caucasian males. Br Med J 1966; 1: 1016-9
76. FERRIS BG, ANDERSON DO, ZICKMANTEL R. Prediction values for screening tests of pulmonary function. Am Rev Respir Dis 1965; 91: 252-61
77. BUIST AS, DUCIC S. Smoking. Evaluation of studies which have demonstrated pulmonary function changes. In: The lung in the transition between health and disease. Lung Biology in health and disease. Vol 12. Eds. Macklem PT, Permutt S 1979 Marcel Dekker

78. COSIO M, GHEZZO H, HOGG JC, CORBIN R et al. The relations between structural changes in small airways and pulmonary function tests. N Engl J Med 1977; 298: 1277-81
79. NIEWOEHRER DE, KLEINERMAN J, RICE DB. Pathologic changes in the peripheral airways of young cigarette smokers N Engl J Med 1974; 291: 755-8
80. HOGG JC, MACKLEM PT, THURLBACK WM. Site and nature of airway obstruction in chronic obstructive lung disease. N Engl J Med 1968;278: 1355-60
81. MACKLEM PT, MEAD J. Resistance of central and peripheral airways measured by a retrograde catheter. J Appl Physiol 1967;22: 395-401
82. SEELY JE, ZUSKIN E, BOUHUYS A. Cigarette Smoking: objective evidence for lung damage in teenagers. Science 1971; 172: 741-3
83. TATTERSALL SF, BENSON MK, HUNTER D, MANSELL A, PRIDE NB, FLETCHER CM. The use of tests of peripheral lung function for predicting future disability from airflow obstruction in middle-aged smokers. Am Rev Respir Dis 1978; 118: 1035-50
84. MARCQ M, MINETTE A. Lung function changes in smokers with normal conventional spirometry. Am Rev Respir Dis 1976; 114: 723-38

85. NEMERY B, MOAVERO NE, BRASSEUR L, STANESCU DC.
Significance of small airways tests in middle-aged smokers.
Am Rev Respir Dis 1981; 124: 232-38
86. GUBERAN E, WILLIAMS MK, WALFORD J, SMITH MM.
Circadian variation of FEV in shift workers.
Br J Industr Med 1969; 26: 121-5
87. MCCARTHY DS, CRAIG DB, CHERNLACK RM. The effect
of acute, intensive cigarette smoking on maximal expiratory
flows and the single-breath nitrogen washout trace.
Am Rev Respir Dis 1976; 113: 301-4
88. FRIDY WW, INGRAM RH, HIERHOLZER JC, COLEMAN MT.
Airways function during mild viral respiratory illnesses. The
effect of rhinovirus infection in cigarette smokers.
Ann Int Med 1974; 80: 150-4
89. CHERNLACK RM, RABER MB. Normal standards for ventilatory
function using an automated wedge spirometer.
Am Rev Respir Dis 1972; 106: 38-46
90. MORRIS JF, KOSKI A, JOHNSON LC. Spirometric standards
for healthy non-smoking adults. Am Rev Respir Dis 1971;
103: 57-67
91. MACFIE AE, HARRIS A, WHITLOCK RML. Transit time
analysis of the forced spirogram in healthy children and
adults. J'Appl Physiol 1979; 46: 263-7

92. NEUBURGER N, LEVISON H, KRUGER K. Transit time analysis of the forced expiratory vital capacity in cystic fibrosis. *Am Rev Respir Dis* 1976; 114: 753-9

93. JORDANOGLU J, TATSIS G, VESLEMES M, CHARALAMPAKIS S, HADJISTAVROU C. Partial effective times of the forced expiratory spirogram in health and mild airways obstruction. *Thorax* 1980; 35: 375-8

94. FLETCHER C, PETO R, TINKER C, SPEIZER FE. The natural history of chronic bronchitis and emphysema. Oxford University Press 1976.

95. BATES DV. The fate of the chronic bronchitic: a report of the 10-year follow-up in the Canadian Dept. of Veteran's affairs co-ordinated study of chronic bronchitis. *Am Rev Respir Dis* 1973; 108: 1043-65.

96. JOHNSTON RN, MCNEILL RS, SMITH DH, LEGGE JS, FLETCHER F. Chronic bronchitis - measurements and observations over 10 years. *Thorax* 1976; 31: 25-9.

97. DOSMAN J. Preventative diagnosis in occupational pulmonary disease. *Ann Intern Med* 1975; 83: 274-6

98. DOSMAN J, MACKLEM PT. Diseases of small airways. *Advances in Int Med* 1977; 22: 355-76

99. ANTHONISEN NR, BASS H, ORIOL A, PLACE REG, BATES DV. Regional lung function in patients with chronic bronchitis. Clin Sci 1968; 35: 495-511
100. BROWN R, WOOLCOCK AJ, VINCENT NJ, MACKLEM PT. Physiological effects of experimental airway obstruction with beads. J Appl Physiol 1969; 27: 328-35
101. HOGG JC, MACKLEM PT, THURLBECK WM. Site and nature of airway obstruction in chronic obstructive lung disease. N Eng J Med 1968; 278: 1355-60
102. WOOLCOCK AJ, VINCENT NJ, MACKLEM PT. Frequency dependence of compliance as a test for obstruction of small airways. J Clin Invest 1969; 48: 1097-1106
103. DOLFUSS RE, MILIC-EMILI J, BATES DV. Regional ventilation of the lung studied with boluses of ^{133}Xe . Respir Physiol 1967; 2: 234-46
104. BUIST AS, VAN FLEET DL, ROSS BB. A comparison of conventional spirometric tests and the test of closing volume in an emphysema screening centre. Am Rev Respir Dis 1973; 107: 735-43
105. BUIST AS, ROSS BB. Quantitative analysis of the alveolar plateau in the diagnosis of early airway obstruction. Am Rev Respir Dis 1973; 108: 1078-87

106. MCFADDEN ER, LINDEN DA. A reduction in maximum mid-expiratory flow rate: a spirographic manifestation of small airways disease. *Am J Med* 1972; 52: 725-37
107. MCFADDEN ER, KIKER R, HOLMES B, DE GROOT WJ. Small airway disease: an assessment of the tests of peripheral airway function. *Am J Med* 1974; 57: 171-82
108. SOBOL BJ. The early detection of airway obstruction: another perspective. *Am J Med* 1976; 60: 619-24
109. BLACK LF, OFFORD K, HYATT RE. Variability in the maximal expiratory flow volume curve in asymptomatic smokers and non-smokers. *Am Rev Respir Dis* 1974; 110: 282-92
110. GREGG I. Epidemiology. Chapter 11 in *Asthma*. Eds. Clark TJH and Godfrey S. Chapman & Hall Ltd. 1977 London
111. MACKLEM PT, FRASER RG, BROWN WG. Bronchial pressure measurements in emphysema and bronchitis. *J Clin Invest* 1965; 44: 897-905
112. MACKLEM PT, WILSON NJ. Measurement of intrabronchial pressure in man. *J Appl Physiol* 1965; 20: 653-63
113. WRIGHT R. Bronchial atrophy and collapse in chronic obstructive pulmonary emphysema. *Am J Path* 1960; 37: 63-71

114. MAISEL JC, SILVERS GW, GEORGE MS, DART GA,
PETTY TL, MITCHELL RS. The significance of bronchial
atrophy. *Am J Path* 1972; 67: 371-83
115. THURLBECK WM, PUN R, TOTH J, FRAZER RG.
Bronchial cartilage in chronic obstructive lung disease.
Am Rev Respir Dis 1974; 109: 73-80
116. DESPAS PJ, LEROUX M, MACKLEM PT. Site of airway
obstruction in asthma as determined by measuring maximal
expiratory flow breathing air and a helium-oxygen mixture.
J Clin Invest 1972; 51: 3235-43
117. DOSMAN J, BODE F, URBANETTI J, MARTIN R, MACKLEM PT.
The use of a helium-oxygen mixture during maximum expiratory
flow to demonstrate obstruction in small airways in smokers.
J Clin Invest 1975; 55: 1090-9
118. PEDERSON OF, CASTILE RG, DRAZEN JM, INGRAM RH.
Density dependence of maximum expiratory flow in the dog.
J Appl Physiol 1982; 53: 397-404.